Institute for Virology in the Department of Pathobiology,
University of Veterinary Medicine Vienna

And

Department of Cancer Immunology and AIDS,
Dana-Farber Cancer Institute, Boston

Subject: Virology

Isolating HIV-1 Envelope Mimotopes Using Polyclonal Sera from Pig-Tailed Macaques Infected with a CCR5-Tropic Subtype-C Simian-Human Immunodeficiency Virus

MASTER THESIS

Submitted for Obtaining the Degree of

MASTER OF SCIENCE

At the University of Veterinary Medicine Vienna

By

Bakk.rer.nat Barbara Bachler

Vienna, July 2010

First Supervisor:

Ruth M. Ruprecht, M.D. Ph.D.

Professor of Medicine; Cancer Immunology/AIDS, Dana-Farber Cancer Institute and Harvard Medical School, Boston, MA

Second Supervisor:

Ao. Univ. Prof. Tzt. Dr. Dieter Klein

Institute for Virology, Department of Pathobiology, University of Veterinary Medicine, Vienna

Reviewer:

Univ. Prof. Dr.rer.nat. Armin Saalmüller

Institute for Clinical Immunology, Department of Pathobiology, University of Veterinary Medicine, Vienna

TABLE OF CONTENTS

LIST OF ILLUSTRATIONS

LIST OF ABBREVIATIONS

General Abbreviations

°C	Degree Celsius
3DEX	3D-Epitope-Explorer
Å	Ångström
Abs	Antibodies
ADCC	Antibody-dependent cellular cytotoxicity
AIDS	Acquired immune deficiency syndrome
APC	Antigen Presenting Cell
BSA	Bovine Serum Albumin
C1-C5	Conserved regions 1-5 on gp120
CA	Capsid protein
CCR5	Chemokine receptor CCR5
CCR5Δ32bp	Genetic variant of CCR5, containing a deletion mutation of a 32 base pair fragment
CD	Cluster of differentiation
$CD4^+$ T cells	T cells expressing the surface receptor CD4
CD4i	CD4 induced (epitope on gp120)
$CD8^+$ T cells	T cells expressing the surface receptor CD8
cDNA	Complementary deoxyribonucleic acid
CHR	C-terminal heptad region (gp41)
CRF	Circulating recombinant forms
CT	Cytoplasmatic tail (gp41)
CTL	Cytotoxic T-cell
CXCR4	Chemokine receptor CXCR4
dH_2O	Distilled water
DMEM	Dulbecco's Modified Essential Medium
DNA	Deoxyribonucleic acid
E.coli	Escherichia coli
ELISA	Enzyme-linked immunosorbent assay
Env	Envelope protein
ER2738	Escherichia coli strain
Fab region	Fragment, antibody binding region
FAS ligand	Transmembrane protein of the tumor necrosis factor family
FCS	Foetal Calf Serum
FITC	Fluorescein Isothiocyanate
FP	Fusion peptide (gp41)
F-pilus	Fertility or sex pilus used by F (fertility) factor positive bacteria for conjugation
g	gram
G	Guanine
Gag	Group specific antigen
Gag-pol	Group specific antigen-polymerase
GALT	Gut-associated lymphoid tissue
gp120	Envelope Glycoprotein 120
gp160	Envelope Glycoprotein 160
gp41	Envelope Glycoprotein 41
H_2O_2	Hydrogen peroxide solution
H_2SO_4	Sulfuric acid
HCl	Hydrogen chloride
HeLa	Immortal cell line named after "Henrietta Lacks"
HIV	Human immunodeficiency virus
HLA	Human leukocyte antigen
HRP	Horseradish peroxidase
IFN-γ	Interferon gamma
IgG	Immunglobulin G
IgM	Immunglobulin M
IL	Interleukin
IN	Integrase
IPTG	Isopropyl-β-D-thiogalactoside
Kb	Kilobase
LacZα	Alpha fragment of a beta-galactosidase monomer
LB	Luria Bertani
LTNPs	Long term non progressors
LTR	Long terminal repeat
M	Molar mass
M13	Bacteriophage strain
M13K07	Helper phage
MA	Matrix protein
mAb	Monoclonal antibody
MHC I	Major histocompatibility complex I
MHC II	Major histocompatibility complex II
ml	Milliliter
MMC	Mucosal mononuclear cells
MPER	Membrane-proximal external region (gp41)
mRNA	Messenger RNA
M-tropic	HIV strains using mainly macrophages as target cells
MVA	Modified vaccinia virus Ankara
N	Nanomolar
nAb	Neutralizing antibody
NaCl	Sodium chloride
NaI	Sodium iodide
NaN_3	Sodium azide
NC	Nucleocapsid protein
NEB	New England Biolabs
Nef	Negative regulation factor
NFκB	Nuclear factor kappa-light-chain-enhancer of activated B cells
ng	Nanogramm
NHR	N-terminal heptad repeat (gp41)
NK cells	Natural killer cells
nm	Nanometer
NMR	Nuclear magnetic resonance
OPD	Ortho-phenyldiamine
p.i.	Post infection
PBS	Phosphate buffered saline
PBMC	Peripheral Blood Mononuclear Cell
PDPL	Phage-displayed random peptide library
pfus/ml	Plaque forming units per milliliter
pH	Measure of the acidity of a solution
Ph.D.-12	Phage Display Library 12mer
Ph.D.-7	Phage Display Library 7mer
Ph.D.-C7C	Phage Display Library cyclic 7mer
pI-pX	Proteins 1-10 of bacteriophage M13
Pol	Polymerase
PR	Protease
PR	Polar region (gp41)
PT	Pig-tailed macaque
R5	CCR5 tropic virus strain
Rev	Regulator of virion gene expression
RF	Replication form
RM	Rhesus macaque
RNA	Ribonucleic acid
RNAPII	RNA polymerase II
RNase H	Endonuclease
rpm	Revolutions per minute
RRE	Rev response element
RT	Reverse transcriptase
SDS	Sodium dodecylsulfate
SHIV	Simian-human immunodeficiency virus
SIV	Simian immunodeficiency virus
SIVcpz	Simian immunodeficiency virus isolated from chimpanzees

SIVmac	Simian immunodeficiency virus isolated from rhesus macaques
SIVmne	Simian immunodeficiency virus isolated from pig-tailed macaques
SIVsmm	Simian immunodeficiency virus isolated from sooty mangabeys
ssDNA	Single stranded deoxyribonucleic acid
SU	Surface protein, gp120
T	Thymine
Tat	Transcriptional transactivator
TCEP	Tris(2-carboxyethyl)phospine
TEM	Transmission electron microscope
TH1	T helper cells 1
TH2	T helper cells 2
TM	Transmembrane protein, gp41
TRIM5alpha	Tripartite motif-containing 5
Tris	Tris(hydroxymethyl)aminomethane
T-tropic	HIV strains using mainly naïve T cells as targets
TZM-bl	Indicator cell line (derivate of HeLA cell line)
UNAIDS	Joint United Nations Programme on HIV and AIDS
V1-V5	Variable loops 1-5 (on gp120)
Vif	Viral infectivity factor
Vpr	Viral protein r
Vpu	Viral protein u
X4	CXCR4 tropic virus strain
X4R5	Dualtropic virus strain (CXCR4 and CCR5)
X-Gal	5-Bromo-4-chloro-3-indolyl-β-D-galactoside
µl	Microliter
µm	Micrometer

Amino Acids

A	Ala	Alanine
C	Cys	Cysteine
D	Asp	Aspartic acid
E	Glu	Glutamic acid
F	Phe	Phenylalanine
G	Gly	Glycine
H	His	Histidine
I	Ile	Isoleucine
K	Lys	Lysine
L	Leu	Leucine
M	Met	Methionine
N	Asn	Asparagine
P	Pro	Proline
Q	Gln	Glutamine
R	Arg	Arginine
S	Ser	Serine
T	Thr	Threonine
V	Val	Valine
W	Trp	Tryptophan
Y	Tyr	Tyrosine

Virus Strains

HIV1157i	HIV-1 isolate from a Zambian infant
CAP210	HIV-1 strain, clade C
Q461d1	HIV-1 strain, clade A
SF162	HIV-1 strain, clade B
SHIV-1157i	SHIV strain containing SIV backbone and envelope from HIV1157, clade C
SHIV-1157ip	Passaged SHIV-1157i (early isolate), clade C
SHIV-1157ipd	Late isolate of SHIV-1157ip, clade C
SHIV-1157ipd3	Late-stage infectious molecular clone #3 of SHIV-1157ipd, clade C
SHIV-1157ipd3N4	Late-stage infectious molecular clone #3 of SHIV-1157ipd containing one additional NF-κB site, clade C
SHIV89.6	SHIV strain , clade B
SIVmac239	SIV isolate from rhesus monkey #239
SS1196.1	HIV-1 strain, clade B

Animal Names

J02185	SHIV-1157ipd3N4-infected pig-tailed macaque
K03135	SHIV-1157ipd3N4-infected pig-tailed macaque
L03165	SHIV-1157ipd3N4-infected pig-tailed macaque
M04123	SHIV-1157ipd3N4-infected pig-tailed macaque
M05118	Naïve pig-tailed macaque
RAo-8	SHIV-1157ip-infected rhesus macaque
RPn-8	SHIV-1157i-infected rhesus macaque

Monoclonal Antibodies

17b	Human monoclonal antibody 17b
2F5	Human monoclonal antibody 2F5
2G12	Human monoclonal antibody 2G12
447-52D	Human monoclonal antibody 447-52D
4E10	Human monoclonal antibody 4E10
IgG1 b12	Human monoclonal antibody IgG1 b12
m9	Human monoclonal antibody m9
X5	Human monoclonal antibody X5

1 INTRODUCTION

1.1. The Human Immunodeficiency Virus (HIV)

The human immunodeficiency virus (HIV) belongs to a subfamily of retroviruses called lentiviruses (BARRE-SINOUSSI et al., 1983). Their group name derived from the Latin word *lentus* which means "slow" and refers to the fact that they can persist and continue to replicate for many years before they cause any obvious signs of disease (long period of incubation). Like all members of the viral family of Retroviridae, HIV is an enveloped virus containing two copies of a single-stranded, positively sensed RNA genome. After infecting target cells, the viral RNA is transcribed into DNA, which in turn has to be integrated into the host genome. Once integrated, the viral DNA is replicated using the cellular machinery and after viral protein production, assembly and maturation, a large number of virus particles are released, ready to infect more target cells (JANEWAY, 2001).

1.1.1. Discovery and Origin of HIV

More than 25 years ago the causative agent of the acquired immune deficiency syndrome (AIDS) was described by three independent research groups (BARRE-SINOUSSI et al., 1983; GALLO et al., 1984; LEVY et al., 1984) and called human immunodeficiency virus (HIV) by the International Committee on the Taxonomy of Viruses (COFFIN et al., 1986b; COFFIN et al., 1986a) shortly afterwards. In 1986, a "new human retrovirus from West African patients with AIDS" (CLAVEL et al., 1986) with 40-60% homologies to HIV-1 was isolated and named as HIV-2. Since their discovery, several epidemiological and genetic studies have shown that HIV-1 and HIV-2 consist of different groups. To date, four groups of HIV-1 are known: M (main/major), O (outlier), N (non-M/non-O/new) and P (PLANTIER et al., 2009). They differ in their genetic variation of the surface envelope glycoprotein gp160 as well as in their geographical distributions. Group M is the most common group causing the majority of infections and can be further subdivided into 11 clades or subtypes (A-H, J and K), with various prevalence in different regions. While clade B is mostly found in Europe and North America, clade C is mainly spread in India, China and sub-Saharan Africa (PERRIN et al., 2003 and figure 1). Additionally, there are circulating recombinant forms (CRFs) due to infections with different subtypes (THOMSON et al., 2002, JULG et al., 2005).

***Figure 1**: Worldwide distribution of the major HIV-1 subtypes and circulating forms (CRFs).*
According to PERRIN et al., 2003

1.1.2. Structure of the Viral Particle

To initiate a successful life cycle, certain molecules on the surface of HIV-1 particles are required. Transmission electron microscopy (TEM) pictures show a round particle (100-120 nm in diameter), spiked with a network of envelope molecules on the outside of the virion. Each spike is formed by a heterotrimer of the non-covalently linked envelope glycoprotein units gp120 (surface glycoprotein, SU) and gp41 (transmembrane glycoprotein, TM), both derived from the gp160 precursor. Each SU domain is heavily glycosylated and after binding of its functional sites (receptor and co-receptor binding sites) to the target cell, conformational changes within the envelope spikes lead to membrane fusion with the target cell.

After completing a full replication cycle, the newly built virion escapes by budding from the host plasma membrane. Therefore, the outer shell of the viral particle contains a phospholipid bilayer and several membrane proteins originated from the host cell. The viral membrane and the linked matrix proteins (MA) compose the outer core of the virus.

The inner core of the virus (virus capsid) appears in a cone-shape and consists of the capsid proteins (CA) and the two single-stranded RNA molecules stabilized by nucleocapsid proteins (NC). Additionally, the capsid contains viral enzymes (reverse transcriptase (RT), RNase H and integrase (IN), see figure 2), two copies of the tRNALys3 (initiator of reverse transcription) and the accessory proteins Nef (negative effector) and Vif (viral infectivity factor). The viral protease (PR), important for the maturation process of the virion, can be found between matrix and capsid (JANEWAY, 2001; PETERLIN et al., 2003; ROUX et al., 2007).

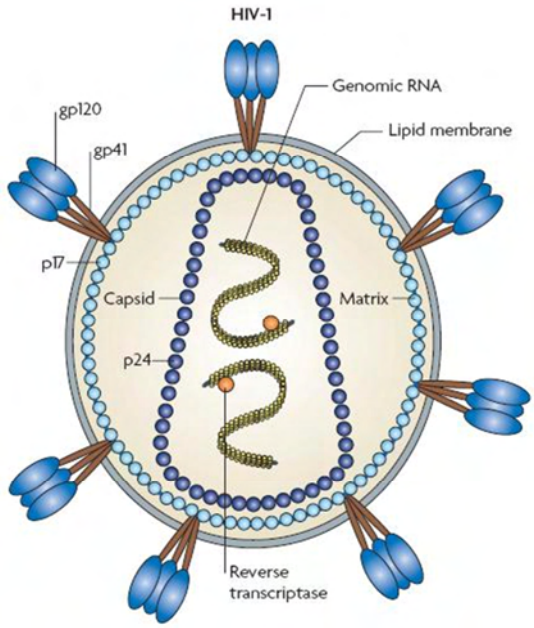

Figure 2: Structure of an HIV-1 particle.
Schematic illustration of the viral particle, showing the viral envelope molecules (made by gp120 and gp41), the matrix proteins (p17), the inner core (composed of capsid proteins, p24) and the two genomic RNA molecules, linked to the viral enzyme reverse transcriptase (from KARLSSON HEDESTAM et al., 2008)

1.1.3. Organization of the Viral Genome

The entire HIV genome is approximately 10 kb in length and contains open reading frames for 16 different proteins, synthesized from at least ten transcripts. On the 5' and the 3' end, the genome is flanked by long terminal repeat sequences (LTRs), required for reverse transcription of the viral RNA, viral integration into the host genome and control of viral gene expression.

The three major genes – *gag* (group-specific-antigen), *pol* (polymerase) and *env* (envelope) – can be found in the genome of all members of the retrovirus family. However, the HIV-1 genome encodes six additional proteins that are important for viral replication: genes encoding for regulatory proteins (transcriptional transactivator (*tat*) and the regulator of virion gene expression (*rev*)) and genes translated into the so-called accessory proteins: negative effector (*nef*), viral infectivity factor (*vif*) and the viral proteins r (*vpr*) and u (*vpu*) (see figure 3).

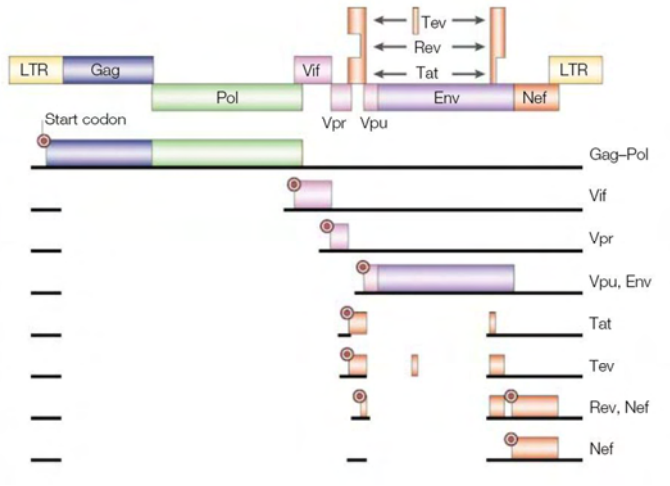

Figure 3**: **The HIV-1 genome and its transcripts.
Spliced and unspliced transcripts are denoted by black lines. Start codons of every transcript are indicated. Explanations see in 1.1.3 and 1.1.5 (figure from PETERLIN et al., 2003).

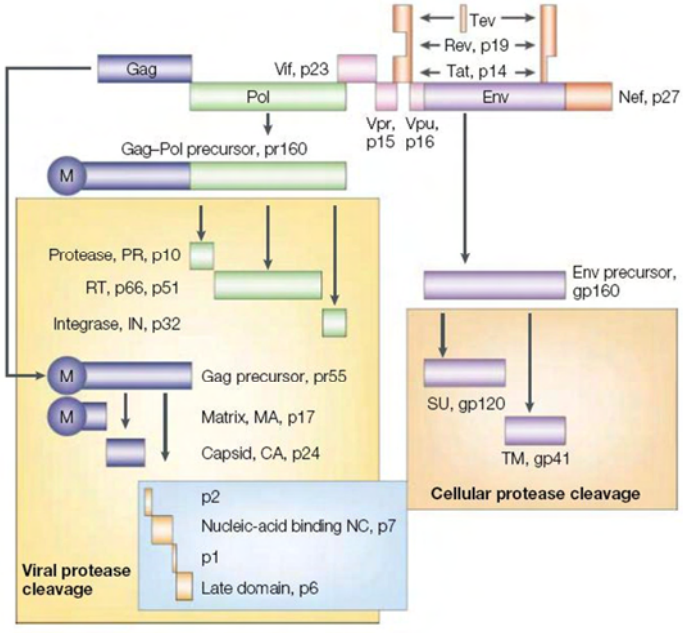

Figure 4**: **HIV-1 proteins.
Protein precursors and processed subunits are shown. Functions of proteins are summarized in 1.1.3 and table 1 (PETERLIN et al., 2003).

All HIV-1 gene products and their functions are summarized in table 1 and the organization within the HIV-1 genome is shown in figure 4. The Gag and Gag-Pol polyprotein precursor (pr160) leads to nine subunits after being processed by the viral protease. *Gag* encodes for the structural proteins of the internal matrix and is first translated into a precursor polyprotein p55, which is later cleaved by HIV proteases into smaller proteins. *Pol* encodes for several viral enzymes, important for viral replication and provirus integration into the host genome. *Env* codes for the Env polyprotein gp160, which is cleaved by cellular proteases into gp120 (SU) and gp41 (TM) (JANEWAY, 2001; PETERLIN et al., 2003). One primary transcript leads to more than 30 different messenger (m)RNAs which encode for all different viral proteins. Depending on the time point within an HIV-infection every transcript is translated differently (see also part 1.1.5).

Table 1: Overview HIV genes and products (according to PETERLIN et al., 2003)

Gene		Gene products and their functions	
gag	*Group-specific antigen* *Gag precursor pr55*	*Core and matrix proteins:* - *MA (matrix, p17)* - *CA (capsid, p24)* - *NC (nucleocapsid, p7)* - *p6, p2 and p1*	Virus assembly and secretion of viral particles
pol	*Polymerase* *Gag-Pol precursor pr160*	*Viral enzymes:* - *Reverse transcriptase (RT, p51; contains RNAse H, p66)* - *Protease (PR, p10)* - *Integrase (IN, p32)*	Viral replication and integration
env	*Envelope* *Env precursor gp160*	*Transmembrane glycoproteins:* - *SU (surface or gp120; binds receptor and co-receptor on target cell)* - *TM (transmembrane or gp41; is required for virus fusion and internalization)*	Surface molecules for interaction with target cell receptors
tat	Transactivator	Transcriptional regulator of the long terminal repeat (LTR)	
rev	Regulator of virion gene expression	Allows export of unspliced and partially spliced transcripts from nucleus	
vif	Viral infectivity factor	Affects particle infectivity	
vpr	Viral protein R	Transport of DNA to nucleus, augments virion production and responsible for cell cycle arrest	
vpu	Viral protein U	Promotes intracellular degradation of CD4 and enhances release of virus from cell membrane	
nef	Negative effector or negative factor	Augments viral replication in vivo and in vitro and downregulates CD4 and MHC class II	

1.1.4. Target Cells and Receptors

HIV can infect several different cells of the immune system, such as T helper cells, macrophages and dendritic cells. For a first interaction with the target cell, the gp120 portion of the virus glycoprotein complex gets in contact with the cell surface receptor CD4. However, to initiate a successful infection, gp120 must also bind to a second receptor in the membrane of the host cell (co-receptor) (see figure 5). The two most common co-receptors are the CC chemokine receptor CCR5 (mainly found on dendritic cells, macrophages and $CD4^+$ memory T cells) and the CXC chemokine receptor CXCR4 (expressed on naïve T-cells). Depending on which one is used, the particular virus strains are referred as R5

("Macrophage"- or M-tropic) and X4 (T-tropic) virus strains, respectively (BERGER et al., 1998). Certain virus strains can use both co-receptors and are therefore named X4R5 strains (dualtropic).

Shortly after the virus has infected its new host, R5 virus strains dominate while utilization of CXCR4 appears usually later in infection. This receptor restriction reflects the infections course of HIV: At the early stage of infection the virus needs CCR5, mainly to transit through dendritic cells and macrophages, while later on mostly $CD4^+$ T cells are infected.

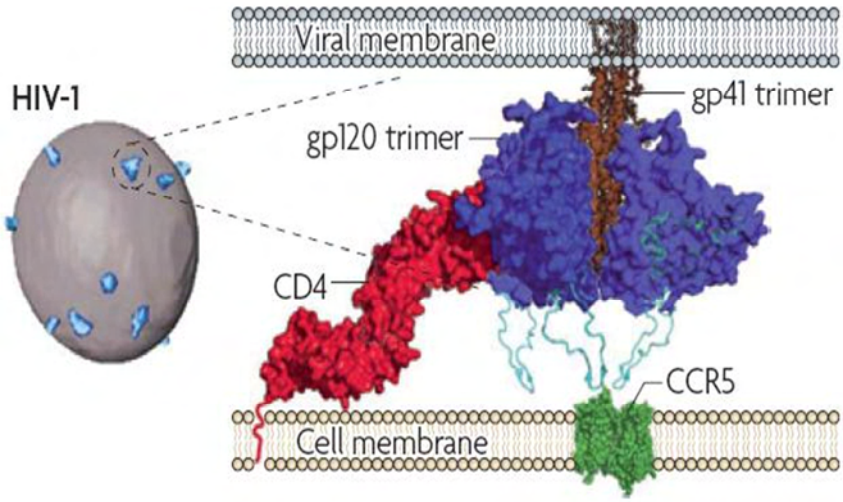

Figure 5**: **Interaction of a HIV-1 virion with the target cell membrane.
For a successful infection, the viral envelope molecules (g120 shown in blue, gp41 in brown) have to get in contact with two cell surface receptors (CD4 receptor shown in red, the CCR5 receptor in green) (KARLSSON HEDESTAM et al., 2008).

1.1.5. The Life Cycle of HIV

A common characteristic of all retroviruses is their life cycle, starting with the entry of the virus into the target cells and ending with the release of new viral particles. The ability to infect particular types of cell, also known as the cellular tropism of the virus, is given by the expression of the receptors on the surface of target cells. Binding of the trimeric envelope complex to the cellular surface receptor CD4 (see figure 5) leads to conformational changes, allowing attachment of the chemokine binding domains of gp120 to a chemokine receptor (either CCR5 or CXCR4). The structural rearrangements allow gp41 to enter the target cell membrane and will eventually end in the fusion of the cellular and viral membranes (MARKOVIC et al., 2004).

Once the virus entered the cell and was uncoated, the positively sensed RNA genome is reverse transcribed (with recombination events) into a negatively sensed complementary DNA (cDNA) using the retroviral enzyme reverse transcriptase (RT) (JANEWAY, 2001). This process of reverse transcription is known to be very error-prone, since the RT does not have any proof-reading function (DAS et al., 1995). Hence, during this step mutations are very likely to occur. Whilst reverse transcription, the mRNA flanking

long-terminal repeats (LTR) are formed playing an important role for viral integration and gene expression. The RT also contains a ribonuclease activity (RNase H) used to degrade the RNA template after the cDNA was synthesized. The double-stranded viral DNA intermediate (also produced by the RT, using the single stranded cDNA as a template) has to enter the nucleus for transcription. For that reason HIV is using a so-called pre-integration complex, containing integrase, matrix, viral protein r (Vpr) and viral DNA. Since the pre-integration complex proteins contain a large number of nuclear-localization signals, the viral DNA can enter the nucleus independently from cell division and nucleus membrane disintegration. With the help of the integrase (IN), the viral DNA can be integrated into the host chromosome (preferentially active genes). Once integrated, the virus is referred as provirus and like other retroviruses, HIV can establish a latent infection and remain quiescent for a long time.

For a successful production of infectious virus particles, from an integrated HIV provirus, not only the cellular RNA polymerase II (for transcription of (-) DNA into messenger (m) RNA) but also the cellular transcription factor NFκB (nuclear factor kappa-light-chain-enhancer of activated B cells) of the host is required. By binding to promoters in the viral 5' LTR region, it is initiating the transcription of viral RNA. The produced primary transcript is spliced in a time-dependent manner to produce more than 30 mRNA species for the viral proteins. The early proteins, Tat, Rev and Nef are fully spliced, while those encoding for the late, mostly structural and enzymatic viral proteins, are singly spliced or unspliced (PETERLIN et al., 2003). The switch between the early and late phases of gene expression is regulated by binding of the early protein Rev to the Rev response element (RRE) in the gene encoding *env*, which allows the transport of singly spliced and unspliced viral mRNA from the nucleus to the cytoplasm.

After the viral transcription and translation is completed, the final step of the life cycle, the assembly of HIV-1 virions starts. The processed glycoproteins gp120 and gp41 are transported to and anchored into the plasma membrane of the host cell. Maturation of the viral particle can occur either in the forming bud or in the immature virion after budding from the infected cell. During this maturation step, HIV proteases cleave several HIV proteins, and enzymes and structural components have to assemble to produce the fully matured HIV virion (GELDERBLOM, 1997).

1.2. HIV Infection and AIDS

The first cases of AIDS were reported in 1981 and according to the **Joint United Nations Programme on HIV and AIDS** (**UNAIDS)** since then, more than 25 million people have died because of AIDS or rather an AIDS-related opportunistic infection. In the year 2008, 33.4 million people worldwide were infected with HIV-1 and 2.0 millions died because of AIDS; making it still one of the most destructive epidemics (UNAIDS, 2009, www.unaids.org, AIDS Epidemic Update November 2009).

Although there are two known types of HIV – HIV-1 and HIV-2 – most AIDS worldwide is caused by the more virulent HIV-1. HIV infections in general are characterized by a high depletion of $CD4^+$ T cells accompanied by an increased susceptibility to infection with opportunistic pathogens (JANEWAY, 2001).

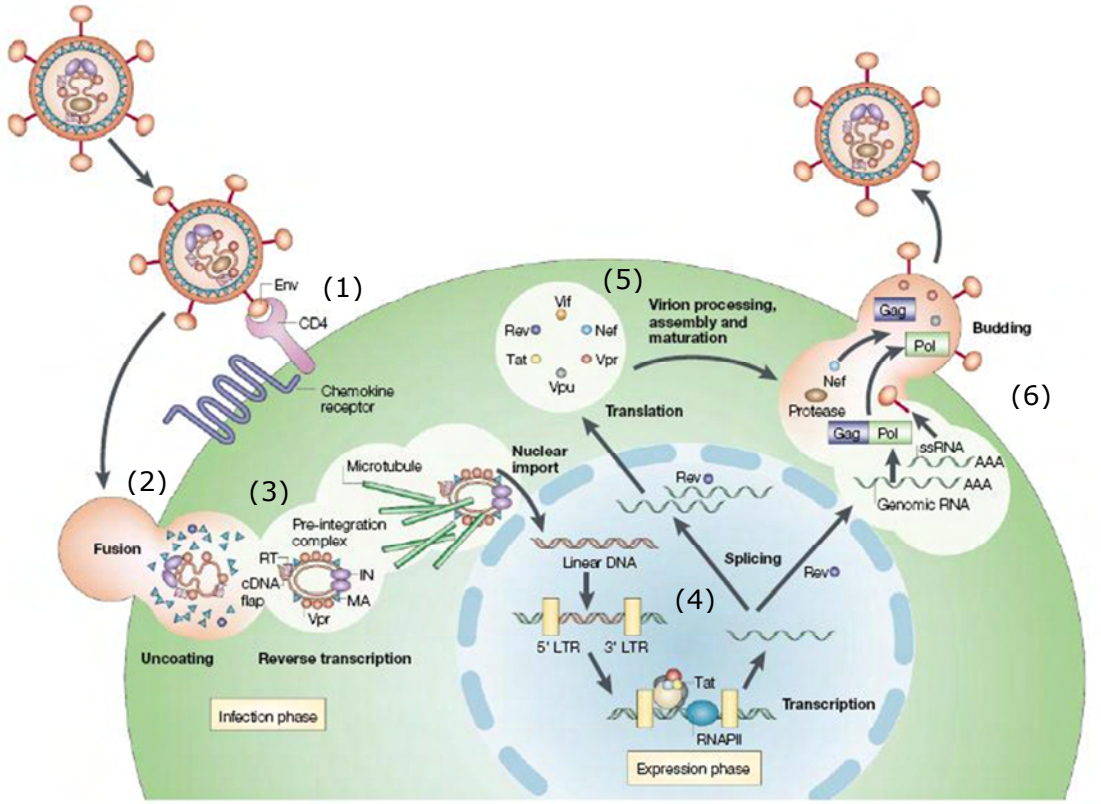

***Figure 6**: **The HIV-1 life cycle**.*
(1) Interaction of cell surface receptors with envelope spike on the virion surface. (2) Virion enters cell by fusion of viral and cellular membranes. (3) The viral capsid is uncoated, reverse transcription starts and the double-stranded viral DNA is transported into nucleus (using the pre-integration complex). (4) Viral DNA is integrated into host genome (now referred as provirus) and RNA transcripts are produced (by RNA polymerase II (RNAPII) and mediated by Tat). (5) Transcripts are transported into the cytoplasm where they are translated into viral proteins (singly and unspliced transcripts are transported by the viral Rev protein). (6) Assembly and maturation of virion. New viral particles are released from the infected cell by budding. Details explained in 1.1.5. (according to PETERLIN et al., 2003).

1.2.1. Infection and Routes of Transmission

To initiate an infection, HIV has to be transferred via body fluids from an infected individual to an uninfected one. Most of the time, HIV is transmitted via sexual exposure using genital tract or rectal mucosa as a primary site of transmission. Other ways are: by transfusion with contaminated blood or blood products, by intravenous drug abuse when contaminated needles are shared or through mother-to-child transmission due to exposure of the infant to contaminated maternal fluids (transit through birth canal, maternal milk). The success rate of virus transmission is dependent on its biologic properties, its concentration in the exposed body fluid and also the nature of the host susceptibility (LACKNER et al., 2007, LEVY, 2009). While the possible routes of transmission are well known, it is still not fully described which mechanism the virus can use to cross the mucosal epithelium and if the virus is transmitted as a free or a cell-bound virus. (MCMICHAEL et al., 2010).

1.2.2. The Biology of an HIV-1 Infection and Progression to AIDS

In general the course of HIV infection can be divided into three stages: the acute stage (primary infection), the clinical latency (chronic or asymptomatic stage) and the clinical manifest stage (AIDS) (see figure 7).

Approximately 10 days after a virus particle was transmitted successfully, the viral RNA can be detected in the plasma of the infected individual (acute or primary infection). The period until detection is known as eclipse phase. After those 10 days, the lymph nodes get infiltrated and new target cells, which are circulating $CD4^+CCR5^+$ memory T cells, can be infected. Now the virus can replicate quickly and spread out to other lymphoid tissues (e.g. gut associated lymphoid tissue (GALT)) to find more memory T cells. A few weeks after infection, (around 3-4 weeks) the intense viral activity can be observed by: the increase in viral RNA copies in the blood, the increase of the $CD8^+$ T-cell population and the presence of serum antibodies against viral proteins (seroconversion). At the time of the peak viremia the amount of $CD4^+$ T cells is low but returns to near normal levels in the blood later. After the active phase of infection (usually 12-20 weeks), the viral load reaches a stable level (viral set point) and the level of $CD8^+$ cells decreases significantly. The infection seems to be controlled caused by the extensive activation of the immune system (asymptomatic period or clinical latency).

During the course of infection, viral escape mutants are selected under the pressure of starting adaptive immune responses (increasing viral diversity, see figure 7) (MCMICHAEL, A.J. et al., 2010; SIMON et al., 2003). Due to mutations in the third variable loop (V3) of g120, a co-receptor switch to CXCR4 can occur, which broadens the virus tropism to naïve T cells. As a result, the $CD4^+$ T cell counts decreases significantly, making the host susceptible to opportunistic infections. The acquired immunodeficiency syndrome is by definition reached at a $CD4^+$ T cell amount below 200 cells/µl in the blood.

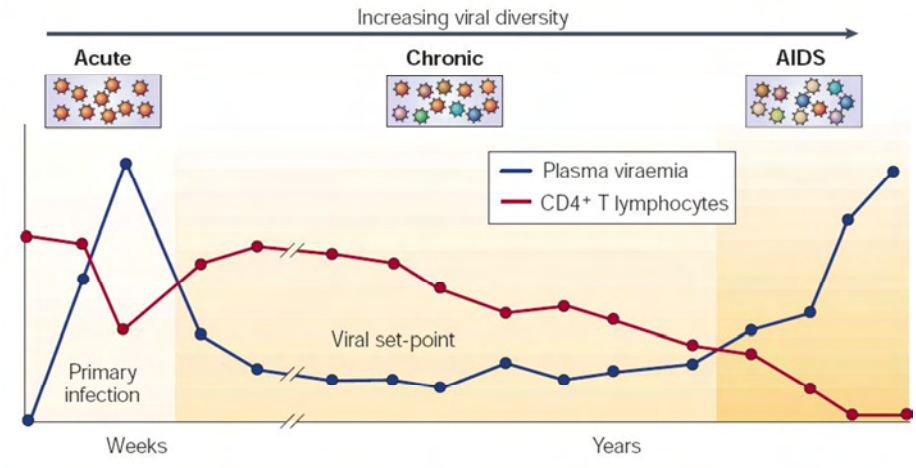

Figure 7: The natural course of an HIV-1 infection.
The figure shows the typical relationship between plasma virus load (blue line) and $CD4^+$ T cell count (red line) over time in an untreated HIV infection. AIDS is defined by the occurrence of opportunistic infections or HIV-1-associated malignancies and a number of CD4+ T lymphocytes below 200 cells/µl. Viral diversity increases over the course of infection due to the continuously high level of viral replication and the error-prone nature of HIV-1 reverse transcription (from SIMON et al., 2003).

The duration of the asymptomatic phase varies among infected people (rapid, slow or long-term non-progressor), with a median of 10 years. However, most of the people infected with HIV will eventually develop AIDS. Only a small percentage of people make antibodies against HIV proteins but do not have any symptoms of progression to AIDS for more than 10 years. Those patients are referred to as long-term non-progressors (LTNPs). Several reasons for the prolonged time of incubation are possible: (1) lower viral set point (PANTALEO et al., 1995), (2) higher diversity in *env* region (MIKHAIL et al., 2003), (3) changes in the variable loop regions of g120 leading to an inhibited co-receptor switch, (4) secreting natural ligands of the CCR5 receptor to an higher extend (MIKHAIL et al., 2003), (5) different HLA (human leukocyte antigen) type expression affecting the quality of the peptide presentation (KASLOW et al., 1996) and (6) mutations, such as the homozygous CCR5Δ32bp deletion leading to non-functional co-receptor proteins (AGRAWAL et al., 2004).

1.2.3. Host Immune Responses to HIV

HIV-1 can activate the innate, as well as the adaptive part of the host immune system both using humoral and cellular components to combat HIV. One of the first reactions to an HIV infection, are increased levels of acute-phase proteins (already detectable in the eclipse phase) and cytokines. As a cellular innate response, natural killer (NK) cells start to lyse infected cells. In the acute phase of an HIV-1 infection also some first antibody-antigen complexes, provided by non-neutralizing IgM molecules, are present (see figure 8).

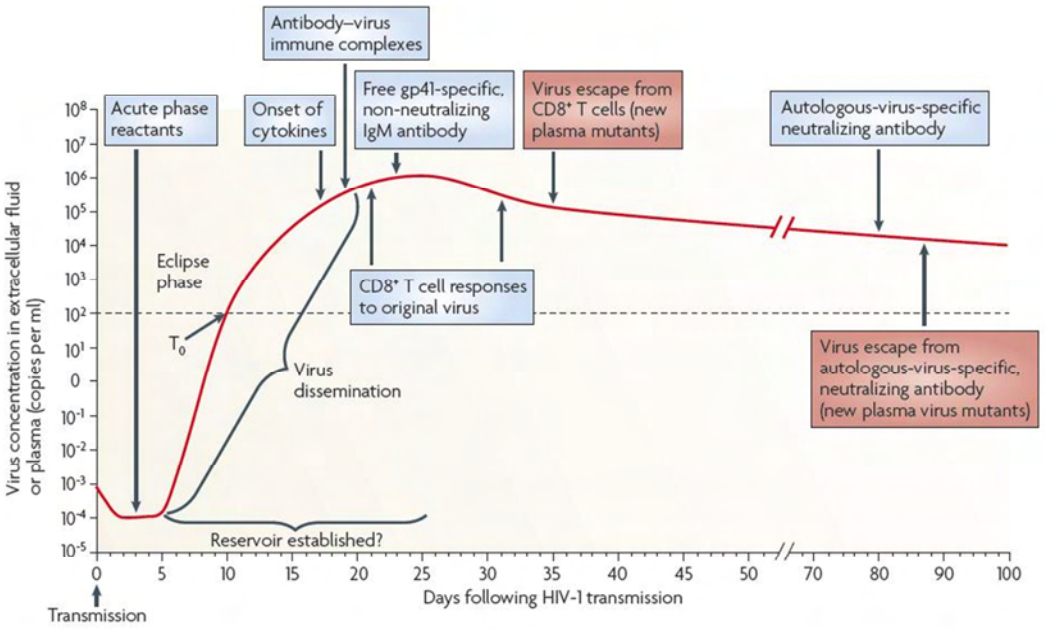

Figure 8: Immune responses to an HIV-1 infection.

The first immune responses to HIV-1 infection can be observed in an increase of acute-phase proteins in the plasma. At the point of virus detection in the plasma (T_0) also increased plasma cytokine levels can be measured. As plasma viremia is increasing, the first antibody–virus immune complexes are detected, followed by HIV-1-specific CD8+ T cell responses and first free gp41-specific, but non-neutralizing IgM antibodies. By the time new plasma mutants develop, complete virus escape from the first CD8+ T cell responses can occur rapidly. Around day 80 after infection the first autologous virus-neutralizing antibodies can be detected and with the following week also antibody escape virus mutants are emerging (according to MCMICHAEL et al., 2010).

Regarding to the adaptive immune system, within weeks after infection, $CD8^+$ T cell (cytotoxic T lymphocytes, CTL) responses are detectable. They get primed for viral peptides, presented on MHC class I molecules and lyse infected cells. $CD4^+$ T cells (T helper cells) on the other hand can recognize viral peptides presented on antigen presenting cells (e.g. dendritic cells) expressing the MHC class II molecule on their cell surface. After being activated they start to produce and secret cytokines: While T_H1 (T helper cells type 1) mainly activate NK cells and macrophages by secreting IL-2 and interferon gamma (IFN-γ), are T_H2 (T helper cells type 2) producing IL-4, IL-5, IL-6 and IL-10 and therefore activating the differentiation of B cells and antibody production in plasma cells (humoral immune response). Most of the produced antibodies are directed against the envelope proteins gp120 and gp41, as well as the capsid protein p24. Antibodies recognizing viral particles can have different protective functions (see figure 9): One of the most important mechanisms is the ability of antibodies to reduce the infectivity of a virus particle, also known as virus neutralization (see also 1.4). Neutralization can occur at several steps in the virus life cycle (see figure 9). First of all, neutralizing antibodies can bind to molecules on the surface of viral particles and thus interfering with their interaction with cellular surface receptors. Additionally, they can also block the fusion of virus and target cell membranes, one of the so-called post-attachment mechanisms. After the virus has entered the cell, antibodies can prevent the virus from uncoating, interrupt the virus assembly and maturation and inhibit the virus from budding out of the cell. Besides those neutralizing activities, antibodies play also an important role in complement induced virolysis, and opsinization and phagocytosis of the viral particles. Furthermore, they can attack virus infected cells using the antibody-dependent cellular cytotoxicity (ADCC) mechanism, primarily mediated through NK cells.

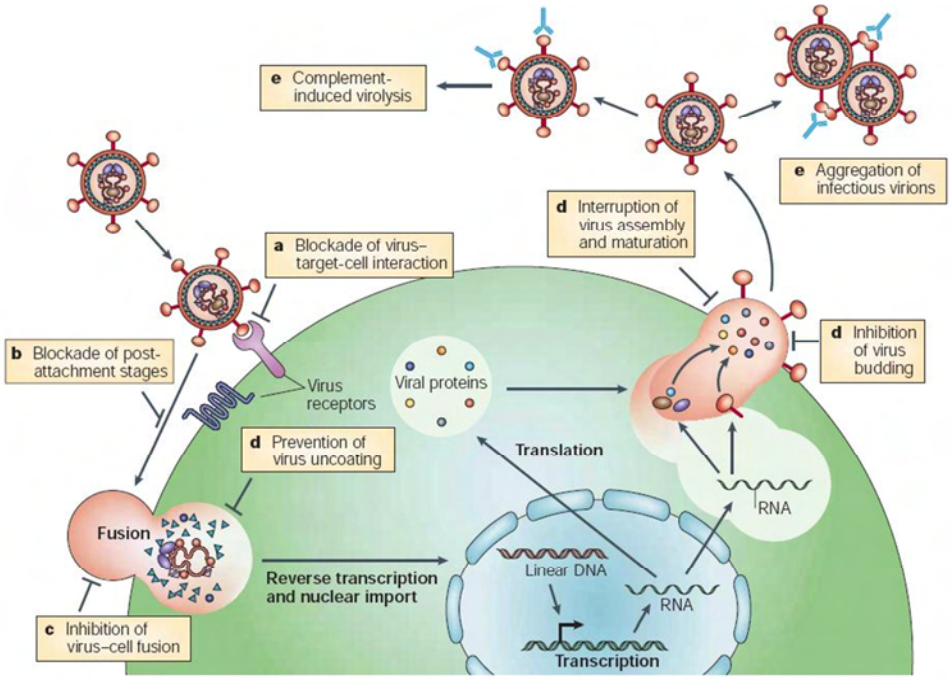

Figure 9: Protective mechanisms against HIV-1 infections mediated by antibodies.
Antibodies can block virus-target cell interactions (a) and prevent fusion of virus and cell membranes (post attachment mechanisms, b-c). Additionally they can block virus-cell fusion (c) or they might be involved in later stages of the life cycle (d-e): preventing uncoating, interrupting virus assembly, preventing maturation and virus budding. Furthermore, antibodies can opsonize and lyse viral particles by inducing complement cascades and ADCC (see text in 1.2.3). (from ZOLLA-PAZNER, 2004).

1.3. Structural Organization of the HIV Envelope Glycoprotein

As mentioned before, the HIV envelope spike (gp160 complex) is organized as a trimeric molecule, containing non-covalently associated gp120 and gp41 molecules. It mediates viral tropism and entry, and is considered as a promising target for neutralizing antibodies to prevent infection of target cells.

1.3.1. Structural Organization of gp120

Looking at the gp120 monomer, it can be divided into five conserved (C1-C5) and five variable (V1-V5) segments. Latter ones can change structure and conformation, allowing the virus to escape the immune response (escape mutants) (KWONG et al., 1998; PANTOPHLET et al., 2006; WYATT et al., 1998; ZOLLA-PAZNER, 2004).

The gp120 core is heart-shaped and can be organized into three areas: the inner domain, the outer domain and the bridging sheet (see figure 10). The inner domain consists mainly of C1 and C5 regions, is free of glycans and generates the major contact interface with gp41. The bridging sheet of the gp120 molecule, which accommodates highly conserved regions, is responsible for receptor (CD4) and co-receptor (CCR5 or CXCR4) binding and provides the link between inner and outer domain (KWONG et al., 1998). The outer domain (outer surface of the envelope) is largely covered by glycans, which is thought to lower the immunogenicity of the viral particles (PANTOPHLET et al., 2006).

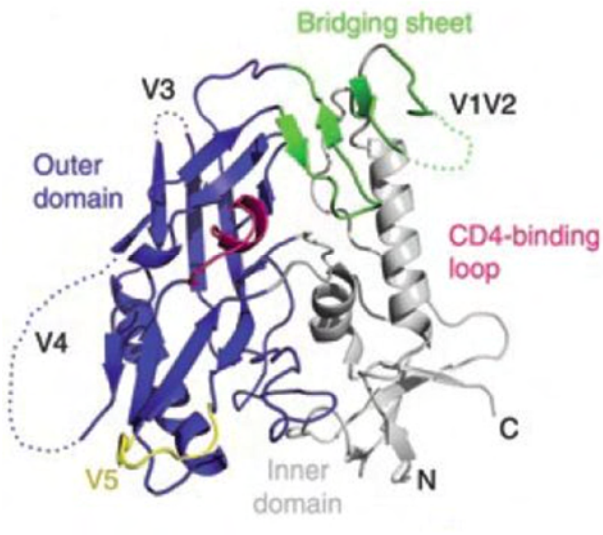

Figure 10: Ribbon representation of a clade C core gp120 structure (CAP210).
The three main domains are shown (outer domain in blue, bridging sheet in green and inner domain in gray). All five variable loops and the CD4-binding loop (pink) are indicated. From DISKIN et al., 2010.

For a first interaction of gp120 and the target cell, certain residues of the CD4 receptor (mostly Phe^{43} and Arg^{59}) get in contact with a “cavity”, formed at the interface of the outer domain, the inner domain and the bridging sheet (*Phe43 cavity*, KWONG et al., 1998). Upon CD4-binding, conformational changes in the gp120 protein occur (V1/V2 and V3 shifts) and lead to the exposure of the highly conserved co-receptor binding site. Important residues for interaction with CCR5 have been mapped to bridging sheet and near the V3 stem (PANTOPHLET et al., 2006). Since the co-receptor binding site is not present until CD4 has bound, antibodies against that area have only a weakly neutralizing activity in vitro (without soluble CD4).

1.3.2. Structural Organization of gp41

The transmembrane part of the Env protein, gp41 attaches the spike to the viral membrane and plays an important role in the fusion process of viral and target cell membranes. The protein is more conserved than gp120 and can be divided into three major domains: the extracellular region (ectodomain), the transmembrane domain (TM) and the cytoplasmic tail (CT) (see figure 11). The ectodomain is mainly involved in the membrane fusion and contains: a N-terminal hydrophobic region (acts as fusion peptide (FP), a polar region PR; two α-helix repeat regions (N-terminal heptad repeat (NHR) and C-terminal heptad repeat (CHR)); a disulfide-bridged hydrophilic loop connecting the two heptad repeats (containing the immunodominant "KLIC" motif, ZOLLA-PAZNER, 2004) and a Trp-rich region (membrane-proximal external region (MPER)) (MONTERO et al., 2008).

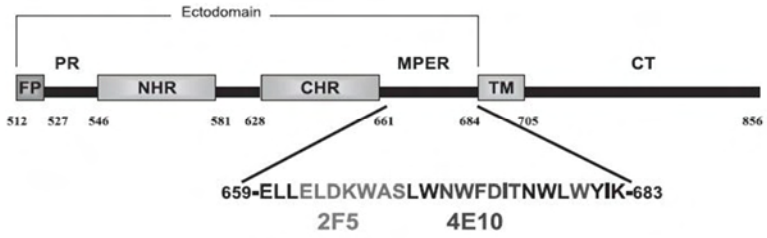

Figure 11: Schematic illustration of gp41 domains.
Organization of all gp41 regions and the epitopes of two human monoclonal antibodies, 2F5 and 4E10 are shown (see also table 2 and figure 12). Explanation see text. From MONTERO et al., 2008.

1.4. Broadly Neutralizing Antibodies and Vaccine Approaches

As mentioned in 1.2.3, antibodies play a very important role in protecting the host against virus infection and one of the most protective steps against HIV is mediated by neutralizing antibodies (nAb) (ZOLLA-PAZNER, 2004). In several passive immunization studies, nAb have shown to be protective in animal models (BABA et al., 2000; FERRANTELLI et al., 2004; FERRANTELLI et al., 2007; MC CANN et al., 2005; PARREN et al., 2001; RUPRECHT et al., 2003). However, the generation of viral nAbs has turned out to be a challenging task (BURTON, D.R. et al., 2004; HOXIE, 2009; MASCOLA et al., 2009; BURTON et al., 2004; STAMATATOS et al., 2009) and only a few broadly reactive human monoclonal antibodies (mAb) have been developed so far (the four most characterized ones are illustrated in figure 12 and their characteristics are summarized in table 2). However, three out of those four antibodies have been linked to autoreactivity (HAYNES et al., 2005).

Some problematic issues in the antibody based vaccine development are: (1) the presence of virus escape mutants due to the fast mutation rate, (2) the shielding of nAb epitopes by variable loops and glycans and (3) the immunodominance of non-neutralizing epitopes (formed by non-functional envelope proteins) often overlapping with epitopes for broadly nAbs.

Table 2: Four of the best characterized human monoclonal antibodies with broadly neutralizing activity.

Human monoclonal antibody	Recognized epitope	Characteristics		Reference
2G12	Oligomannose residues on gp120	Poorly immunogenic	Prevents virus entry	TRKOLA et al., 1996; SCANLAN et al., 2002; TRKOLA et al., 1996
IgG1 b12	CD4-binding domain of gp120	Highly immunogenic; first broadly neutralizing mAb identified	Prevents CD4 attachment	BARBAS et al., 1992; BURTON et al., 1994
2F5	Transmembrane-proximal region of gp41 ectodomain	Poorly immunogenic, but broadly neutralizing	Inhibits fusion process	TRKOLA et al., 1995; PARKER et al., 2001
4E10	Transmembrane-proximal region of gp41 ectodomain	Poorly immunogenic, but broadly neutralizing	Inhibits fusion process	ZWICK et al., 2001

To date, researchers in the field of HIV vaccine development follow two main strategies. As mentioned above, one of them concentrates on developing vaccines that elicit neutralizing antibodies. Another way to fight against lentiviral infections is focusing on the generation of virus specific $CD8^+$ T cells (cytotoxic T cells, CTL). Such a vaccine-induced cellular immune response cannot prevent the HIV infection itself. However, infected cells are killed before new viral particles are released which would help to control the HIV infection. The $CD8^+$ T cell vaccines include plasmid DNA encoding HIV genes, recombinant modified vaccinia virus Ankara (MVA), recombinant adenovirus-5 and recombinant vesicular stomatitis virus (AMARA et al., 2001; JOHNSTON et al., 2007; MCMICHAEL, 2006; ROSE et al., 2001; SHIVER et al., 2002).

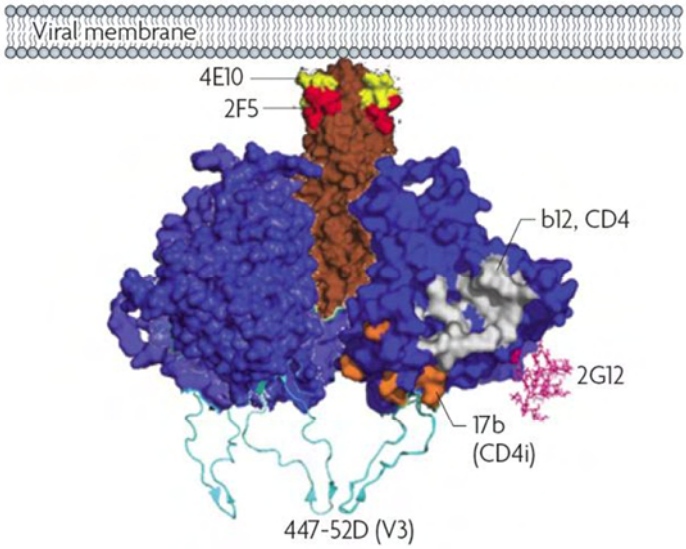

Figure 12: Model of the HIV-1 envelope spike showing epitopes of broadly neutralizing monoclonal antibodies.
The HIV-1 envelope trimer, with gp41 (brown) and gp120 (blue), is shown. The epitopes for the two broadly neutralizing gp41 antibodies 4E10 (yellow) and 2F5 (red) are illustrated. The two broadly neutralizing gp120 antibodies 2G12 (recognizing a carbohydrate cluster (pink)) and b12 recognizing an epitope overlapping with the CD4-binding site on gp120 (gray) are indicated as well. Additionally, the epitope of a CD4 induced antibody 17b (orange) and a V3-loop directed antibody 447-52D (light blue) are shown (from KARLSSON HEDESTAM et al., 2008).

1.5. The SHIV/Macaque Model in AIDS Research

Simian immunodeficiency virus (SIV) is a, to HIV-1 and HIV-2, closely related group of viruses, which is found naturally in African primate species. According to phylogenetic analyses, some SIV lineages have co-evolved with their hosts, while others have shown a cross-species transmission from simians to humans and became pathogenic for the new host. The direct ancestry of HIV-1 originated from a SIV strain (SIVcpz), found in chimpanzees (*Pan troglodytes troglodytes*) and was transferred to the human population via cross-species transmission during the 20th century (HOLMES, 2001; HUET et al., 1990). HIV-2 on the other hand, might have evolved from another SIV strain (SIVsmm), which can be found in sooty mangabeys (*Cercocebus atys*) (HIRSCH et al., 1989).

Up to now, three main SIV strains have been isolated and designated after their species of origin: SIVmac (rhesus macaque, *Macaca mulatta*), SIVsmm (sooty mangabey, *Cercocebus atys*) and SIVmne (pig-tailed macaque, *Macaca nemestrina*) and all of them share the common ancestor SIVsmm, which generally causes no pathogenesis in its natural hosts. After experimental inoculation of SIV strains into several Asian macaque species, like rhesus, pig-tailed or cynomolgus monkeys an AIDS-like pathogenesis was observed and indeed, SIV infection of macaques had become the animal model of choice for HIV and AIDS research (HU, 2005).

1.5.1. The Use of SHIV Strains in HIV research

The general idea of a simian human immunodeficiency virus (SHIV) construct, is to combine HIV-1 genes (vpu, tat, rev, and env) with a SIVmac239 backbone in a chimeric virus (HU, 2005). Several advantages of SHIV strains over SIV led to a widespread application in the current HIV research (summarized in KRAMER et al., 2007). The most obvious advantage is based on the fact, that SHIV strains encode HIV-1 *env* and therefore allows direct testing of HIV-1 *env* based vaccines and isolating of novel anti-HIV-1 neutralizing antibodies from infected animals. Furthermore a “heterologous virus challenge” approach in vaccine studies can be used to reflect the viral complexity in real life (VLASAK et al., 2006). A third, very important benefit of constructing SHIV strains is the possibility to study HIV-1 *env* evolution in infected primates to find out if it follows a similar way as it was observed in infected humans (HOFMANN-LEHMANN et al., 2002).

Since the introduction of SHIV models into the AIDS vaccine development, three generations of SHIV constructs have been developed. The first generation encodes *env* genes of laboratory-adapted HIV-1 strains, and pathogenicity was observed only after serial passages of the parental SHIV constructs in macaques. Indeed, the next generation (such as SHIV89.6P) encodes *env* genes of HIV-1 isolates from patients progressed to AIDS. However, those constructs seem to act dualtropic in vitro, while they are exclusively X4 in vivo. The third, and most recent generation of SHIV constructs (also SHIV-1157ipd3N4, see 1.5.2) encodes *env* genes of primary R5 HIV-1 isolates (available SHIV strains are summarized in KRAMER et al., 2007).

1.5.2. SHIV-1157ipd3N4, a CCR5-tropic Clade C Strain

Most of the so far developed SHIV strains utilize envelope genes, derived from HIV-1 clade B strains. Since clade B strains represent around 10% of worldwide infections, the available SHIV strains do not reflect the genetic diversity of the HIV-1 epidemic. The much more dominant subtype of HIV-1 is clade C, which comprise more than 50% of all infections. Moreover, HIV mostly uses the mucosal transmission route to spread from an infected individual to an uninfected one. Again, none of the so far available SHIV strains had been reported to be mucosally transmissible. Finally, an exclusive R5 tropism represents a more biologically relevant co-receptor usage than dual tropic SHIV strains, such as SHIV89.6, which has been widely used as challenge virus (KRAMER et al., 2007).

Those facts taken together led to the construction of a highly replication competent, mucosally transmissible R5 Clade C SHIV strain (SONG et al., 2006) (see table 3). It expresses *env* of a relatively recently transmitted HIV isolate (HIV1157i) from a 6-month-old Zambian infant born to an HIV-1 positive mother. An infant rhesus macaque (RPn-8) was inoculated intravenously with the original molecular clone (SHIV-1157i), which was passaged through other rhesus monkeys (leading to SHIV-1157ip). Afterwards, the late-stage virus (SHIV-1157ipd) was isolated and characterized. To increase the virulence, SHIV-1157ipd3N4 was constructed by introducing an additional NF-κB binding site (see 1.1.5). Song and co-workers were able to transmit SHIV-1157ipd3N4 intrarectally to rhesus monkeys of both Indian and Chinese origin. Additionally, this clade C SHIV strain can also be used to infect pig-tailed macaques, shown in a recent study (HO et al., 2009).

1.5.3. Macaca nemestrina vs. *Macaca mulatta*

The degree of viral infectivity and disease susceptibility is often dependent on the species of macaques used in a study. In general, three subspecies of Asian macaques are popular for the research of AIDS pathogenesis: *Macaca mulatta* (rhesus macaques), *Macaca fascicularis* (cynomolgus macaques) and *Macaca nemestrina* (pig-tailed macaques). While many studies provided a detailed insight into the biology of viral infection and pathogenesis in rhesus macaques, not much is known about the outcome of primate lentiviral infections in other macaque species, such as pig-tailed macaques (HO et al., 2009).

In 1992, Agy and co-workers inoculated eight pig-tailed macaques with either cell-associated or cell-free suspensions of HIV-1. They described a successful infection of the Peripheral Blood Mononuclear Cells (PBMCs) and sustained seroconversion to a broad spectrum of HIV-1 proteins. Thus, they concluded *Macaca nemestrina* as an “animal model for HIV-1 infections for evaluating the pathogenesis of acute HIV-1 replication and candidate vaccines and therapies” (AGY et al., 1992).

Considering pig-tailed macaques as an animal model for HIV-1 infections, there are some key points to keep in mind (HO et al., 2009). First, although all three of the mentioned macaque subspecies share the same ancestor, *Macaca fascicularis* and *Macaca mulatta* are more closely related to each other than to *Macaca nemestrina*. Keeping that in mind, genetic implications affecting components of the adaptive

immune response (T-cell receptor diversity and MHC molecules) should be considered when evaluating the pathogenesis of lentiviral infections. Second, pig-tailed macaques do not produce the restriction factor TRIM5α, used by rhesus macaques to inhibit lentiviral replication (STREMLAU et al., 2004). Therefore, they might be more susceptible for HIV-1 infections than other subspecies. Third, some studies showed that pig-tailed macaques are also more susceptible for lentivirus-induced disease. Since the response to HIV-1 infections in humans can be highly diverse, pig-tailed macaques could be considered as a useful animal model to evaluate different disease outcomes in different subspecies.

Table 3: Nomenclature of clade C SHIV strains

Name of strain	Explanation	Reference
SHIV-1157i	original molecular clone, not yet adapted to rhesus monkeys SIV backbone + *env* of HIV-1 clade C from a Zambian infant **i = infant**	SONG et al., 2006
SHIV-1157ip	early biological isolate after passage through five rhesus monkeys **p = passaged** (monkey-adapted)	
SHIV-1157ipd	late biological isolate **d = disease** (isolated from an infected animal with disease - AIDS)	
SHIV-1157ipd3	late-stage infectious molecular clone #**3**	
SHIV-1157ipd3N4	extra NF-κB binding site added (two rather than one)	

1.6. Epitope Identification and the Phage Display Approach

1.6.1. Epitope Mapping in General

A specific interaction of antigens and their corresponding antibodies requires certain related regions, referred as epitopes (located on the antigen) and paratopes (found on the antibody), respectively. Identifying the sequence and structure of such an epitope, accordingly termed as epitope mapping, can be helpful to study protein-protein interactions, to determine protecting (neutralizing) sites and eventually for the production of epitope-based vaccines (GERSHONI et al., 2007; WANG et al., 2004).

Depending on the location of the amino acid residues within the peptide, epitopes can be divided into two groups: the discontinuous (conformational) and continuous (linear) ones. Conformational epitopes are characterized by having the amino acid residues, responsible for the interaction with the paratope, spread all over the primary sequence. However, a protein folding can bring them together to build a certain

contact area. Linear epitopes, on the other hand have contacting amino acid residues in close proximity already in their primary sequence (WANG et al., 2004).

Some popular epitope mapping techniques are: (1) using an array of overlapping synthetic peptides (pepscan), (2) co-crystillization of the antigen:antibody complex and nuclear magnetic resonance (NMR), (3) computational docking, (4) binding analysis (ELISA, dot blot, Western Blot assays) and (5) the directed mutagenesis approach (summarized in GERSHONI et al., 2007). All these methods try to determine an exact structure or sequence of the antigen in question. A very different approach is testing the binding capacity of random peptides representing a huge diversity of possible combinations of amino acid residues. In 1986, Geysen and co-workers showed peptides having not exactly the same sequence as the native epitope of an antigen, but are capable of interacting with the paratope in a similar way as the native one. These peptides are referred as mimotopes because they "mimic" those specific antigenic determinants (GEYSEN et al., 1986). One widely used methodology to screen for such mimotopes is the phage display technology.

1.6.2. Epitope Identification Using the Peptide Phage Display Technology

This pretty simple and rapid selection technique was first described by George Smith in the year 1985 and is based on a modified bacteriophage (simply called phage), which expresses a library of peptide or protein variants on its surface (SMITH, 1985). Some key features of the phage display method had led to a widespread usage in many different research areas, including epitope mapping of antibodies, identification of receptor agonists and antagonists, finding enzyme substrates and inhibitors, analysis of protein-protein interactions and last but not least, vaccine design (examples discussed in BRATKOVIC, 2010, IRVING et al., 2001, KRUMPE et al., 2007, SZARDENINGS, 2003, WANG et al., 2004). General facts about phage display are described in BARBAS et al., 2001. One of the advantages of this methodology is due to the ability to provide a physical link between phenotype (exposed protein on the surface of the phage virion) and genotype (phage genome encodes sequence of each protein variant to be displayed), achieved by cloning a foreign gene into a gene encoding a capsid structural protein (KONTHUR, Z. et al., 2002). Another reason for the popular usage of the phage display technology is probably the complexity of peptides being displayed. Using random sequences, a large library containing a high amount of different peptide sequences can be obtained (10^8 to 10^{11} individual variants) (KRUMPE et al., 2007).

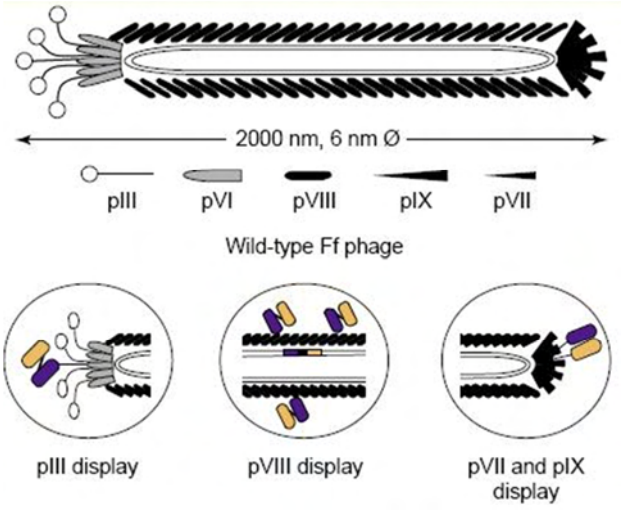

Figure 13: Structure of a wildtype filamentous bacteriophage (Ff phage) and the three main surface display variants.
The most common approach for peptide display is to fuse the foreign sequences to the amino terminus of pIII or pVIII. (KONTHUR et al., 2002)

The most common phages are the filamentous ones (see figure 13), including M13 strains (KEHOE et al., 2005; SIDHU, 2001). They wild type M13 phage is about 900-2000 nm long and only 6 nm in diameter. The virion contains a circular single stranded DNA (ssDNA) genome which is coated with 2700 copies of the major coat protein pVIII. The genome is quite flexible and therefore large inserts of foreign sequences can be introduced without affecting its replication cycle and packaging process immoderately (SZARDENINGS, 2003, BOTTGER et al., 2009, KEHOE et al., 2005, WANG et al., 2004). To initiate the bacterial infection, the phage capsid protein pIII has to attach to the sexual pilus (F-pilus) of its host Escherichia coli (E. coli). The positive, single stranded phage genome is injected into the target cell and a complementary, negative strand is synthesized using the bacterial polymerase. After forming the double stranded phage genome (also known as replication form, RF), the host protein synthesis machinery is used and all of the eleven phage-encoded proteins are produced (KEHOE et al., 2005). Some of these proteins are involved in the replication process (pII, pV and pX) and some are required for assembly and export (pI, pIV and pXI). However, most of them are structural proteins (coat proteins pIII, pVI, pVII, pVIII and pIX), being inserted into the inner bacterial cell membrane upon synthesis. While five copies, each of pIII and pVI are incorporated at one end and of pVIII and pIX at the opposite end of the virion, pVIII is surrounding the phage genome (figure 13). Of note, and important for the phage display technology, M13 is a non-lytic bacteriophage. Infected cells still grow and divide, although at half the rate of uninfected bacteria (KEHOE et al., 2005).

The screening process of a phage-displayed peptide library is usually performed using an affinity selection, also called biopanning. The whole procedure is summarized in figure 14. Target molecules (e.g. monoclonal antibodies, polyclonal sera, enzymes, enzyme substrates or receptor domains) are immobilized on solid surfaces (e.g. paramagnetic beads or ELISA plate well) and incubated with the peptide library. Peptides to be displayed are often fused to the amino terminus of the phage capsid protein pIII on the “head” of the virion (see figure 13). Unbound phages (displayed peptides were not specific for target molecules) are washed away, while specific binding phages are eluted (e.g. using a pH shift) and amplified using E. coli strains. By performing several rounds of selection, positive clones are enriched and can be identified using an enzyme-linked immunosorbent assay (ELISA). By sequencing the genome of specifically bound phages, the displayed peptides can be deduced and common motifs detected.

1.6.3. Phage Display to Identify Promising HIV-1 Vaccine Candidates

As mentioned above, the phage display technology has been used in several research areas to develop novel therapeutics or diagnostic reagents. Successful examples have targeted different kind of cancers, viral, bacterial or parasitic infections, autoimmune disorders, thrombosis or inflammation (examples are summarized in BRATKOVIC, 2010, IRVING et al., 2001, KRUMPE et al., 2007, SZARDENINGS, 2003, WANG et al., 2004). In the field of HIV research, the phage display technique is, amongst others, used for: (1) B-cell epitope mapping (ENSHELL-SEIJFFERS et al., 2003); (2) isolation and characterization of human antibodies or Fab-fragments by screening human antibody libraries; (KOEFOED et al., 2005; MOULARD et al., 2002); (3) epitope mapping of well known neutralizing monoclonal antibodies against

HIV-1 (XIANG et al., 2003) and (4) reverse vaccinology approaches for the identification of novel epitopes (HUMBERT et al., 2006). Several studies have shown that peptides, based on certain areas of the HIV-1 envelope protein are able to induce a high immune response in mice and rabbits (HEWER et al., 2003; MCGAUGHEY et al., 2003). Furthermore, the immunization of mice or monkeys with mimotopes isolated by screening peptide libraries, exposed promising immunogens, eliciting cross-clade neutralizing antibodies (DI MARZO VERONESE et al., 1994; HUMBERT et al., 2008a) and even led to protection against SHIV-89.6PD challenges in rhesus macaques (CHEN et al., 2001).

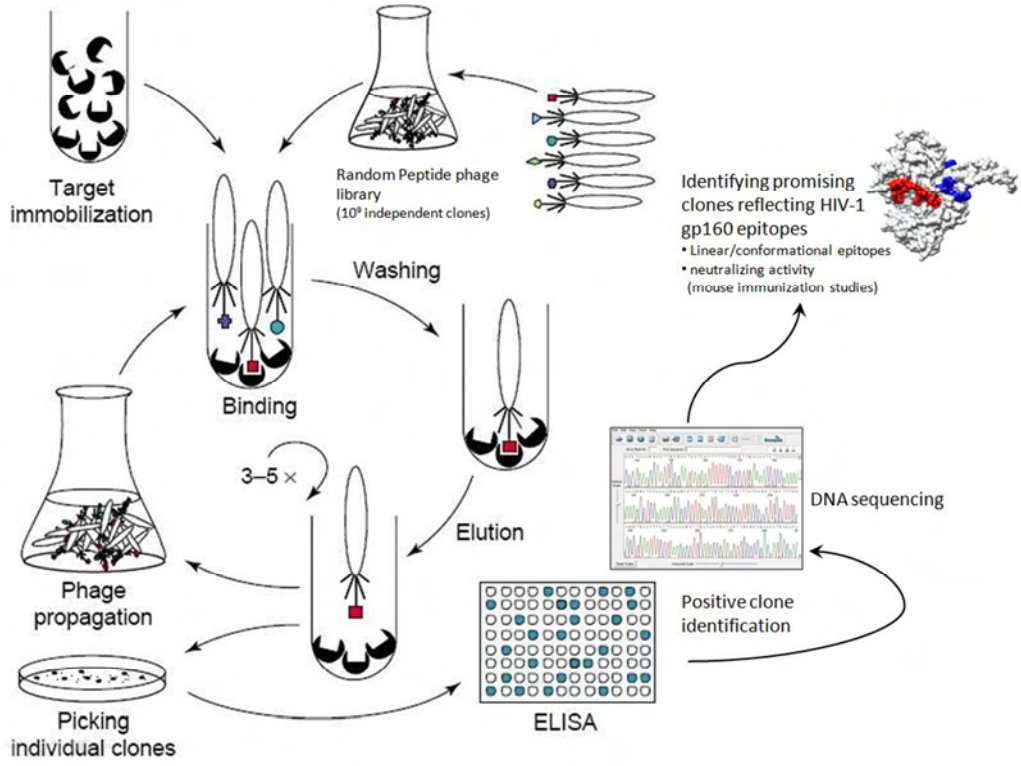

Figure 14: ***General principle of the Peptide Phage Display Technology, illustrated on HIV-specific epitopes.*** In vitro selection of specific peptides during cycles of biopanning and propagation. The phage DNA of selected positive clones is sequenced and further analyzed to identify promising clones mimicking HIV-1 gp160 epitopes (figure adapted to KONTHUR et al., 2002).

1.7. Aim of Thesis

1.7.1. Isolation of Mimotopes Representing New Epitopes for Neutralizing Antibodies Using the Phage Display Technology

In 2008, the Ruprecht Laboratory published a study, where they isolated mimotopes using polyclonal sera from a CCR5-tropic subtype-C SHIV-infected rhesus macaque (*Macaca mulatta*) by screening a random peptide library (HUMBERT et al., 2008a). After analyzing those recombinant peptide phage sequences for conformational and linear homologies to gp160 (by computational and experimental methods), promising mimotopes were used in a novel DNA prime/phage boost immunization strategy. For the first time they could show that the C-terminal domain of gp120 can induce cross-clade neutralizing antibodies in

immunized mice and were able to confirm that the combination of phage display and computational analysis can be used to identify new immunogens, capable of inducing broadly reactive neutralizing antibodies.

In the following study, a similar goal should be approached, but this time by evaluating the antibody response of a different subspecies. Thus, polyclonal sera of CCR5-tropic subtype-C SHIV-infected pig-tailed macaques (*Macaca nemestrina*) were screened using the phage display technology (methodology summarized in figure 14). Three different selection strategies were performed with a special focus on the identification of novel gp160 specific epitopes, with the potential to be recognized by neutralizing antibodies. Isolated mimotopes should be analyzed for linear, as well as conformational homologies to the envelope protein by using a developed SHIV-1157ipd3N4 gp120 model and the software 3DEX. Promising candidates should be evaluated according their cross recognition activity and possible conformational dependencies should also be shown experimentally.

1.7.2. Three Different Selection Strategies

Strategy 1: Isolation of Highly Specific Mimotopes Representing Motifs of SHIV-1157ipd3N4 gp160

By depleting all non-SHIV specific antibodies (polyclonal serum of a naïve animal as a negative selector was used), we hypothesized that highly specific phagotopes, mimicking epitopes of SHIV-1157ipd3N4 gp160 will be enriched after three rounds of selection.

Strategy 2: Isolation of Common Mimotopes Representing Motifs of SHIV-1157ipd3N4 gp160

By using three different SHIV-1157ipd3N4-infected pig-tailed macaques as positive selectors (based on a strategy called sequential antigen panning by ZHANG et al., 2004), we hypothesized that we would be able to isolate common mimotopes present in all three infected animals. To deplete all non-SHIV specific antibodies, a naïve animal was used as negative selector.

Strategy 3: Isolation of Potentially Neutralizing Mimotopes by Depleting Binding-Only Antibodies

By performing a selection using polyclonal serum samples from a SHIV-1157ipd3N4-infected pig-tailed macaque with high neutralizing antibody titer as a positive selector and a SHIV-1157ipd3N4-infected pig-tailed macaque with low neutralizing antibody titer as a negative selector, we hypothesized that we can select for neutralizing antibody mimotopes by depleting binding-only antibodies.

2 ANIMALS, MATERIALS AND METHODS

2.1. Four Pig-Tailed Macaques Infected with SHIV-1157ipd3N4

The animal samples, used in the following project, were derived from a recently published in-vivo study (HO et al., 2009). Some important results are summarized in this introducing chapter. For more details, readers are referred to the original publication. All experiments were performed under the approval of the Institutional Animal Care and Use Committee at the University of Washington and animals were kept according to established National Institutes of Health guidelines.

In this study, four juvenile pig-tailed macaques (see part 1.5.3) were inoculated intrarectally with the chimeric virus strain SHIV-1157ipd3N4 (see part 1.5.2). At specific time points (pre- and post-inoculation), tissue and blood samples have been collected and parameters like viral loads, T-cell subsets and antibody responses have been examined.

2.1.1. Infectivity and Viral load

All four inoculated macaques (J02185, K03135, L03165, M04123) became infected confirming the susceptibility of this macaque subspecies to the R5-tropic subtype-C SHIV strain. Animal M04123 had to be euthanized after two weeks of infection because of complications during the intestinal biopsy procedure. The three remaining animals have shown peak plasma viral loads around 7.6×10^6 viral RNA copies/ml two weeks after inoculation. In two of the three animals plasma viremia persisted. Only animal J02185 was able to control the viral replication below the level of quantification (100 copies/ml).

2.1.2. T-cell Subsets

$CD3^+CD4^+$ T lymphocyte levels in the duodenum were measured by flow cytometry and a dramatic depletion of 92-97% of the total $CD4^+$ T-cell population in the duodenal mucosa were observed 3-4 weeks after infection. Other mucosal tissues, like the colon and the lung have shown a severe loss of the $CD3^+CD4^+$ T cells as well. Furthermore, this depletion of $CD4^+$ T cells led to a decrease of the CD4:CD8 T cell ratios during the acute infection (23-fold decrease in the duodenum). Looking at the amount of the duodenal $CD4^+CCR5^+$ T cells, a significant decrease after 2-3 weeks post inoculation was observed in all four infected animals. However, by week 20-24 the percentages of this cell population had been recovered in all three remaining animals.

2.1.3. Antibody Responses

In addition, the antigen-specific antibody responses after the acute phase of SHIV-1157ipd3N4 infection were monitored in the three remaining animals. Four weeks after infection, SIV-specific and HIV-1 gp120

specific antibodies were detected and these antibody titers continued to increase (throughout the study period).

Neutralizing antibody activities were measured using a pseudotyped virus assay. Animals K03135 and L03165, which had a high and persistent viral load, also showed great levels of nAb activities against HIV-1 strains, like Q461d1, SF162 and SS1196.1.

Table 4: Pig-tailed macaques from the previous study. (HO et al., 2009)

Animal	short description (immunopathogenesis, clinical history)
M05118	- naïve pig tailed macaque that was never inoculated with any HIV-, SIV-, or SHIV-strain
M04123	- had to be euthanized after two weeks of infection because of complications during the intestinal biopsy procedure
L03165	- died during a mucosal sampling procedure 48 weeks after infection - showed persistent viremia - had normal peripheral $CD4^+$ T-cell levels - had reduced platelet count and moderate decrease in the albumin:globulin protein ratio - greater levels of neutralizing antibody activities compared to animal J02185
J02185	- was able to control the virus replication by week 6 p.i - showed the highest degree of CD3+CD4+ T cell depletion in the duodenum by 4 weeks p.i. - lowest antibody titer against SIVmac whole virus and HIV-1_{SF162} gp120 - low levels of neutralizing antibody activities
K03135	- viremia persisted during the year-long study - showed detectable viral load in mucosal mononuclear cells (MMC) in its duodenum (between weeks 10 and 16 p.i.). - greater levels of neutralizing antibody activities compared to animal J02185 - between week 77 and week 80 after inoculation a heart murmur was observed and at week 83 the animal had to be euthanized (personal communication with Dr. Shiu-Lok Hu)

2.2. Evaluating Antibody Responses in SHIV-1157ip3N4-Infected Pig-Tailed Macaques

2.2.1. Evaluating Anti-Monkey IgG Species Specificity

As a secondary -peroxidase conjugated- antibody in the Enzyme-linked immunosorbent assay (ELISA) and for immobilization of monkey antibodies during the iterative panning process (coating of paramagnetic beads, see 2.3.1), an anti-monkey IgG (Immunoglobulin G) antibody was used. According to the manufacture's product description, the antiserum was developed in rabbits using monkey IgG, purified from pooled rhesus monkey sera (Sigma Aldrich, Product No. M0278). Since the test samples of the following study were derived from pig-tailed macaques, we had to confirm that the anti-monkey IgG antibody is as specific for *Macaca nemestrina* as it is for *Macaca mulatta*. This was done via ELISA, by coating the polyclonal serum on a microtiter plate.

Instruments and Plates	**Companies**
▪ ELISA reader - Mithras LB 940 Software: MikroWin2000	Berthold Technologies,
▪ Automated plate washer ELx405RS	BioTek Instruments Inc.,
▪ 96 Well ELISA Microplates (Microlon 600)	Greiner-Bio-One GmbH, Product No. 655081
Buffers and Chemicals	
▪ Coating buffer Carbonate-bicarbonate buffer	Sigma-Aldrich, Product No. C3041-100CAP
▪ Blocking buffer (PBSCT) 3% N-Z Case Plus in 1x Phosphate Buffered Saline (PBS)/0.5% Tween-20	Sigma Aldrich, Product No. N4642 Invitrogen, Product No. 70013-032 Sigma-Aldrich, Product No. P2287
▪ Phosphate-citrate buffer pH 5.0	Sigma-Aldrich, Product No. P4809
▪ Ortho-phenyldiamine (OPD)-tablets 30 mg substrate/tablet	Sigma-Aldrich, Product No. P8412
▪ 30% Hydrogen peroxide solution (H_2O_2)	Sigma-Aldrich, Product No. H1009
▪ Sulfuric acid (H_2SO_4), 1 N	Titrisol, VWR International, LLC; Product No. 9981-2
Antibodies	
▪ Rabbit Anti-Monkey IgG (whole molecule) Peroxidase Conjugate	Sigma-Aldrich, Product No. A 2054
Samples	**References**
▪ Sera of SHIV-1157ipd3N4-infected pig-tailed macaques Animal K03135 week 68, 80 and 83b nec (necropsy sample) Animal J02165 week 36 and 68 Animal L03165 week 36	HO et al., 2009 see Table 4
▪ Serum of naïve pig-tailed macaque Animal M05118	
▪ Serum of SHIV-1157ip-infected rhesus monkey Animal RAo-8	HUMBERT et al., 2008b

A microtiter plate was coated with the test sera (100 µl per well), diluted in coating buffer starting with a 1:250 dilution (5-times serial dilutions, in duplicates). After incubation over night at 4°C, the plates have been washed three times with dH_2O and blocked with 3% PBSCT (200 µl per well) for 1-2 hours at room temperature. Following a three times washing step with dH_2O the peroxidise conjugated rabbit anti-monkey antibody, diluted 1:2,000 (also in 3% PBSCT) was added (100 µl per well), incubated for 1-2 hours at room temperature and afterwards washed five times with dH_2O. The plate was developed using 100 µl/well of the substrate-buffer solution, containing hydrogen peroxide (H_2O_2) in phosphate-citrate buffer and ortho-phenylenediamine (OPD) as substrates. The OPD substrate produces a soluble product that is yellow-brown in color and after stopping its reaction with 100 µl/well of 1 N H_2SO_4 it can be read at 490/620 nm.

2.2.2. Presence of Binding Antibodies against HIV Envelope Proteins

Before starting to isolate mimotopes using sera of SHIV-1157ipd3N4-infected pig-tailed macaques, the presence of HIV envelope specific antibodies in the test samples had to be confirmed. Therefore a HIV-1/2 specific Western Blot, which shows the reactivity of antibodies with individual HIV viral antigens and an indirect Enzyme-linked immunosorbent assay (ELISA) showing specific binding of serum antibodies to gp120 (SHIV-1157ip), were performed.

Binding Antibodies Detected via Western Blot

Kits ▪ QualiCode™ HIV-1/2 Western Blot Kit	**Company** Immunetics, Catalog No. DK-C152-024
Samples ▪ Sera of pig-tailed macaques Animal K03135 week 0, 68, 80 and 83b nec Animal J02165 week 0, 36 and 68 Animal L03165 week 0, 36 Animal M05118 (naïve animal)	**Reference** HO et al., 2009 see Table 4

The assay was performed according to the manual of the QualiCode™ HIV-1/2 Western Blot Kit. The stripes were developed for seven minutes in the provided substrate solution. After drying, they were analyzed according to the reference card, also provided with the kit. As a negative control, all pre-bleed samples (week 0) of the infected animals and a naïve animal were tested.

Binding Antibodies Detected via ELISA

Materials and Buffers for ELISA see 2.2.1.
Same samples tested as by Western Blot.

A microtiter plate was coated with 50 ng/well (in 100 µl coating buffer) of the gp120 (1157ip) protein. After incubation over night at 4℃ the plates have been w ashed three times with dH_2O and blocked with 3% PBSCT (200 µl per well) for 1-2 hours at room temperature. Following a three times washing step with dH_2O, the test samples were added (starting with a dilution of 1:1,000, 4-times serial dilutions, also in 3% PBSCT) to the microtiter plate and incubated over-night at 4℃. On the next day, the bound antibodies were detected using the peroxidase conjugated rabbit anti-monkey IgG, diluted 1:2,000 in 3% PBSCT. The plates was developed and read as described in 2.2.1.

2.2.3. Presence of Neutralizing Antibodies

For this study, all data on neutralizing antibody levels were taken from the original publication (HO et al., 2009) and from figure 46 (personal communication with Dr. Shiu-Lok Hu) where neutralizing antibody activities have been measured using a pseudotyped virus assay in TZM-bl cells. TZM-bl cells are modified

HeLa cells that express luciferase and β-galactosidase under the control of the HIV LTR. Thus, they can be used as reporter cell lines and neutralization of HIV or SHIV can be measured as function of reductions in Tat- regulated luciferase reporter gene expression after a single round of infection (quantified as relative luminescence units (RLU)) (MONTEFIORI, D.C., 2009).

2.3. Isolation of Mimotopes

2.3.1. Preparation of Paramagnetic Beads

Instruments	**Companies**
▪ Dynal MPC™-S Magnetic Particle Concentrator	Invitrogen
▪ Rotator LABQUAKETM	Dynal Biotech Inc., Barnsted/Thermodyne
▪ Nikon Eclipse TE300 fluorescence microscope equipped with a Nikon N70 camera	DSC Optical Services Inc., Newton MA
Software: MetaMorph®	Molecular Devices
Buffers	
▪ Coupling Buffer (Buffer B) 0.1 M borate buffer ph 9.5	Sigma-Aldrich, Product No. B0252
▪ Washing and Storage Buffer (Buffer C) PBS (ph 7.4) with 0.1% (w/v) Bovine Serum Albumine (BSA)	Sigma-Aldrich, Product No. A2058
▪ Blocking Buffer (Buffer D) PBS (pH 7.4) with 0.5% (w/v) BSA	
▪ PBS/0.02% NaN_3	Sigma-Aldrich, Product No. S8032
Antibodies and Beads	
▪ Anti-Monkey IgG (whole molecule) Affinity Isolated Antigen Specific Antibody	Sigma-Aldrich, Product No. M0278
▪ Anti-rabbit IgG-FITC conjugate	Sigma-Aldrich, Product No. F7512
▪ Dynabeads® M-280 Tosylactivated	Dynal A.S., Product No. 142.04

Paramagnetic beads (Dynabeads M-280 tosylactivated) were coated with a rabbit anti-monkey IgG (M0278, Sigma Aldrich) to immobilize antibodies present in the used polyclonal pig tailed monkey sera. Buffers B, C and D were prepared according to Dynabeads ® M-280 Tosylactivated Manual (Rev.no. 008; 08-11-18).

Washing, ligand-coupling and blocking of paramagnetic beads: 1 ml of the beads in the storing solution was transferred into a new 2 ml tube. By using a magnetic chamber the beads are bound to the magnet and after removing the supernatant the beads were washed once by adding 1 ml of the Coupling Buffer and afterwards resuspended in 1 ml of the same buffer. According to the manufacturer's instructions, 5 µg of the rabbit anti-monkey IgG Antibody were added to $2x10^9$ beads per milliliter and

incubated for 16 hours at 37℃. To avoid that the beads settle down they were incubated while shaking at 220 rpm. After the antibody was coupled to the beads, remaining free tosylactivated groups have been blocked. The supernatant was removed and the beads were washed twice with 1 ml Buffer C (4℃) for five minutes, while rotating. Afterwards the beads have been resuspended in 1 ml Blocking Buffer and incubated for four hours shaking at 220 rpm (at 37°C). Then the beads were once more washed with 1 ml Buffer C (4℃) rotating for five minutes and resuspended in 1 ml buffer C (4℃). For the storage of the beads 0.02% NaN_3 was added.

Detecting coated antibodies using a FITC conjugated secondary antibody: To make sure that the coating was successful, the coated beads have been incubated with a secondary antibody, conjugated to the fluorophore, fluorescein Isothiocyanate (FITC). Thus, a successful coating can be confirmed by detecting the secondary antibody with the fluorescence microscope. The coated beads (10 µl in 1 ml PBS) were incubated for 60 minutes rotating, at room temperature with 7 µl of an anti-rabbit IgG-FITC antibody (Sigma Aldrich, Product No. F7512). As a control, uncoated (but blocked) paramagnetic beads were incubated with 7 µl of the same FITC conjugated antibody. As an additional control we included another 10 µl of beads (coated and uncoated) but without the secondary antibody. After incubation, the beads were washed three times with 1 ml PBS and a dilution of 1:120 was transferred to a 96-well tissue culture plate for examination under the fluorescence microscope.

2.3.2. Phage Display Selection (Biopanning)

Instruments	**Companies**
▪ Dynal MPC™-S, Magnetic Particle Concentrator	Invitrogen, Dynal Biotech Inc., Barnsted/Thermodyne
▪ Rotator LABQUAKETM	Beckman Coulter™
▪ Table Top Microfuge 22R	Beckman Coulter™
▪ Centrifuge Avanti J-25	
Buffers, Chemicals, Media	
▪ Blocking Buffer PBSG Phosphate Buffered Saline (PBS)/0.25% gelatin	Spectrum, Product No. GE105
▪ Washing Buffer PBSGT PBSG/0.5% (w/v) Tween-20	Sigma-Aldrich, Product No. P2287
▪ Phage Precipitation Buffer 20% (w/v) polyethylene glycol (PEG)-8000/2.5 M Sodium chloride (NaCl)	Sigma-Aldrich, Product No. 81268 Sigma-Aldrich, Product No. S3014
▪ Elution Buffer Glycine/Hydrochloric acid (HCl) 0.2 M, pH 2.2, supplemented with 1 mg/ml BSA	Sigma-Aldrich, Product No. G2879 Sigma-Aldrich, Product No. A3059 Sigma-Aldrich, Product No. A2058
▪ Neutralization Buffer Tris-HCl 1 M (TRIZMA® hydrochloride Reagent Grade), pH 9.1	Sigma-Aldrich, T3253
▪ PBS/0.02% NaN_3	Sigma-Aldrich, Product No. S8032
▪ Luria Bertani (LB)- media LB broth tablets (10 g/L Enzymatic digest of casein, 5 g/L Yeast extract (low sodium), 5 g/L Sodium chloride, 2g/L Inert agents (necessary for tableting process), dissolved in dH_2O	Sigma Aldrich, Product No. L7275

Antibodies, Beads and Kits	
▪ Rabbit anti-monkey IgG	Sigma-Aldrich, Product No. M0278
▪ Dynabeads® M-280 Tosylactivated	Dynal A.S., Product No. 142.04
▪ Ph.D.™ Phage Display Library Kit containing the Escherichia coli ER2738 host strain	New England Biolabs; E8110S
Samples	**Reference**
▪ Sera of pig-tailed macaques (see	HO et al., 2009
▪ Table **5**)	

The Phage Display Library (according to Ph.D.™ Phage Display Libraries Instruction Manual from New England Biolabs, Version 1.0, 6/09): For mapping HIV-1 specific antibody epitopes Ph.D.™ Phage Display Libraries from New England Biolabs were screened using polyclonal serum samples of different time-points from SHIV-1157ipd3N4-infected pig-tailed macaques (selection strategies see 1.7.2). The Ph.D.™ (phage display) system is based on a modified M13 phage vector which displays peptides as N-terminal fusions to the phage minor coat protein pIII. This protein is present in five copies grouped at one end of the M13 virion. It can bind to the F-pilus of the recipient bacterial and is therefore important for the phage infectivity (see 1.6.2). The M13 genome contains only the fused copy of the gene encoding for the pIII protein (gIII), and as a result all five pIII proteins are carrying displayed peptides.

The company NEB offers three different pre-made phage display peptide libraries (Ph.D.-12, Ph.D.-C7C, Ph.D.-7; see figure 15) which were tested in parallel in three different reactions. Two of the libraries consist of linear (heptapeptide (Ph.D.-7) and dodecapeptide (Ph.D.-12)) peptides, while the third library (heptapeptide (Ph.D.-C7C)) displays the peptides as a loop to the target. Each of them shows complexities of 10^9 independent clones. Thus, most of all possible 7-mer peptide sequences (20^7 or $1.28x10^9$) can be encoded. The 12-mer library on the other hand, only reflects a small part of the possible $4.1x10^{15}$ sequences. In both linear libraries (7-mer and 12-mer), the first residue of the peptide-pIII fusion is the first position of the random peptide sequence. The first residues in the cyclic library are Ala and Cys before the randomized peptide sequence starts (see figure 15 and figure 17). Between the pIII sequence and the displayed peptide, a short linker sequence can be found: GLY-GLY-GLY-SER.

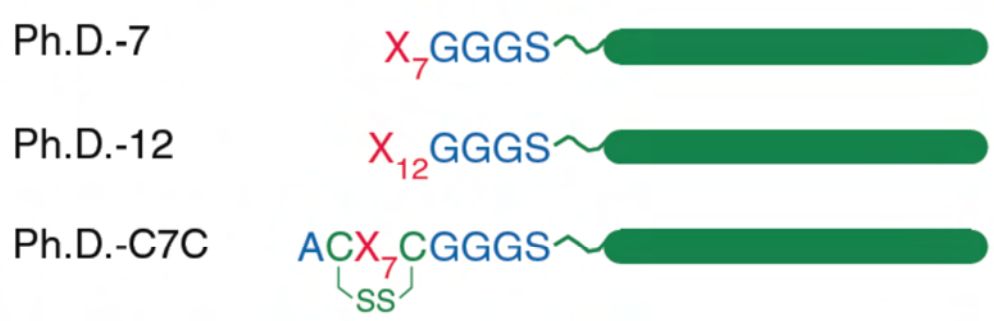

Figure 15: Three pre-made phage display peptide libraries from NEB.
M13 phage body and the pIII protein are shown in green. The linker sequence (GGGS) is illustrated in blue and the random peptide sequence in red (with the peptide length in subscript). The 7mer peptide sequence of the Ph.D.-C7C library is flanked by two cysteine residues, resulting in a loop formation of the displayed peptide (according to *Ph.D.™ Phage Display Libraries Instruction Manual* from New England Biolabs, Version 1.0, 6/09).

Escherichia coli ER2738 host strain:

F´ *proA+B+ lacIq* Δ*(lacZ)M15 zzf::Tn10 (TetR)/fhuA2 glnV thi* Δ*(lac-proAB)* Δ*(hsdMS-mcrB)5* (rk– mk– McrBC–) grown in Luria Bertani (LB)- media.

The used E.coli host strain (also from New England Biolabs) is a robust F^+ strain with a rapid growth rate. Cultures for M13 propagation were inoculated from colonies grown on LB-Agar plates containing tetracycline (to select for presence of the F-factor, since the F-factor of ER2738 contains a mini-transposon which confers tetracycline resistance). For the phage amplification no tetracycline was added to the media.

"Wildtype phage" (M13KE): M13KE Phage is a suspension of infectious virions derived from the Ph.D. cloning vector, M13KE (New England Biolabs). It does not display any peptides and was therefore used as a negative control in all performed phage ELISAs.

The Biopanning process: To isolate highly specific phages three rounds of selection were performed. In general the biopanning process comprises three steps: incubation of antibodies with library, removal of the nonbinding phage and amplification of the binding phage (see figure 16). Depending on the selection strategy different positive (samples containing the antibodies of interest, e.g. neutralizing antibodies; in this study also referred as "positive serum") and negative selectors (e.g. samples from naïve animals to remove non-HIV-1 specific antibodies; also "negative serum") have been used (see table **5**).

In the following part the biopanning process is summarized (see also figure 16). For all three selection strategies the iterative panning procedure was the same, only the used positive and negative selectors varied according to the particular hypothesis (see 1.7.2).

First positive selection: 100 µl of the coated paramagnetic beads (see part 2.3) per reaction were washed with 1 ml PBS, resuspended in 497 µl blocking buffer PBSG and incubated with 3 µl of the positive pig-tailed monkey sera for two hours (rotating at room temperature). Afterwards the beads were washed 5 times with the washing buffer PBSGT and the phage-displayed peptide libraries were added (10 µl in 490 µl PBSG). All three libraries were tested at the same time, preparing a different reaction for each one. The beads have been incubated over night, rotating at 4℃. On the next day the supernatant was taken off, the unbound phages were washed away (10 times with washing buffer PBSGT) and the specifically bound phages were eluted by pH shift (10 minutes, rotating, at room temperature) using 500 µl of the elution buffer (pH 2.2). The supernatant, containing the eluted phages was immediately neutralized with 75 µl of 1 M Tris-HCl (pH 9.1) and used for the first negative selection.

First negative selection: 100 µl of coated beads per reaction have been washed with 1 ml PBS and resuspended in blocking buffer PBSG. This time 3 µl of the negative sample were added and incubated for two hours. After washing the beads for 5 times with PBSGT they were incubated with 500 µl of the first positive eluate (in 55 µl of 10x PBSG) overnight, rotating at 4℃.

Table 5: Overview of used serum samples for performed biopannings (PT = pig-tailed macaques, nAb = neutralizing antibodies, *biopanning code* was assigned for each biopanning for a better differentiation later on. Information about neutralizing antibody activity see figure 46).

Strategy	Biopanning Code	Positive Selector			Negative Selector			Titered Eluate
		Animal	Time Point	Description	Animal	Time Point	Description	
Strategy 1 High Neutralizing vs. Naive	**BB-a**	K03135	week 83b (necropsy sample)	SHIV-1157ipd3N4-infected PT with high binding and nAb titer	M05118	06/30/2009	naïve PT	3rd positive
	BB-b							2nd positive
Strategy 2 Common Motifs	**BB-i**	K03135	week 83b (necropsy sample)	SHIV-1157ipd3N4-infected PT with high binding and nAb titer	M05118	06/30/2009	naïve PT	3rd positive
		J02185	week 36	SHIV-1157ipd3N4-infected PT with low binding and nAb titer				
		L03165	week 36	SHIV-1157ipd3N4-infected PT with high binding and nAb titer				
Strategy 3 High Neutralizing vs. Low Neutralizing	**BB-k**	K03135	week 68	SHIV-1157ipd3N4-infected PT with high binding and nAb titer	J02185	week 68	SHIV-1157ipd3N4-infected PT with low binding and nAb titer	3rd positive

First amplification: For the amplification of specifically bound phages, the E. coli host strain ER2738 (glycerol stock supplied with the Phage Display Peptide Library Kit von NEB) was used. After streaking it onto a LB-Agar plate and incubating over night at 37℃, single clones can be picked, grown in LB-media (over-night culture, 220 rpm, 37℃) and 1:100 dilut ions be used for the amplification. Since unspecific antibodies should have bound to the anti-monkey antibodies, immobilized on the paramagnetic beads during the over-night incubation (negative selection), the specific antibody-phage complexes in the supernatant were used for amplification (500 µl in 25 ml LB-media, containing 1:100 over-night culture of ER2738). After 4.5 hours, shaking at 220 rpm (37℃) the amplified phages have been centrifuged at 8,000 rpm for 30 minutes and the supernatant was transferred into fresh 50 ml tubes containing 1/3 of the phage precipitation buffer (PEG/NaCl). To precipitate the phages, they have been incubated over night at 4℃ and centrifuged for 45 minutes at 8,000 rpm at 4℃ on the following day. The white phage pellet was resuspended in 1.5 ml PBS and transferred into a 2 ml tube. After centrifugation for 5 minutes at 12,000 rpm (to get rid of residual E. coli), the supernatant was transferred into a new 2 ml tube containing 1/3 of the phage precipitation buffer (PEG/NaCl). To precipitate the phages, they have been incubated for 2

hours on ice and then centrifuged for 20 minutes (8,000 rpm at 4℃). The white phage pellet was resuspended in 200 µl PBS, containing 0.02% NaN_3 and stored at 4℃.

To increase the amount of specifically binding phages a second round of selection (positive and negative) and amplification was necessary.

Second round: The second positive selection was performed according to the first positive selection, but this time the amplified phages have been used for the overnight incubation (150 µl of the phages in 300 µl dH2O and 50 µl 10x PBSG). For the second negative selection, the eluted (specifically binding) phages were added and for the second round of amplification, the second negative supernatant was used.

Third round: The third positive selection was performed as described for the previous positive selections, by adding the propagated phages from the second amplification. The eluted phages can be used for phage titering to select for single phage clones.

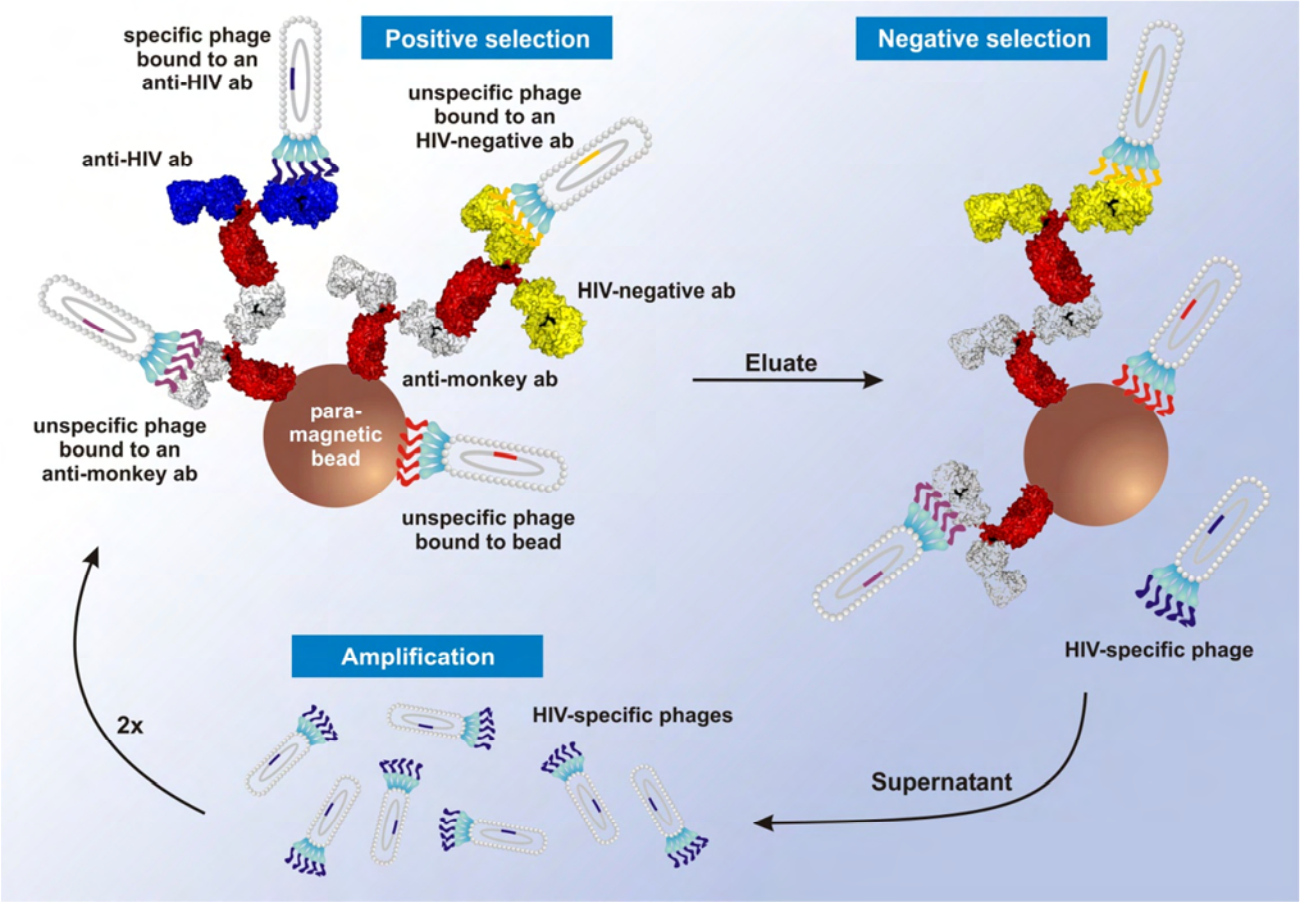

***Figure 16**: Affinity selection of HIV-specific phages (biopanning).*
Each round of selection consists of a positive selection and a negative selection, followed by an amplification of specifically bound phages. Two rounds of negative selection and three rounds of positive selection were performed for each biopanning. Anti-HIV antibodies are shown in blue and HIV-negative antibodies in yellow. More detailed description see text (figure was prepared by Michael Humbert, Ph.D).

Description of used biopanning code: For a simple differentiation of all performed biopannings and the resulting mimotopes, a simple code was developed.

BB – a – 12 – A3
(Example of one phage clone)

BB	Initials of operator
a	Number of biopanning (e.g. “a” was the first biopanning performed in that study)
12	Used phage library, according to New England Biolabs (Ph.D.-**12**, Ph.D.-**C**7C, Ph.d.-**7**)
A3	Phage clone # (according to coordinates on a 96-well plate) – see 2.3.4 and 2.3.5

2.3.3. Phage Titering and Determination of Phage Concentration

Instruments and Plates	**Companies**
▪ Neslab GP-200 water bath	Fisher-Scientific
▪ Petri Dish for LB Agar plates	BD Falcon™, Product No. 351029
Buffers, Chemicals, Media	
▪ Luria Bertani (LB)- media LB broth tablets (10 g/L Enzymatic digest of casein, 5 g/L Yeast extract (low sodium), 5 g/L Sodium chloride, 2g/L Inert agents (necessary for tableting process), dissolved in dH_2O	Sigma Aldrich, Product No. L7275
▪ Luria Bertani (LB)- Agar LB Agar capsules (10 g/L Tryptone, 5 g/L Yeast extract, 10 g/L Sodium chloride, 15 g/L Agar), dissolved in dH_2O	MP Biomedicals LLC, Product No. 3002-221
▪ Top Agar Capsules	Bio 101 Inc., Product No. 3002-521
▪ IPTG (isopropyl-β-D-thiogalactoside)	Fermentas, R0392
▪ X-Gal (5-Bromo-4-chloro-3-indolyl-β-D-galactoside)	Fermentas, R0402

In order to get single phage clones, the eluted phages from the third positive selection of each biopanning have been titered. Additionally, the second positive eluate of the first biopanning was titered (for a better differentiation later on, clones derived from the third positive eluate were referred as BB-a and clones from the second positive eluate as BB-b).

To titer eluted phages, a 10-times dilution series of $1:10^4$ - $1:10^6$ was prepared and 10 µl of each dilution were added to 200 µl of an ER2738 over-night culture, vortexed quickly and incubated for five minutes at room temperature. The infected cells were transferred into 3 ml of pre-warmed top agar (56℃), vortexe d briefly and immediately poured onto a pre-warmed LB/IPTG/Xgal Agar plate (20 ml LB-Agar containing a

1:1,000 IPTG/X-Gal solution). After cooling for a few minutes, the plates have been inverted and incubated overnight at 37℃. On the next day, plate s were analyzed and transferred to 4℃. Since the phages were derived from the cloning vector M13mp19, which carries the lacZα gene and the used E.coli strain (ER2738) is an α-complementing strain, titered plaques appeared blue after plating them onto agar containing X-Gal and IPTG (see Ph.D.™ Phage Display Libraries Instruction Manual from New England Biolabs, Version 1.0, 6/09). To determine the phage concentration the blue clones have been counted (using plates that had around 10^2 plaques), multiplied by the dilution factor to get the phage titer in plaque forming units (pfus/ml).

2.3.4. Picking and Amplification of Single Clones

Plates	**Comapany**
▪ Microtest™ Tissue Culture Plate, 96 well (flat bottom with low evaporation lid)	BD Falcon™, Product No. 353072

To avoid contaminations between single clones the plates for picking should not have more than 100-150 plaques.

Using a sterile pipette tip single blue plaques were stabbed from the titering plate and transferred to a 96-well tissue culture plate (flat bottom), containing 200 µl LB media. If agar plates have been stored for longer than two days at 4℃ before picking, a 1:100 diluted over-night culture was added to the 96-well plates. For every library, 94 single clones have been picked. The last two wells contained the negative controls for the phage ELISA (see 2.3.5): As an unspecific phage control M13KE (infectious virion derived from the Ph.D. cloning vector, M13KE; New England Biolabs) was used. The second negative control did not contain any phages (LB media only). The plates have been shaken over-night at 170-180 rpm (37℃).

2.3.5. Phage ELISA

To determine if a selected phage clone is sufficient to bind the target specifically, a phage ELISA was performed. Bound phages can be detected using a mouse anti-M13 monoclonal antibody that is conjugated to horseradish peroxidase (HRP/Anti-M13 monoclonal conjugate; GE Healthcare; Product No. 27-9421-01) and reacts with the bacteriophage M13 major coat protein product of gene VIII.

Materials and buffers for ELISA see 2.2.1

One microtiter plate per library was coated with 100 µl per well of a 1:5,000 dilution (in coating buffer) of the target sample (positive selector in biopanning) and a control plate per library was coated in the same way using the non-specific sample (negative selector in biopanning). After incubation over night at 4°C the plates have been washed three times with dH_2O and blocked with 3% PBSCT (200 µl per well, for 1-2

hours at room temperature). The plates have been washed three times and 60 µl of each phage clone (transferred directly from tissue culture plate, coordinates are the same as on ELISA plates) and 40 µl 3% PBSCT were added. The wild type phages and the 'LB media only' control were transferred as well. The plates have been incubated over night at 4°C. On the next day the bound phages were detected using the anti-M13 antibody (conjugated to peroxidase), diluted 1:2,000 in 3% PBSCT. The plates were developed and read as in 2.2.1

2.3.6. Amplification of Positive Clones, Preparation of ssDNA and Sequencing

Instruments	**Companies**
▪ Table Top Microfuge 22R	Beckman Coulter™
Buffers, Chemicals, Media	
▪ Phage Precipitation Buffer	
20% (w/v) polyethylene glycol (PEG)-8000/2.5 M Sodium chloride (NaCl)	Sigma-Aldrich, Product No. 81268 Fisher Scientific, Product No. S271-3
▪ Iodide Buffer	
10 mM Tris-HCl (TRIZMA® hydrochloride Reagent Grade, pH 8.0), 1 mM EDTA (Ethylenediaminetetraacetic acid disodium salt dehydrate), 4 M sodium iodide (NaI)	Sigma-Aldrich, Product No. T3253 Sigma-Aldrich, Product No. ES2SS Sigma-Aldrich, Product No. 383112
▪ PBS/0.02% NaN_3	Sigma-Aldrich, Product No. S-8032
▪ 100% ethanol	Sigma-Aldrich, Product No. E7023
Primer	
▪ -96 gIII sequencing primer (100 pmol/µl) Sequence: 5' CCC TCA TAG TTA GCG TAA CG 3'	Invitrogen, OligoPerfect™ Designer

Clones that showed a specific binding in the phage ELISA were selected for preparation of single stranded DNA (ssDNA) and phage stock solution. The remaining culture (which was not used for phage ELISA) from positive clones was transferred into 14 ml snap-cap tubes containing 2 ml LB media and was shaken for at least 4.5 hours (37°C, 220 rpm). If the culture was already older than 2 days, a 1:100 diluted over-night culture of ER2738 was added to the LB media. After the single phage amplification, the culture was transferred into a 2 ml tube and centrifuged at 13,000 rpm for 10 minutes (to get rid of the bacteria). The supernatant was divided into two tubes. 500 µl of the supernatant were used for ssDNA preparation (added to 200 µl of phage precipitation buffer). In parallel, the phage stock of the single clone was prepared using 1.5 ml of the supernatant (added to 500 µl of the phage precipitation buffer). To precipitate the phages, they have been incubated on ice for at least two hours or at 4°C over night. Afterwards, they were centrifuged at 13,000 rpm for 20 minutes (4°C). For the phage stock the white phage pellet was resuspended in 200 µl PBS containing 0.02% NaN_3 and stored at 4°C until further usage. For the ssDNA preparation, the white phage pellet was resuspended in 100 µl iodide buffer, vortexed and 300 µl of 100% ethanol (-20°C) were added. The pellet was centrifuged at 13,000 rpm for 20 minutes. After aspirating the

supernatant, the pellet was washed with 300 µl 70% ethanol and once more centrifuged at 13,000 rpm for 20 minutes. Now, the ssDNA pellet can be dried for 1 to 2 hours and after resuspending in 20 µl dH_2O used for the sequencing reaction.

The prepared ssDNA was transferred into a sequencing plate (12 µl of each clone) and used as template for the dideoxy sequencing reaction, performed by the **Dana Farber/Harvard Cancer Center - DNA Sequencing Facility (Boston, MA)**. Additionally 12 µl of primer -96gIII (figure 17) were prepared, for each clone to be sequenced (end concentration of 1.6 pmol/µl).

2.4. Analyzing Isolated Mimotopes – Computational Work

2.4.1. Analyzing Sequences and Linear Alignments

After receiving the results, the sequences have been analyzed according to the sequencing guidelines of the instruction manual, provided by the *Ph.D.™ Phage Display Libraries Kit* from New England Biolabs. There are several points to consider when translating the phage ssDNA into the corresponding amino acid sequence.

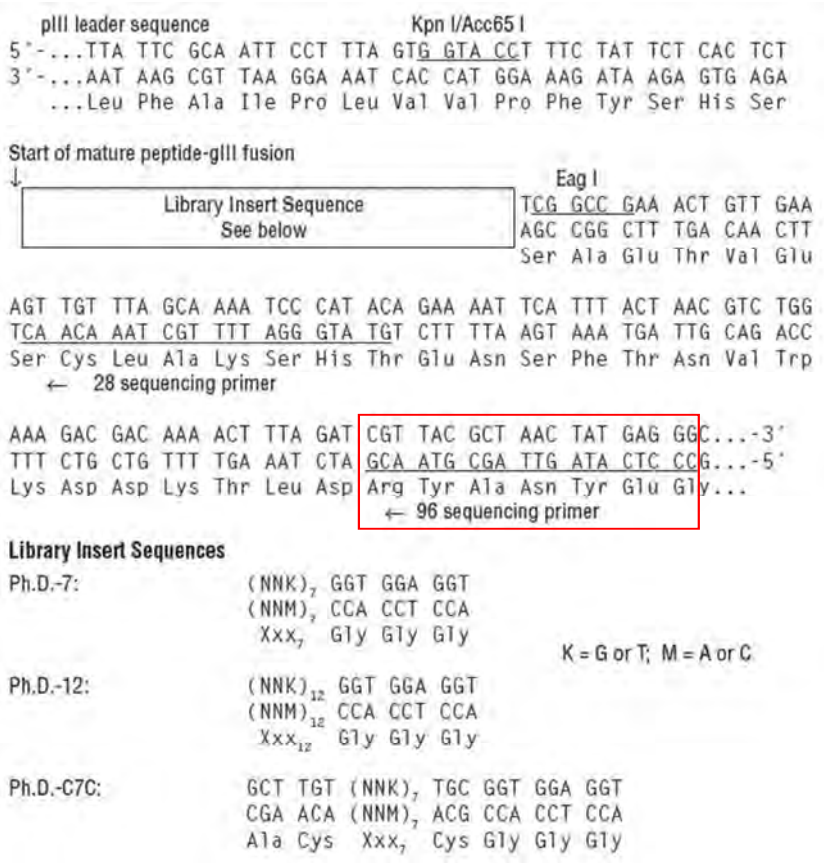

Figure 17: Sequence of random peptide-gIII fusions.
Position of library insert sequence is shown. Primer sequence of used -96gIII is boxed in red.

(1) The received sequence corresponds to the anticodon strand of the template. Thus, the complementary strand was translated.

(2) The third nucleotide of each codon has to be either guanine (G) or thymine (T).

(3) Glutamine in ER2738 is suppressing TAG stop codons. Since this strain was used to amplify the isolated phages, TAG is considered as glutamine codon when translating.

The translated sequences were first grouped according to similar peptide motifs. Afterwards the motifs were analyzed for linear homology to SHIV-1157ipd3N4 gp160 using the BioEdit Sequence Alignment Editor (HALL, 1999).

2.4.2. Modeling of SHIV-1157ipd3N4 gp120

To allow the identification of conformationally dependent mimotopes via software for three-dimensional (3D) analysis (see 2.4.3), a model of the SHIV-1157ipd3N4 gp120 monomer was developed. Using the software Discovery Studio (Accelrys Software, Inc.) protein modeling and energy calculations were performed by Jennifer Watkins, Ph.D. Based on a sequence alignment with the core structure, corresponding to the X-ray structure of JR-FL (HUANG et al., 2005) (pdb code 2B4C), a model of SHIV-1157ipd3N4 gp120 was calculated. V1, V2, and V4 loops were added to the core structure and refined by the loop refinement program. Energies were calculated using CHARMM (Chemistry at Harvard Macromolecular Mechanics). Solvent factors were introduced applying the implicit of distance-dependent dielectrics model, and energy minimization of Env loops was performed using Steepest Descent followed by Conjugate Gradient algorithms.

2.4.3. Conformational Alignments using 3DEX

After analyzing isolated mimotopes for linear homologies with the SHIV-1157ipd3N4 gp160 sequence, they were further compared with the developed SHIV-1157ipd3N4 gp120 model (see 2.4.2) to identify conformational homologies. Using the 3D-Epitope-Explorer (3DEX) software (SCHREIBER et al., 2005) linear peptide sequences can be projected onto the 3D surface structure of a target protein. The mapping of conformational epitopes is based on an algorithm allowing the analysis of single amino acids of a linear peptide sequence with regard to their physicochemical neighborhood in the 3D structure. The discontinuous epitope is identified based on preselected parameters like distance of Cα- or Cβ-atoms of the amino acids in the 3D structure (between 4 and 10 Å), string length (frame size) and surface exposure. The mimotope sequence to analyze is divided into a set of overlapping subsequences or strings (frame size selectable between 3 and the maximum length of the peptide sequence), starting with the first string at the N-terminus and moving with following strings towards the C-terminus of the peptide. For every string, the neighborship between single amino acids in the 3D structure (based on the preselected distance of Cα- or Cβ-atoms) is analyzed and those strings representing potential spatial neighbors are listed in a table with their respective amino acid positions in the protein sequence. In figure 18 a screenshot of a typical peptide sequence analysis using the 3DEX software is shown (from SCHREIBER et al., 2005). The target protein (SHIV-1157ipd3N4 gp120 monomer) was imported as tertiary protein sequence (pdb file) into the 3DEX software (see 2.4.2). The mimotope sequences to be analyzed were imported as text files. Potentially conformational mimotopes were grouped according to their peptide motifs.

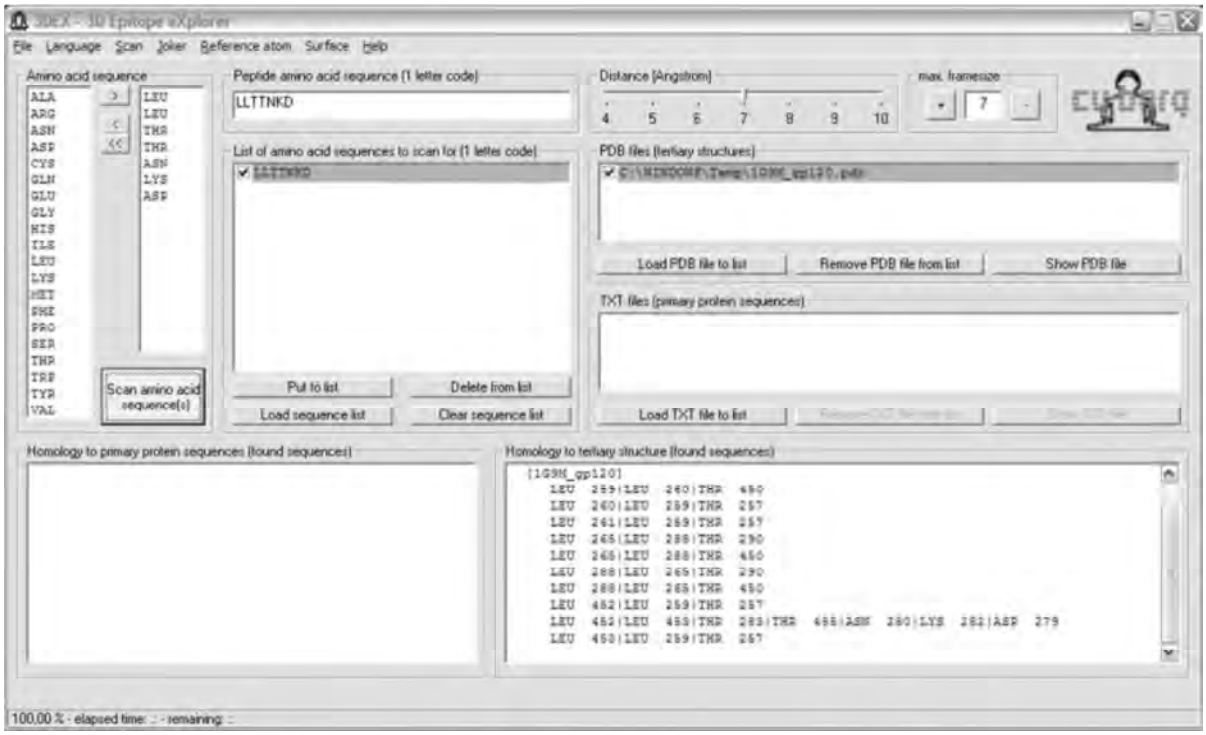

Figure 18: Screenshot of 3DEX - 3D Epitope Explorer.
Typical analysis of a peptide motif LLTTNKD, compared with the HIV-1 gp120 pdb file (1G9M; KWONG et al., 2000). The preselected parameters included a distance of 7 Å and a maximal frame size o f 7. At the bottom right, the possible conformational epitopes are shown.

2.4.4. Visualizing Potential Mimotopes Using CHIMERA Software

Using the UCSF Chimera package from the Resource for Biocomputing, Visualization, and Informatics at the University of California, San Francisco (PETTERSEN E.F. et al., 2004), residues of potential conformationally dependent mimotopes, identified using the software 3DEX (see 2.4.3), were visualized and analyzed with respect to their surface location on the SHIV-1157ipd3N4 gp120 monomer (by applying the surface command).

2.5. Analyzing Isolated Mimotopes – in-vitro *Experiments*

2.5.1. Verifying Specificity of Interesting Clones

Since the first phage ELISA was a high-throughput screening, a second phage ELISA was performed to confirm the specific binding of the isolated and sequenced clones to antibodies from the polyclonal serum sample. Thus, five µl of the purified phages were amplified using a 1:100 diluted overnight culture of ER2738 (96 well plates containing 200 µl LB media per well). This time every phage was checked in triplicates to rule out potential false positive binders. Coating, blocking and developing of the ELISA plates were performed as described in the first phage ELISA (see 2.3.5). Wild type phage M13KE and ‘LB media only’ were included as negative controls.

2.5.2. Cross-Reactivity of Isolated Mimotopes Among Different Animals and Different Time-Points

Mimotopes were evaluated according to their cross-reactivity with different time points of animal K03135 and with samples of the other two SHIV-1157ipd3N4-infected pig-tailed macaques. Therefore, a phage ELISA was performed by coating the serum samples on ELISA plates and adding phages on the next day (every clone was tested in duplicates).

Buffers and Instruments used, see 2.2.1

Antibodies
- Anti-M13 monoclonal HRP conjugate

Companies
GE Healthcare

Samples
Sera of pig-tailed macaques:
K03135 week 0 (pre-bleed)
K03135, eleven time-points between week 28 and 83
J02185 week 68
L03165 week 48

Reference
HO et al., 2009

As described for the phage ELISA (in 2.5.1), single phage clones have been amplified over night (using 5 µl of the stock solution in LB media and 1:100 ER2738 over night culture) and 60 µl of the phage culture were added to 40 µl of 3% PBSCT on the coated ELISA plates. As negative controls, M13KE wild type phages and 'LB media only' have been included. On the next day, bound phages were detected using the anti-M13 antibody (conjugated to peroxidase), diluted 1:2,000 in 3% PBSCT. The plates was developed and read as in 2.2.1.

2.5.3. Conformational ELISA

Instruments
- NanoDrop 1000 Spectrophotometer
  Software: ND-1000 V.3.7.1

Companies
Thermo Scientific

Buffers, Chemicals, Media
- Bond-Breaker® TCEP (Tris(2-carboxyethyl) phosphine) Solution , 0.5M, neutral pH — Thermo Scientific, Product No. 77720
- SDS (sodium dodecylsulfate), dissolved in dH_2O — Sigma-Aldrich, Product No. L4390

Antibodies
- Rabbit Anti-Monkey IgG (whole molecule) Peroxidase Conjugate — Sigma-Aldrich, Product No. A 2054
- Mouse Anti-M13 pIII Monoclonal Antibody — New England Biolabs, Product No. E8033S
- Peroxidase AffiniPure Goat Anti-Mouse IgG + IgM (H+L) — JacksonImmuno Research Laboratories, Inc., Product No. 115-035-044

To show if isolated mimotopes are structurally dependent, a conformational phage ELISA was performed, comparing the binding capacity of native and reduced phages. Phages were reduced by resuspending them in coating buffer containing 10 mM TCEP/2% SDS and boiling them for 2 minutes. Every phage clone was coated in duplicates (native as well as reduced).

Approximately 10^{12} phages per well (native or reduced) have been coated. The concentration was determined using the NanoDrop and its UV/VIS Absorbance module, which allows the instrument to function as a conventional spectrophotometer. The equation used to determine the phage concentration per milliliter is based on the nucleotide content of a phage particle and the molar extinction coefficient (BARBAS et al., 2001). Samples were scanned at 269 and 320 nm. 2 µl of each phage solution (resuspended in 1x PBS) were used (recommended by NanoDrop 1000 Spectrophotometer, V3.7 User's Manual, 7/08, page, section 7). To calculate the virion concentration (in phage particles/ml), the following equation was applied (BARBAS et al., 2001).

1) The corrected absorbance A* = measured A_{269} - measured A_{320}

2) Phage particles / ml = $\left(\frac{A^* \times 6 \times 10^{16}}{7250}\right) \times 10$

7250 = number of nucleotides in the phage genome (according to manual of Ph.D.TM Phage Display Libraries Kit from New England Biolabs).
Multiplied by 10, as the NanoDrop measures absorbencies for 1 mm path length (NanoDrop 1000 Spectrophotometer, V3.7 User's Manual, 7/08, page, section 7).

Equation 1: Spectrophotometric quantitation of phage particles per ml.

After coating the phages on a microtiter plate (10^{12} phages in 50 µl, per well, over night at 4℃), washing and blocking the plates (as already described in 2.2.1), the serum samples were added in a 1:500 (50 µl/well) dilution and incubated over night at 4℃. T o confirm that the reduced phages bind to the microtiter plate surface as well as native phages do, a mouse anti-pIII antibody was included as a control (1:250, diluted in 3% PBSCT). On the next day, the secondary antibody was added (rabbit anti-monkey HRP antibody, diluted 1:2,000; 50 µl/well). To detect the bound phages in the control wells, an anti-mouse HRP antibody (also diluted 1:2,000; 50 µl/well) was used. Both antibodies were incubated for 1 hour at room temperature. The plates were developed and read as already described in 2.2.1.

3 RESULTS

3.1. Evaluating Antibody Responses in SHIV-1157ipd3N4-Infected Pig-Tailed Macaques

Before starting with the isolation of HIV-1 gp160 specific mimotopes, we evaluated the polyclonal sera of SHIV-1157ipd3N4-infected pig-tailed macaques in terms of their antibody titers.

3.1.1. Evaluating Anti-Monkey IgG Species Specificity

In order to use the rhesus macaque specific anti-monkey antibody in the ELISA (as a peroxidase-conjugated secondary antibody) and for the iterative panning process (coating of paramagnetic beads, not conjugated) the sub-species cross-reactivity of the antibody with *Macaca nemestrina* had to be confirmed. Thus, the polyclonal sera of all pig-tailed samples used in that study were assessed according their specific binding to the anti-monkey antibody. In figure 19, the ELISA results are shown.

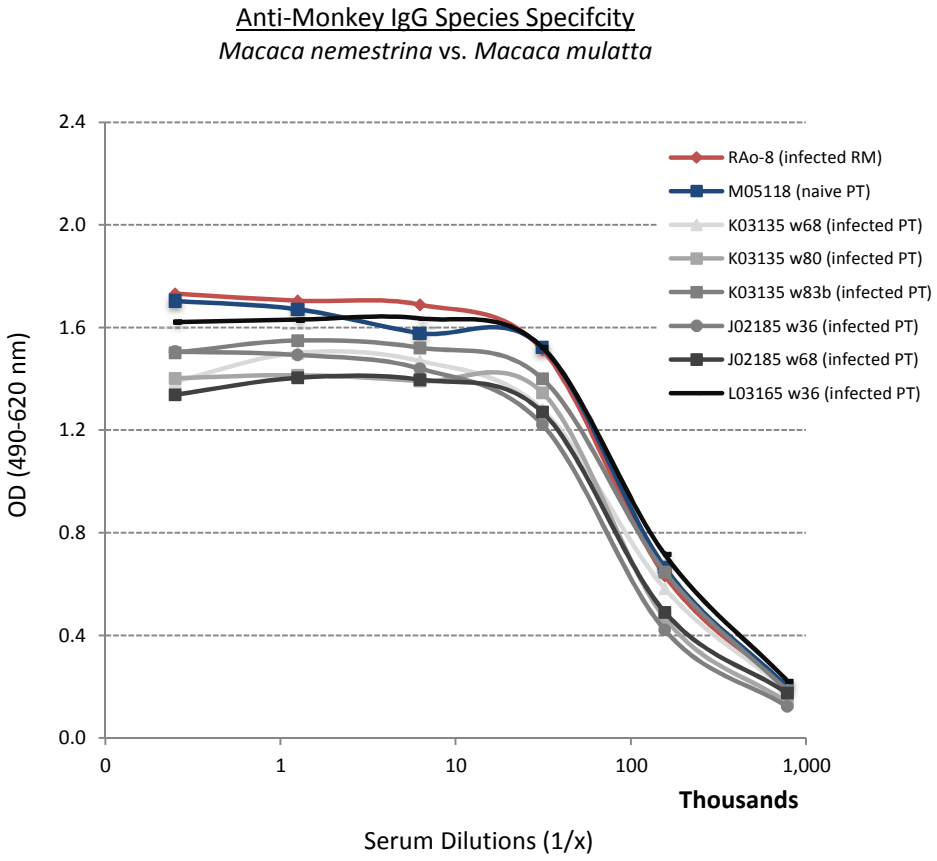

Figure 19: Evaluating anti-monkey IgG species specificity.
SHIV-1157ip infected rhesus macaque sample (red) in comparison with a naïve pig-tailed macaque sample (blue) and six different SHIV-1157ipd3N4-infected pig-tailed macaque samples (in grey).

The peroxidase-conjugated anti-monkey antibody recognized serum antibodies of all tested samples (pig-tailed (PT) samples in comparison to a serum sample of a rhesus macaque (RM)). Although produced using IgG from rhesus macaques, the secondary antibody is able to detect RM antibodies as well as PT antibodies and was therefore used in the following experiments.

3.1.2. Binding Antibodies Detected via Western Blot

Before starting to isolate mimotopes using sera of SHIV-1157ipd3N4-infected pig-tailed macaques, the presence of HIV envelope specific antibodies in the test samples were confirmed. A HIV-1/2 specific Western Blot, which shows the reactivity of antibodies with individual HIV viral antigens was performed. In figure 20, the results are shown. As already described in the original publication about the pathogenicity of SHIV-1157ipd3N4-infected pig-tailed macaques (HO et al., 2009), all three infected animals developed HIV-1 specific antibody responses. Also consistent with the previous study we could show that animal J02185 developed a lower titer of binding antibodies than the other two tested animals (K03135 and L03165). No negative control (provided with the kit, naïve samples or pre-bleeds, respectively) showed any signal but the control band on the bottom. The positive and weak positive control (also provided with the kit) showed all of the expected bands (according to Western Blot manual).

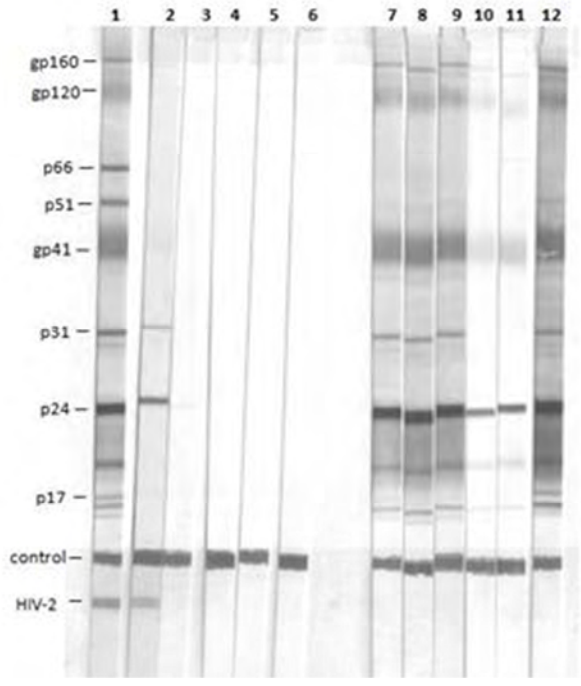

Stripe No.	Sample
1	positive control (provided with kit)
2	weak positive control (provided with kit)
3	negative control (provided with kit)
4	naïve animal (M05118)
5	K03135 week 0 (pre-bleed)
6	J02185 week 0 (pre-bled)
7	K03135 week 68
8	K03135 week 80
9	K03135 week 83b (necropsy sample)
10	J02185 week 36
11	J02185 week 68
12	L03165 week 36

***Figure 20**: HIV-1 specific antibodies detected via Western Blot.*
The tested samples and their respective stripe numbers are listed in the right panel. A positive, a weak positive and a negative control provided with the kit was included (stripe no. 1-3). The serum sample of a naïve pig-tailed animal and the pre-bleed sample of animal K03135 and animal J02185 were tested as well. All the bands showed the required control bands on the bottom. None of the negative controls reacted with any HIV-1 specific antibodies.

3.1.3. Binding Antibodies Detected via ELISA

To confirm the presence of binding antibodies in the sera of SHIV-1157ipd3N4-infected pig-tailed macaques against gp120, an indirect ELISA was performed. Thus, the gp120 trimeric protein (SHIV-1157ip) was coated on an ELISA microtiter plate and incubated with the test samples. In figure 21, the results are shown. As already observed with the Western Blot, all the tested samples showed binding antibodies against the gp120 protein, with animal J02185 having the lowest titer.

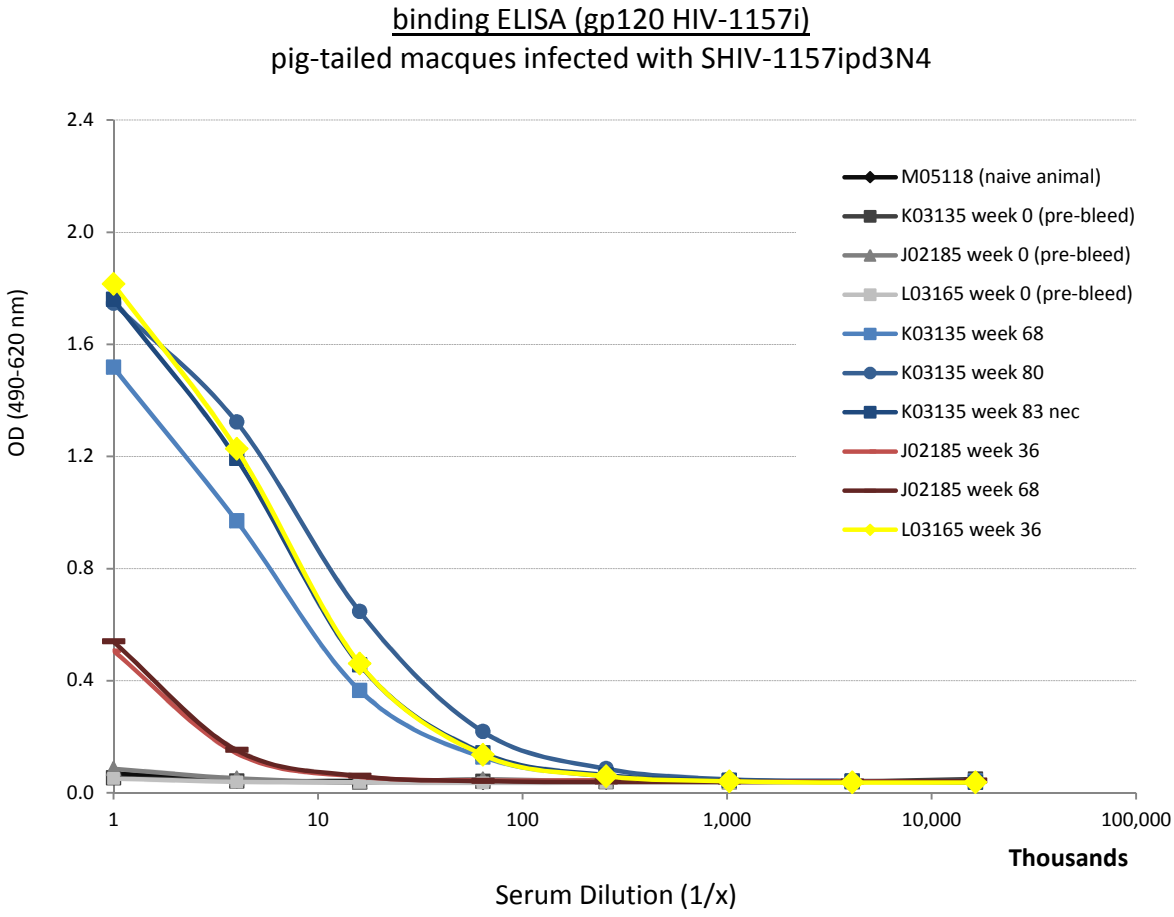

Figure 21**: **gp120 specific antibodies detected via indirect ELISA.
Control samples are shown in black and grey. Samples of animal K03135 are shown in blue, of animal J02185 in orange/red and of animal L03165 in yellow. None of the negative controls reacted with the gp120 antigen, while all the SHIV-1157ipd3N4 infected pig-tailed macaques clearly showed binding antibody titers. Again, animal J02185 had the lowest titer.

3.2. Isolation of Mimotopes

Since both of the performed assays revealed HIV-1 envelope specific antibody titers in the polyclonal serum of all three SHIV-1157ipd3N4-infected pig-tailed macaques, we went one step further and started the isolation of mimotopes. Before the actual screening process can start, anti-monkey antibodies had to be immobilized on a solid matrix used in the panning procedure (paramagnetic beads).

3.2.1. Preparation of Paramagnetic Beads

Tosylactivated, paramagnetic beads were coated with a rabbit anti-monkey IgG for immobilization of antibodies, present in the used polyclonal pig tailed monkey serum samples. After the coating process, the beads were incubated with a FITC-conjugated anti-rabbit IgG antibody and the successful coating was shown under the fluorescence microscope by detecting the FITC conjugated secondary antibody. In figure 22 the results are illustrated. Only in the wells containing coated beads, incubated with the FITC conjugated secondary antibody, a fluorescence signal was detectable. All the negative controls (uncoated beads without secondary antibody (E), uncoated beads with secondary antibody (F) and coated beads without secondary antibody (G) did not show any fluorescence signal. The corresponding bright field images are shown in the upper panels A-D. All pictures were made with 20x magnification.

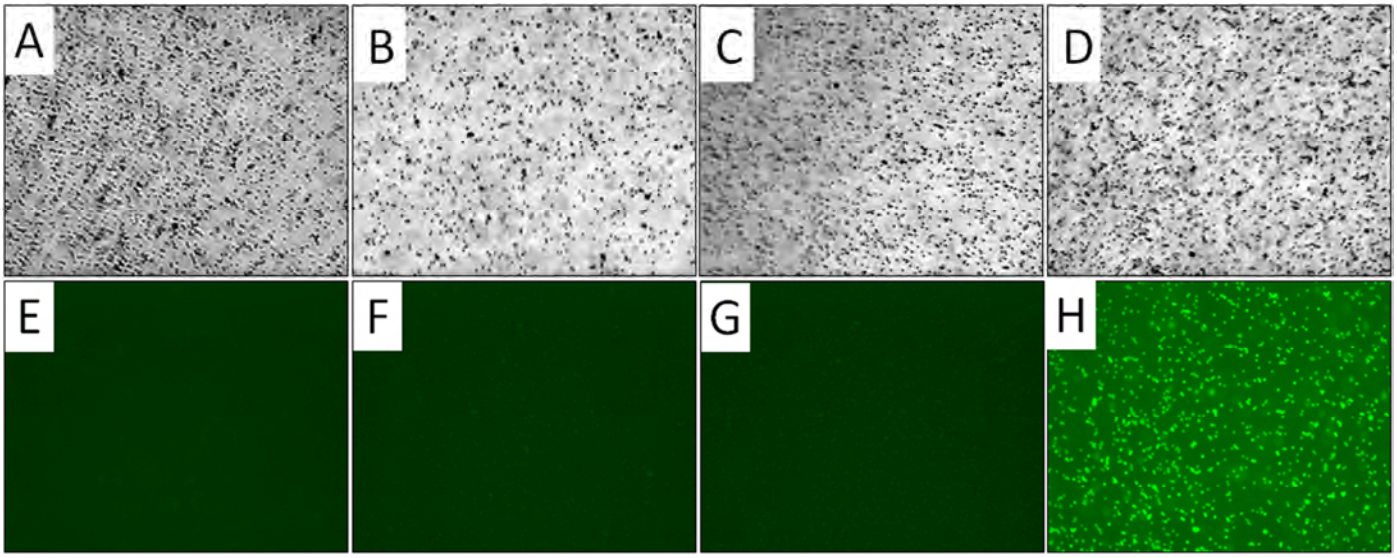

Figure 22**: **Bright field and fluorescence microscope results.
A-D bright field images (20x magnification): **A** uncoated beads without FITC, **B** uncoated beads with FITC, **C** anti rhesus monkey (a-RM) beads without FITC, **D** a-RM beads with FITC; **E-H** fluorescence images (20x magnification): **E** uncoated beads without FITC Ab, **F** uncoated beads with FITC Ab, **G** a-RM beads without FITC Ab, **H** a-RM beads with FITC Ab

Since anti-monkey antibodies were successfully immobilized on the paramagnetic beads, they could have been used for the following panning procedure.

3.2.2. Phage Display Selection (Biopanning)

To isolate specific phages, three rounds of (1) incubation of immobilized serum antibodies with peptide phage library, (2) removal of non-binding phages and (3) amplification of the specific binding phages have been performed. After every positive round the specific binding phages have been eluted by pH shift. In total, three different biopannings have been carried out.

3.2.3. Phage Titering, Determining Phage Concentration and Picking of Single Clones

Either the second positive or the third positive eluate of each performed biopanning was titered and depending on the amount of blue appearing (infected) plaques on the agar plate, the concentration (in plaque forming units (pfus)/ml) was estimated (see table 6). An average concentration of 10^6 – 10^9 was observed. A total of 1,128 phage clones have been picked and tested in a phage ELISA.

***Table 6**:* Phage titering results and estimated phage concentration of all three performed biopannings

Strategy	Biopanning	Titered	Estimated Concentration (pfus/ml)			# of Picked Clones		
			7mer	12mer	C7Cmer	7mer	12mer	C7Cmer
1	BB-a	3rd positive eluate	10^8	10^6	10^5	94 clones each (total of 1,128 clones)		
	BB-b	2nd positive eluate	10^7	10^7	10^6			
2	BB-i	3rd positive eluate	10^8	10^8	10^8			
3	BB-k	3rd positive eluate	10^9	10^9	10^9			

3.2.4. Phage ELISA and Sequencing of Positive Clones

As a first high-throughput screening, picked clones were analyzed by phage ELISA for their specific binding to antibodies of the particular target sample (positive selector used in biopanning). All performed phage ELISAs together led to approximately 38% positive clones (426 out of 1128, for sequential biopanning only clones positive for all three selectors were calculated).

Strategy 1 - Isolation of Highly Specific Mimotopes Representing Motifs of SHIV-1157ipd3N4 gp160 (BB-a and BB-b). In figure 23**,** one example of a typical phage ELISA is shown. Phage clones of the titered third positive eluate (BB-a, 12mer library) were screened and most of the clones showed a high specific binding for the positive serum (animal K03135, week 83 necropsy sample in this case), which confirmed that the affinity selection had worked. To be counted as 'positive for target molecules', the binding signal for the positive selector had to be at least three times higher, than for the negative selector as well as for the included wild type phage control. The phage ELISA results of the linear and the cyclic 7mer library can be found in 8.3. (see figure 47). The linear 7mer library showed almost the same results as the linear 12mer library. With the cyclic 7mer library, only a few positive clones were detected and chosen for sequencing. The screening of phage clones from only two rounds of positive selection (2nd positive eluate) led to similar phage ELISA results as seen with the third positive eluate (data not shown), although three rounds of selection showed approximately 25% more positive clones. Out of 576 picked clones (BB-a and BB-b together), 246 positive clones have been detected (43%) and 60 have been used

for sequencing of the phage ssDNA to identify - for target samples specific - peptide motifs (see also table 7).

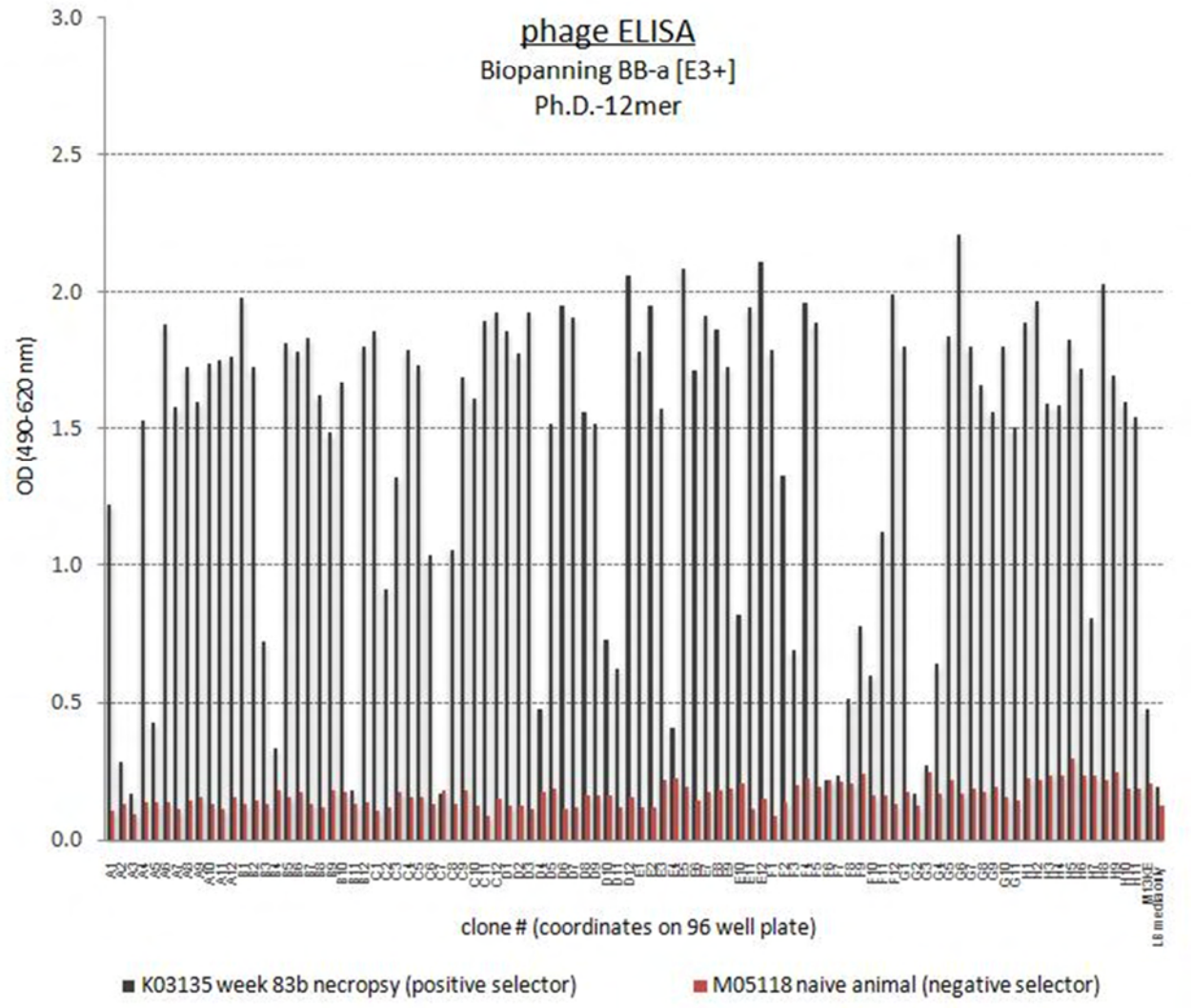

Figure 23*: *Typical phage ELISA (BB-a, 12mer library, 3rd positive eluate).
To identify positive clones after three rounds of selection, a simple phage ELISA was performed. For each library, 94 clones have been screened. As negative controls, the wild type phage M13KE and 'LB media only' were included as well. The binding of phage clones to the positive selector (animal K03135, week 83b necropsy sample) is shown in dark grey and the reaction with antibodies from the naïve serum is shown in red. Antibodies of the naïve serum recognized none of the 94 tested clones (all the other phage ELISAs are illustrated in appendix).

Strategy 2 - Isolation of Common Mimotopes Representing Motifs of SHIV-1157ipd3N4 - Sequential Biopanning (BB-i). In figure 24, the phage ELISA result of the sequential biopanning (BB-i) is shown. All common mimotopes (positive for all three positive selectors but no specific binding to antibodies of the negative serum) are illustrated. Again, the linear 12mer library led to the most positive clones but only 16 out of 96 clones showed a positive signal for all three used positive selectors (17%). With the 7mer library no common clones were isolated (most of them were only positive for the third positive selector, L03165 week 36) and with the cyclic 7mer library a few common clones were selected (data not shown). For sequencing 49 positive clones (30 of the 12mer library and 19 of the cyclic 7mer library) have been

chosen (see table 7). In every phage ELISA the M13KE wild type phage and the LB media only control were included. Of note, the signal for the wild type phage was higher than seen in the other phage ELISAs, and as mentioned before, only signals 3-times higher than for M13KE can be considered as 'truly' positive. To rule out false positive signals, a second phage ELISA was performed with all the sequenced clones (see 3.4.1).

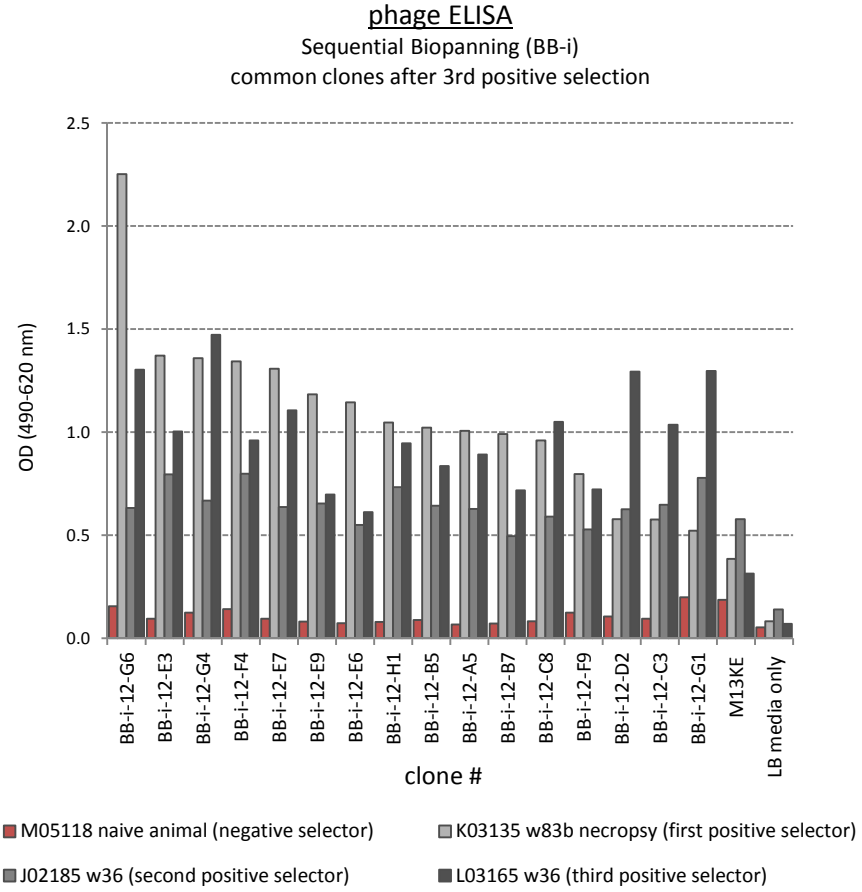

Figure 24: Phage ELISA results of sequential biopanning (BB-i).
Only common clones (positive for all three positive selectors and negative for the negative selector) are shown. As a negative selector a naïve pig-tailed macaque serum sample was used (shown in red). All three positive selectors (SHIV-1157ipd3N4 infected pig-tailed macaques) are shown in grey. As a negative control wild type phage M13KE and LB media only was included as well.

Strategy 3 - Isolation of Potentially Neutralizing Mimotopes by Depleting Binding-Only Antibodies (BB-k). The phage ELISA results of the third selection strategy (BB-k) led to positive clones in all three of the performed reactions (57% in total, see figure 48) and 60 positive clones were chosen for sequencing – all showing at least three times higher binding signals compared to background signal (sample of animal J02185 and M13KE wild type phage control).

After positive clones have been identified by phage ELISA, 169 single clones of all three performed biopannings have been amplified and prepared for ssDNA sequencing. In table 7, the amount of picked and sequenced clones of each biopanning and each library is summarized.

3.3. Analyzing Isolated Mimotopes – Computational Work

According to the sequencing guidelines of the instruction manual from New England Biolabs, the resulting sequences have been analyzed.

Unexpectedly, only recombinant peptide phage sequences of biopanning BB-b (2nd positive eluate, first selection strategy) showed the two flanking cysteine residues, characteristic for the cyclic 7mer library. BB-a (3rd positive eluate, same biopanning) sequences instead displayed a linear 7mer motif, and BB-i (3rd positive eluate of sequential biopanning) and BB-k (3rd positive eluate of third selection strategy) a linear 12mer motif. No cyclic 7mer motif without those flanking cysteine residues was selected for any further analysis. Thus, 122 out of 169 sequenced clones (approximately 11% of all, with phage ELISA, tested clones) have been evaluated experimentally and with computational methods.

3.3.1. Analyzing Sequences and Linear Alignments

The translated peptide sequences were grouped according to similar motifs and checked for linear homologies with SHIV-1157ipd3N4 gp160. For a better overview, the resulting alignments are discussed and illustrated for each selection strategy separately, and in combination with the conformational alignments (see 3.3.3 - 3.3.5).

3.3.2. Modeling of SHIV-1157ipd3N4 gp120 and 3DEX

One of the main goals in that study was to analyze isolated mimotopes regarding their conformational homologies with the HIV envelope proteins. Thus, a computational based model of the SHIV-1157ipd3N4 gp120 monomer was developed by Jennifer Watkins, Ph.D., which can be used for the analysis with 3DEX. The resulting model is shown in figure 25. It was visualized using the surface command of the CHIMERA software and its variable loops were highlighted.

The pdb file of SHIV-1157ipd3N4 gp120 and the text file of all peptide sequences to be analyzed were imported into the 3DEX program and analyzed with the following parameters. (1) As reference atom, the Cα-atom was selected; the distance between the atoms was preselected with 8 Å, and the frame size started with five, but was increased up to 12 in some cases. Most of the isolated peptide sequences gave many hits. Only sequences with homologies of at least five amino acid residues for 12mer mimotopes and at least four amino acid residues for 7mer mimotopes have been considered for further analyses. The probability *p,* to find a certain motif of 4 or even 5 amino acid residues on gp120 is much lower than 1% (considering the number of possible amino acid residues (20), number of residues to find (4 or 5) and total amount of residues of the SHIV-1157ipd3N4 gp120 model (397)) (see equation 2).

Equation 2: Calculating probability p to find a certain motif of four amino acid residues on gp120.

$$p = \left(\frac{1}{20}\right)^4 \times 397 = 0.0025$$

Potential conformational mimotopes, identified by 3DEX, were visualized with the help of the CHIMERA package. The analysis was performed with special focus on their location on the surface of the SHIV-1157ipd3N4 gp120 protein, preferably overlapping with neutralization sites or known domains important in HIV-1 entry (CCR5 and CD4 binding sites). In figure 32, the promising peptide motifs after 3DEX and CHIMERA analysis are summarized and their location is indicated. The corresponding figures for each mimotope can be found in 8.4. Those mimotopes have been chosen for further analysis.

All mentioned amino residue positions on gp120 are referring to the particular amino acid residues in the SHIV-1157ipd3N4 model. An alignment with the published HIV-1 subtype B strain JR-FL (PDB-ID: 2B4C), including the amino residues important for the interaction with CD4 (highlighted in red) and CCR5 (highlighted in blue), respectively, is shown in 8.5. Variable loops are indicated in green.

The resulting mimotope motifs are discussed with regard to their particular selection strategy. Of note, 3DEX gave more hits than summarized in figure 32. However, those mimotopes were considered as the most promising ones and thus selected for further analysis.

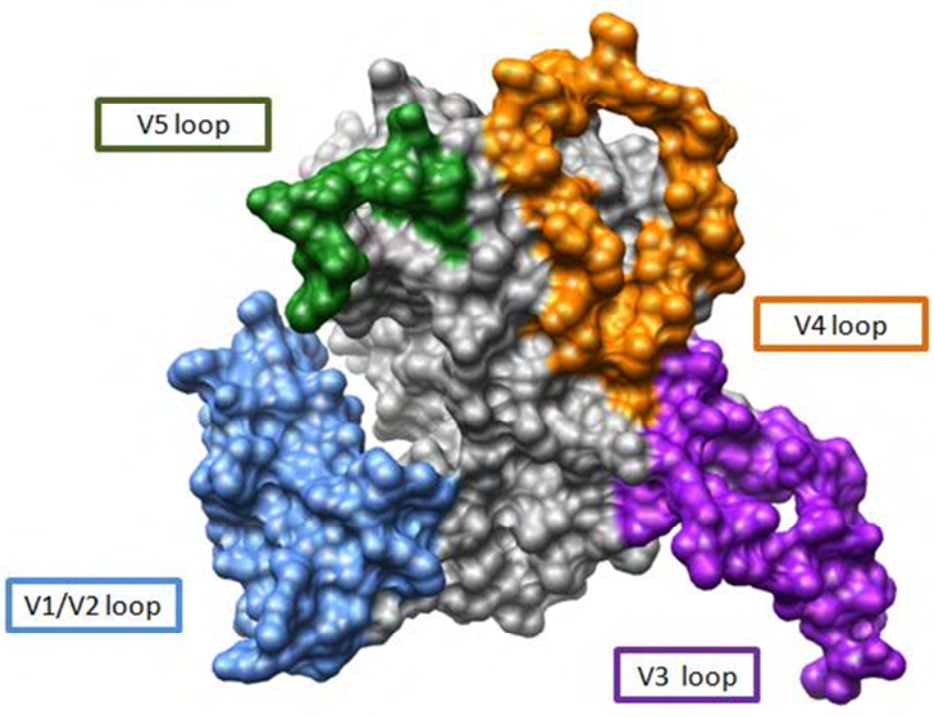

Figure 25: ***SHIV-1157ipd3N4 gp120 monomer.***
The developed SHIV-1157ipd3N4 gp120 monomer model is shown. Visualized using the pdb file of the model and the CHIMERA software by applying the surface command. The variable loops 1 and 2 are highlighted in blue, the V3 loop in purple, the V4 loop in orange and V5 in green. The constant parts of the protein are shown in grey.

3.3.3. Strategy 1 - Isolation of Highly Specific Mimotopes Representing Motifs of SHIV-1157ipd3N4 gp160 (BB-a and BB-b)

The aim of the first selection strategy was to isolate mimotopes representing motifs of SHIV-1157ipd3N4 gp160. Since we used the serum sample of a naïve animal as a negative selector, we hypothesized that we could select for mimotopes highly specific for HIV proteins by depleting all non-HIV specific antibodies.

In figure 27, isolated phagotopes of biopanning BB-a and BB-b are shown. They were aligned and grouped according to their linear sequence. One motif – **PI**x**D**x**T** – was recurring frequently. None of the selected mimotopes showed any obvious linear homology to the SHIV-1157ipd3N4 gp160 sequence or any other SHIV-specific proteins (analyzed using BLASTp, National Center for Biotechnology Information, http://blast.ncbi.nlm.nih.gov/Blast.cgi). However, neutralizing antibodies often target conformational epitopes. Thus, isolated mimotopes were analyzed for structural homology to gp120 using the established SHIV-1157ipd3N4 model and 3DEX.

With this approach we were able to identify some interesting mimotopes which seem to overlap with either the CCR5 binding site (shown in blue) or the CD4 binding site (shown in red). One of those CCR5 mimotopes is illustrated in figure 26 (clone BB-a-12-C12). Of particular interest, one of the CD4bs clones (BB-a-12-G6) with the sequence TSMGQND is overlapping with the Phe43 cavity, which was described to be important for the interaction with the CD4 receptor (see 1.3.1.). Besides those 'CCR5'- and 'CD4'-mimotopes, one peptide sequence (clone BB-b-12-B7) mimicked a discontinuous epitope on the V3 loop, partly overlapping with the immunodominant 'GPG' motif ($S^{219}G^{221}A^{225}A^{228}G^{230}D^{231}$, figure 32 and 8.4).

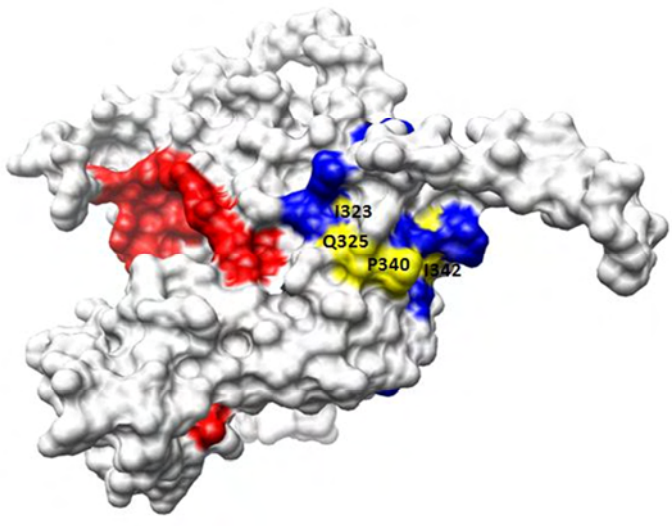

Figure 26: 3DEX result of clone BB-a-12-C12.
Visualized using the CHIMERA software and the SHIV-1157ipd3N4 gp120 model. Residues involved in the interaction with the CD4 receptor are highlighted in red, residues important for the interaction with the chemokine receptor CCR5 in blue. Mimotope sequence ($I^{323}Q^{325}P^{340}I^{342}N^{345}$, identified by 3DEX, is shown in yellow.

Linear Alignment: Phagotopes Biopanning BB-a and BB-b																			
Phagotopes		Sequences																	
Group 1								**P**	**I**	**I**	**D**		**T**						
BB-a-12-F4		K	A	Q	S	H	P	P	I	I	D	F	T						
BB-a-12-D6							A	G	I	I	D	S	T	D	N	A	S	P	
BB-a-7-E10 and b-7-C11	2x						F	P	I	I	D	S	T						
BB-b-7-D12							F	P	I	Y	D	T	T						
Group 2								**P**	**I**	**D**	**D**	**R**	**T**						
BB-a-7-D9							Q	P	I	D	D	Y	S						
BB-a-12-H2			S	W	L	H	N	P	I	D	D	T	T	R					
BB-a-12-A6							N	P	I	D	D	R	T	L	R	W	C	W	
BB-a-12-H8					K	P	G	P	I	D	D	N	T	H	W	T			
BB-a-7-D6							A	P	Q	D	D	R	A						
BB-a-12-F12		K	Q	L	H	S	M	P	Q	D	D	F	S						
BB-a-12-F5						S	W	G	D	D	D	T	T	N	P	T	L		
BB-a-12-H1								I	I	D	D	R	T	L	S	T	K	D	W
BB-b-12-A1								V	I	D	D	R	A	S	S	W	W	T	S
BB-b-12-C4								T	I	D	D	R	T	S	L	S	L	L	K
BB-b-12-F6		S	I	N	S	Q	S	G	I	D	D	R	S						
BB-b-12-H4								V	L	D	D	R	T	T	S	P	S	F	D
BB-b-7-D5							Q	P	N	D	D	Y	S						
Group 3								**P**	**I**	**N**	**D**		**T**						
BB-a-7-A10							Y	P	I	N	D	F	A						
BB-a-7-C2							T	P	I	N	D	S	T						
BB-a-7-H10								L	I	N	D	A	T	Y					
BB-a-12-B1		S	T	T	Q	R	Q	P	I	N	D	H	T						
BB-a-12-C11						N	Q	P	I	N	D	H	T	G	L	V	A		
BB-a-12-C12					T	I	Q	P	I	N	D	A	T	H	T	H			
BB-a-12-D1							A	P	I	N	D	F	T	G	T	L	W	S	
BB-a-12-D3							S	P	I	N	D	R	T	S	K	Y	T	L	
BB-a-12-E2		S	S	C	G	L	S	P	I	N	D	F	S						
BB-a-12-E5						N	N	P	Q	N	D	A	T	W	V	P	L		
BB-a-12-G6					T	S	M	G	Q	N	D	Y	T	G	A	W			
BB-a-12-E7			I	Q	P	P	I	P	I	N	D	S	A	Y					
BB-b-7-D11							V	P	I	N	D	H	T						
BB-b-12-A11		T	W	S	A	S	N	P	I	N	D	R	T						
BB-b-12-C9							A	P	I	N	D	F	T	G	T	L	W	S	
BB-b-7-B8							G	A	I	N	D	A	T						
BB-b-12-G4					A	Y	P	P	I	N	D	A	T	Q	F	Q			
BB-b-12-C2 and b-12-C3	2x	G	V	T	L	H	Y	G	I	N	D	Q	T						
BB-b-12-C7 and b-12-D2	2x					I	T	G	I	N	D	S	T	L	D	M	R		
BB-b-7-C12								A	I	N	D	R	T	T					
BB-b-7-B1								A	I	N	D	S	T	R					
BB-b-7-A2								S	I	N	D	A	T	S					
BB-b-7-E6								V	I	N	D	S	T	T					
Group 4		**no recurring motifs**																	
BB-a-12-E8					S	H	M	G	P	H	T	F	T	Q	F	S			
BB-b-c-D9 and b-c-D12	2x				Q	P	H	S	W	L	G								
BB-b-c-F12					L	S	L	L	L	H	L								
BB-b-7-B5					Q	M	P	S	Y	L	T								
BB-b-12-A4					G	P	I	V	D	S	T	H	E	S	S	T			
BB-b-12-B7					L	T	R	S	G	A	A	G	D	L	T	L			

***Figure 27**: Linear Alignment BB-a and BB-b.*

Resulting phagotopes of BB-a and BB-b, divided into 4 different groups (according to similar motifs). Clones of group 4 did not show any recurring motifs. Phagotopes of group 1, 2 and 3 showed an abundant occurring motif (PIXDXT), but no linear similarities to SHIV-1157ipd3N4 gp160 or any other HIV-specific proteins (analyzed using BLAST, National Center for Biotechnology Information). Identical clones are indicated with a "2x" in the second column.

3.3.4. Strategy 2 - Isolation of Common Mimotopes Representing Motifs of SHIV-1157ipd3N4 - Sequential Biopanning (BB-i)

To isolate mimotopes represented in all three SHIV-1157ipd3N4-infected pig-tailed macaques, a sequential antigen panning was performed. Using three different positive selectors one very common motif was selected - the immunodominat ^{589}KLIC^{592} motif (amino residues according to the published SHIV-1157ipd3N4 gp160 sequence; Accession. No. DQ779174) on gp41 (around 70% of all BB-i peptide sequences). Besides that motif, mimotopes of another well known epitope - ^{221}GPG^{223} on the tip of the V3 loop - were isolated. Additionally, a **P**xxx**IE**x**TT** motif and some single sequences were identified, which could not have been aligned with the linear gp160 sequence. All non-KLIC sequences have been further analyzed for conformational similarities with 3DEX and the SHIV-1157ipd3N4 model. All BB-i sequences are aligned in figure 28.

Linear Alignment: Phagotopes Biopanning BB-i (Sequential BP)																		
Phagotopes		Sequences																
Group 1: KLIC (gp41)		**L**	**G**	**I**	**W**	**G**	**C**	**S**	**G**	**K**	**L**	**I**	**C**	**T**	**T**	**A**	**V**	**P**
BB-i-12-A5		V	S	T	A	S	C	S	G	K	L	F	C					
BB-i-12-B5		V	S	T	A	S	C	S	G	K	L	F	C					
BB-i-12-B7						T	C	Y	G	K	L	E	C	T	P	H	A	
BB-i-12-C3			S	G	L	Q	C	Y	G	K	L	W	C	S				
BB-i-12-C8						G	C	T	G	K	L	M	C	S	Y	V	H	
BB-i-12-D2			S	L	P	G	C	H	G	K	M	L	C	R				
BB-i-12-E3		V	S	T	A	S	C	S	G	K	L	I	C					
BB-i-12-E7		V	S	T	A	S	C	S	G	K	L	F	C					
BB-i-12-E9		V	S	T	A	S	C	S	G	K	L	F	C					
BB-i-12-F4					S	T	C	M	G	R	L	M	C	T	L	G		
BB-i-12-G1			S	L	P	G	C	H	G	K	M	L	C	R				
BB-i-12-G4						G	C	T	G	K	L	M	C	S	Y	V	T	
BB-i-12-G6					N	M	C	S	G	H	L	I	C	L	D	W		
BB-i-12-D11			S	G	L	Q	C	Y	G	K	L	W	C	S				
BB-i-12-E2				T	D	R	C	S	G	R	I	I	C	H	Q			
BB-i-12-E8						N	C	S	G	S	L	I	C	A	R	P	H	
BB-i-12-H2					N	E	C	F	G	Q	L	I	C	R	E	D		
BB-i-12-B12			S	L	P	G	C	H	G	K	M	L	C	R				
BB-i-12-H5					V	Q	C	D	G	K	L	R	C	M	A	W		
BB-i-12-H7			S	G	L	Q	C	Y	G	K	L	W	C	S				
Group 2: V3 loop (gp120)		**N**	**N**	**T**	**R**	**K**	**S**	**I**	**R**	**I**	**G**	**P**	**G**	**Q**	**A**	**F**	**Y**	**A**
BB-i-12-G3					A	K	T	I	F	Y	G	P	Y	N	S	V		
BB-i-12-G7					A	K	S	I	H	I	A	P	N	T	M	L		
BB-i-12-H1					A	K	T	V	S	V	G	P	G	L	S	G		
Group 3						**P**				**I**	**E**		**T**	**T**				
BB-i-12-E12			T	S	A	P	L	M	P	I	E	D	T	T				
BB-i-12-B2			G	L	P	P	T	Q	A	I	E		T	T	L			
Group 4		**no recurring motifs**																
BB-i-12-E4					F	R	S	H	D	A	W	V	L	Q	Y	Y		
BB-i-12-F6					S	E	R	D	F	V	H	T	Y	Y	F	G		
BB-i-12-G9					N	L	D	P	E	S	W	I	K	V	Y	Y		
BB-i-12-B8					M	K	P	Y	S	S	D	K	W	P	W	H		
BB-i-12-G2					S	V	E	A	L	W	D	Q	W	T	R	T		

Figure 28: Linear Alignment BB-i.

Resulting phagotopes of BB-i have been divided into 4 groups. One very common motif was selected - the KLIC motif on gp41 (group 1). In group 2, another well known motif is shown – the V3 loop epitope GPG. Additionally, a PxxxIExTT motif and some single sequences were observed, which could not have been aligned with the gp160 sequence.

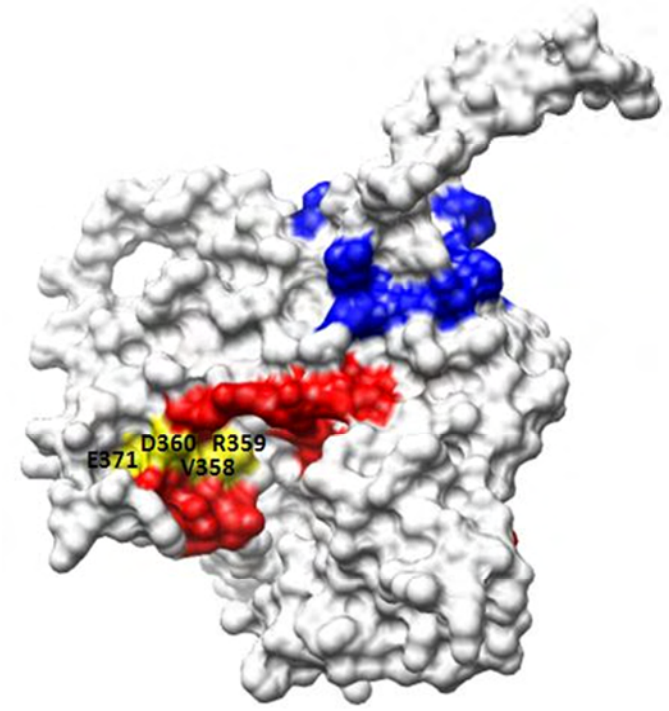

Figure 29: 3DEX result of clone BB-i-12-F6.
Visualized using the CHIMERA software. Residues involved in the interaction with the CD4 receptor are highlighted in red, with the chemokine receptor CCR5 in blue. Mimotope sequence ($E^{371}R^{359}D^{360}F^{373}V^{358}$), overlapping with the CD4 binding site is shown in yellow.

Six mimotopes from the sequential biopanning have been considered for further analysis after comparing the peptide sequences with the SHIV-1157ipd3N4 gp120 monomer model. Another clone (BB-i-12-G7) was overlapping with the CCR5 binding site, two clones (BB-i-12-F6 (shown in figure 29) and BB-i-12-H1) with the CD4 binding site and two clones could be mapped to the surface of the V1 (BB-i-12-B8) or rather the V4 (BB-i-12-G2) loop.

One of the "KLIC" mimotopes (BB-i-12-E3) was included in further in-vitro analysis ('Top 35' mimotopes) as well, but was not analyzed by 3DEX (figure 32 shows only 34 out of 35 most promising mimotopes).

3.3.5. Strategy 3 - Isolation of Potentially Neutralizing Mimotopes by Depleting Binding-Only Antibodies (BB-k)

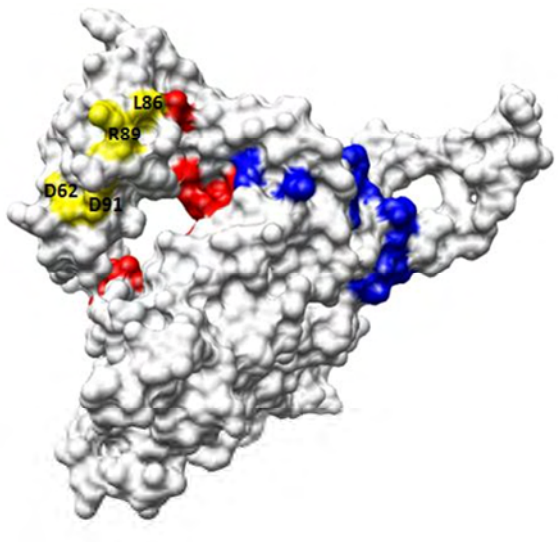

Figure 30: 3DEX result of clone BB-k-7-B12.
Visualized using the CHIMERA software. Residues involved in the interaction with the CD4 receptor are highlighted in red, with the chemokine receptor CCR5 in blue. Mimotope sequence on the V2 loop surface is shown in yellow ($A^{85}L^{86}R^{89}D^{91}D^{62}G^{61}F^{70}$).

For strategy 3, we hypothesized that by depleting binding only antibodies - by using a serum sample with a low nAb titer as a negative selector and using a serum sample with a high titer of neutralizing antibodies as a positive selector - we could enrich for phages representing neutralizing epitopes. After a linear alignment with the SHIV-1157ipd3N4 gp160 sequence most of the selected mimotopes showed homology to a certain part on the V2 loop (^{73}TTEIR^{77}). Additionally, we selected some phages with no obvious linear homology to Env and one KLIC mimotope. All of the in figure 31 shown sequences were used for analysis with the SHIV-1157ipd3N4 gp120 model and the 3DEX software.

Linear Alignment: Phagotopes Biopanning BB-k																			
Phagotopes		Sequences																	
Group 1							**R**	**D**	**D**	**G**	**F**								
BB-k-7-A6 and 7-B8	2x				V	Y	T	D	D	G	F								
BB-k-7-G12					V	Y	R	D	D	G	F								
BB-k-7-B12					A	L	R	D	D	G	F								
BB-k-12-B10			D	Q	T	F	R	D	D	G	F	P	V	T					
Group 2: V2 loop		**C**	**S**	**F**	**N**	**V**	**T**	**T**	**E**	**I**	**R**	**D**	**K**	**K**	**Q**	**K**	**V**		
BB-k-7-A11							T	T	E	I	R	T	V						
BB-k-12-B3							T	T	E	V	W	T	G	D	L	L	T	P	
BB-k-7-D10							T	T	E	V	Q	T	V						
BB-k-7-E5							T	T	E	I	R	T	R						
BB-k-7-F11							T	T	E	I	R	T	D						
BB-k-12-D6							T	T	E	R	L	T	L	A	L	N	S	V	
BB-k-7-G7							T	T	E	V	P	T	Y						
BB-k-7-G8							T	T	E	I	R	T	V						
BB-k-12-D11			I	H	H	R	G	T	E	I	R	T	H	Q					
BB-k-12-D5							S	T	E	I	R	T	H	N	Y	W	A	L	
BB-k-12-D8					Y	V	G	T	E	I	L	T	V	D	L	W			
BB-k-12-C6				S	P	P	G	T	E	I	M	T	W	R	M				
BB-k-12-G2		N	F	M	A	W	G	T	E	I	Q	T	W						
BB-k-12-H9						M	G	T	E	I	L	T	Q	S	T	T	A		
BB-k-12-C8					H	A	G	T	E	I	Q	T	S	N	H	L			
BB-k-12-A3		G	M	K	N	F	G	T	E	Y	R	T	M						
BB-k-12-D9 and B9	2x	T	V	T	N	L	G	T	E	L	M	T	K						
BB-k-12-E6				E	N	H	G	T	E	V	K	T	L	S	V				
BB-k-12-A10 and H6	2x			T	N	Y	G	T	E	K	F	L	G	M	V				
BB-k-12-F4					S	Y	G	T	E	R	Q	T	L	K	H	Y			
BB-k-7-C6						G	G	T	E	R	F	T							
BB-k-12-E7					I	L	G	T	E	V	M	T	L	K	R	T			
BB-k-12-H1					S	A	G	T	E	V	P	T	W	V	R	K			
BB-k-12-B7			V	P	S	H	G	T	E	V	F	T	R	Q					
BB-k-12-H8			D	Y	R	W	G	T	E	V	I	T	F	R					
BB-k-12-C12								T	E	I	Q	T	V	T	H	A	Q	S	R
BB-k-12-H10							H	T	E	I	Q	T	Y	T	S	L	L	T	
BB-k-7-B9							S	T	E	V	R	T	M						
BB-k-7-F12							S	T	E	V	R	T	V						
BB-k-12-G7							S	T	E	V	R	T	T	T	H	S	T	P	
BB-k-12-A8				M	H	Q	S	T	E	V	Q	T	L	L	G				
Group 3: KLIC (gp41)		**L**	**G**	**I**	**W**	**G**	**C**	**S**	**G**	**K**	**L**	**I**	**C**	**T**	**T**	**A**	**V**	**P**	
BB-k-12-A12						M	C	S	G	Q	L	V	C	L	S	M	S		
Group 4		**no recurring motifs**																	
BB-k-7-B10 and k-7-H8	2x				W	P	L	I	Y	Y	T								
BB-k-12-F5					W	V	P	Q	R	T	H	M	S	I	P	H			

Figure 31: Linear Alignment BB-k

Resulting phagotopes of BB-k have been divided into 3 different groups. The most frequent linear motif mimicked a 4 amino acid long part on the V2 loop. Additionally, we selected some phages with no obvious linear homology to the same SHIV-1157ipd3N4 gp160. All of them were included in the 3DEX analysis using the SHIV-1157ipd3N4 gp120 model.

The analysis with 3DEX led to one mimotope overlapping with the CCR5 binding site (BB-k-12-B3), but most of the peptide sequences where located either very close to the CD4 binding site (on the V2 or on the V5 loop, respectively) or overlapping with the Phe43 cavity. Two clones, with the motif 'RDDGF' were assigned to the V2 loop surface by 3DEX. One of them (BB-k-7-B12) is shown in figure 30.

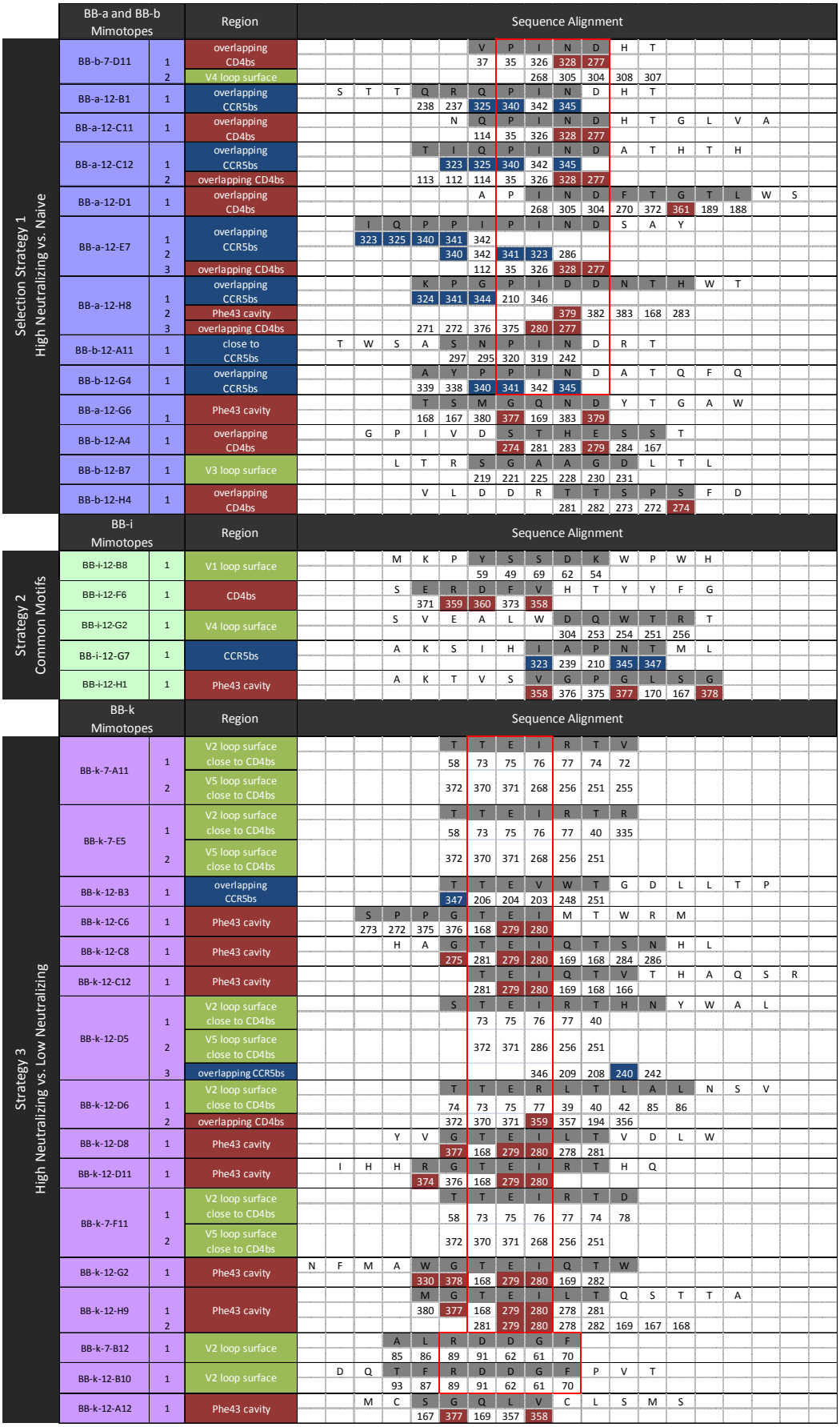

Figure 32: Most promising 3DEX results

The top 34 mimotopes out of 3 biopannings are shown. Peptide sequences overlapping with the CCR5 binding site (CCR5bs) are highlighted in blue, those in contact with the CD4 binding site (CD4bs) in red, and those somewhere on the surface of a variable loop in green. Similar motifs are boxed in red.

3.4. Analyzing Isolated Mimotopes – in-vitro *Experiments*

3.4.1. Verify Specificity of Interesting Clones – Phage ELISA

To confirm the specific binding of all sequenced clones, an additional phage ELISA was performed. This time, each single clone was tested in triplicates. The wild type phage M13KE and 'LB media only' were included as negative controls. Only clones that were confirmed to be positive for their particular positive serum sample were considered for further analysis. In figure 33, one phage ELISA for some clones of the first biopanning (BB-a and BB-b) is illustrated. The average binding signal of all three wells plus standard deviation is shown.

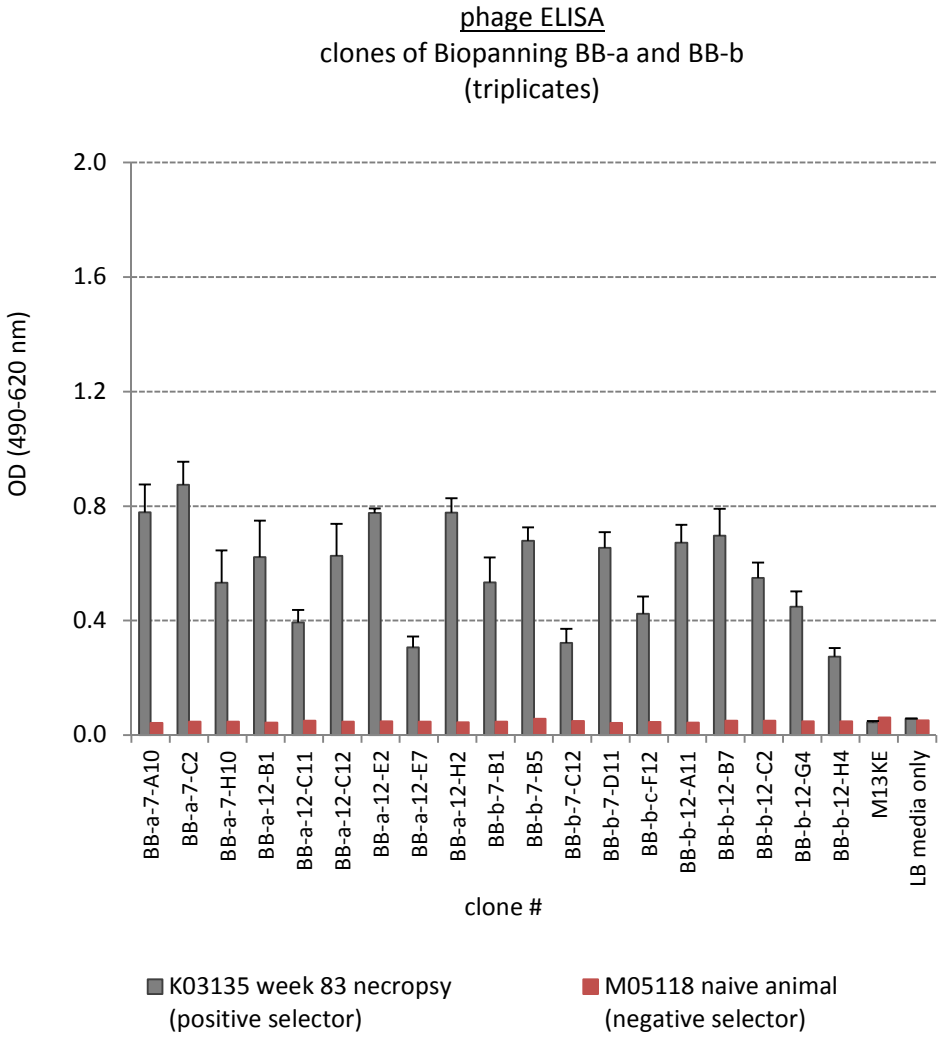

Figure 33: Phage ELISA - BB-a and BB-b.
Some of the sequenced clones are shown (19 out of 50). Positive selector K03135 week 83 (necropsy sample) is shown in grey and the negative selector (naïve animal M05118) in red. To be positive for the target sample, clones have to show a 3-times higher binding for the SHIV-1157ipd3N4 infected serum sample than for the non-infected sample and for the wild type phage control. Negative control 'LB media only' was included as well.

For the sequential biopanning, clones showed a much lower binding specificity than seen with the first biopanning, when using only one positive selector for every round of selection. In many cases, there was barely a three times higher binding signal for all three positive selectors compared to the naïve animal M05118 and the wild type phage M13KE (see figure 34). However, most of the clones were positive for animal K03135 and L03165. Since 70% of the isolated mimotopes showed homologies with an already well known motif - the immunodominant loop KLIC on gp41 - only five clones have been considered for further analysis (BB-i-12-G7, BB-i-12-F6, BB-i-12-H1, BB-i-12-B8 and BB-i-12-G2; see figure 39).

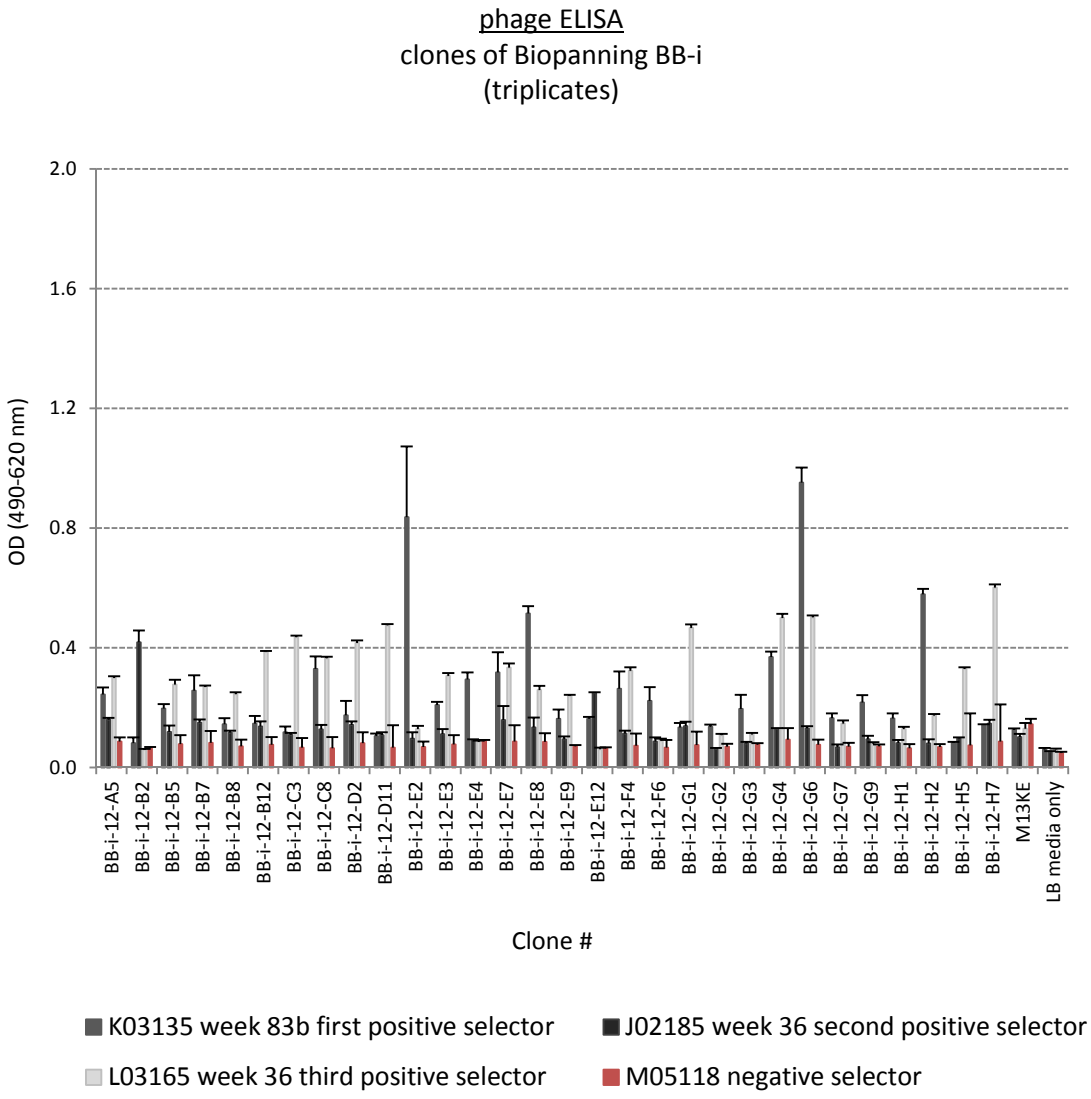

Figure 34: Phage ELISA - Sequential Biopanning (BB-i).
All three positive selectors (K03135 week 83b (necropsy sample), J02185 week 36 and L03165 week 36 are shown in grey, the negative selector (M05118, naïve animal) is shown in red. Most of the clones showed hardly a higher binding specificity than the negative selector. Especially for J02185 - the animal with the lowest antibody titer – most clones did not show a (three times higher) specific binding activity. Negative controls (M13KE and LB media only) were includes as well.

In the case of the third biopanning (BB-k), a high binding specificity for most of the clones was observed (see figure 35) and 16 out of 42 sequenced clones have been selected for further analysis.

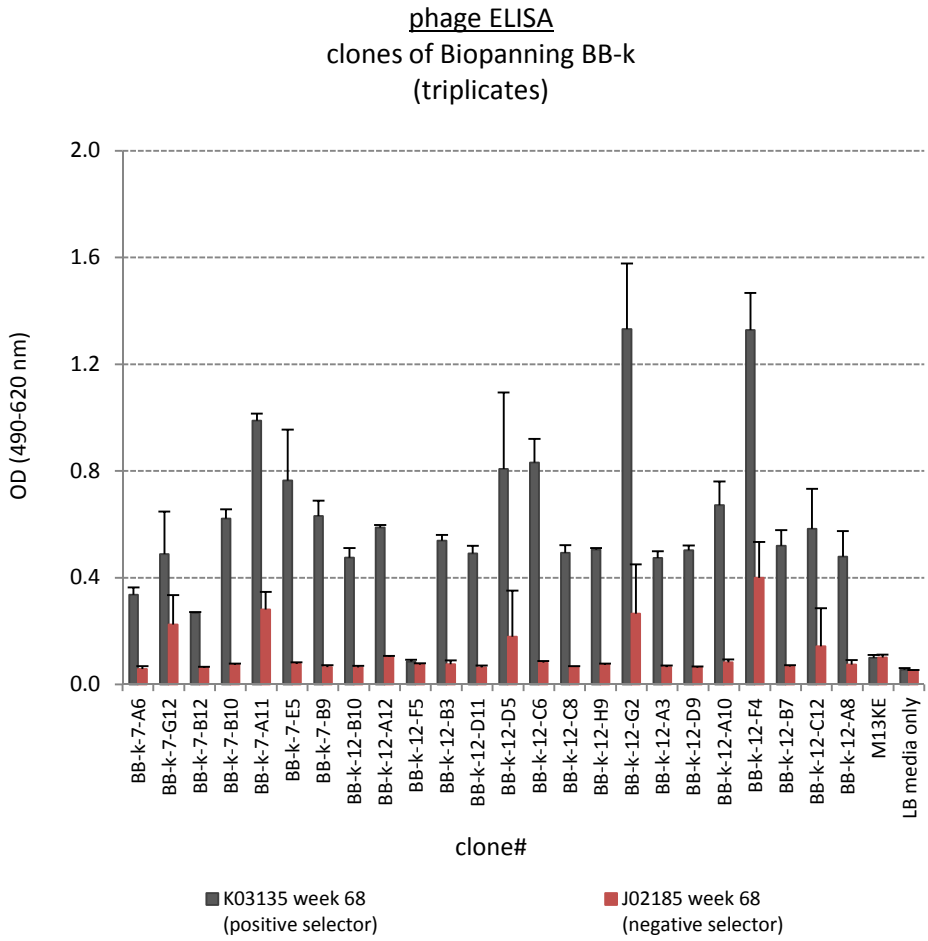

Figure 35: ***Phage ELISA - BB-k.***
Positive selector (animal K03135 week 68) is shown in grey and the negative selector (J02185 week 68) in red. Most of the tested clones showed a binding signal at least 3 times higher than the background signal (negative selector). Both negative controls (M13KE and LB media only) showed only background binding as well.

3.4.2. TOP 35 - Most Promising Mimotopes

After linear alignments, 3DEX analysis and phage ELISA, 35 mimotopes from all three performed biopannings remained as promising candidates. In Table 7, all three performed biopannings are summarized. Out of 1,228 screened clones, 169 have been sequenced (15%) and 122 have been further analyzed according to their homology to the SHIV-1157ipd3N4 envelope proteins. A total of 35 promising candidates (approximately 3%) have been selected and their cross reactivity pattern and their conformational dependence was evaluated (see 3.4.3 and 3.4.4).

Table 7: Summarized results of all three performed biopannings (calculated percentages for each performed selection strategy refer to total amount of analyzed sequences).

Selection Strategy		Strategy 1 High Neutralizing vs. Naïve	Strategy 2 Common Motifs	Strategy 3 High Neutralizing vs. Low Neutralizing
Biopanning Code		**BB-a and BB-b**	**BB-i**	**BB-k**
Sequenced (total amount)		60	49	60
Sequenced Ph.D. 12mer		37	30	30
Sequenced Ph.D. 7mer		17	0	15
Sequenced Ph.D. C7Cmer		6	19	15
Sequences Analyzed (total amount)		**50**	**30**	**42**
Linear Homologies	**no similarities with gp160**	50	7	9
	similarities with gp120	0	3	33
	similarities with gp41	0	20	0
Conformational Homologies	**similarities with gp120**	**84% (42)**	**23% (7)**	**67% (28)**
	similarities with gp41	not tested	not tested	not tested
Top 35 Mimotopes (further analyzed)		**26% (13)**	**20% (6)**	**38% (16)**

3.4.3. Cross Reactivity of Isolated Mimotopes – Cross ELISA

To assess the cross reactivity pattern of all Top 35 mimotopes, they were tested against 13 SHIV-1157ip4N3-infected serum samples (plus one pre-bleed and one naïve sample). The binding signals of each mimotope and each time-point were examined in ratio to the binding signal of each clone with a naïve pig-tailed macaque serum sample (M05118). Clones have been considered as positive when they showed a three times higher binding activity to the test sample compared to the sample of the naïve animal and compared to the binding activity of the wild type phage control (M13KE). In every ELISA a 'LB media only' control was included as well. In figure 36 all binding patterns are summarized and highlighted using a color code.

	K03135 w0	K03135 w28	K03135w44	K03135 w52	K03135 w60	K03135 w64	K03135 w68	K03135 w72	K03135 w76	K03135 w80	K03135w83	K03135 w83b	L031365 w48	J02185 w68
BB-a-12-B1	0.9	1.2	1.2	1.1	1.1	1.0	1.2	1.0	1.3	1.3	14.0	14.6	1.0	1.1
BB-a-12-C11	1.2	1.1	0.9	0.9	1.0	1.2	1.5	1.0	1.2	1.2	15.3	15.9	1.1	1.0
BB-a-12-C12	0.8	1.1	0.9	0.9	0.9	0.8	1.3	0.9	0.9	1.2	11.2	10.6	0.8	0.9
BB-a-12-D1	1.3	1.2	1.1	1.0	1.0	1.2	1.0	1.1	0.9	1.8	17.5	18.5	1.0	1.0
BB-a-12-E7	0.8	1.0	0.8	1.0	0.9	1.0	1.2	1.0	0.9	1.1	10.5	9.7	1.0	0.9
BB-a-12-G6	1.2	1.3	1.0	1.3	1.0	1.1	1.2	1.0	1.1	1.1	13.8	13.0	0.9	0.9
BB-a-12-H8	0.8	1.1	0.9	1.1	1.0	1.0	1.3	1.0	1.0	1.2	13.6	15.0	1.3	0.9
BB-a-c-D2	1.1	0.9	0.9	1.1	1.0	0.9	0.9	1.0	0.9	1.0	13.6	12.2	1.0	0.9
BB-b-12-A11	0.9	0.7	0.9	1.0	0.9	0.8	0.8	0.8	0.9	5.3	18.7	15.4	0.7	1.0
BB-b-12-A4	0.9	0.8	0.7	0.8	0.8	0.9	0.7	0.8	0.9	0.9	15.7	15.1	0.9	0.8
BB-b-12-B7	1.1	1.0	1.2	1.2	1.0	1.0	1.3	1.0	1.1	3.2	11.8	10.4	0.7	0.8
BB-b-12-G4	0.8	0.9	0.9	1.1	1.0	1.2	1.2	1.0	1.2	1.3	17.1	15.8	1.0	1.0
BB-b-12-H4	0.9	1.1	1.2	1.4	1.2	1.6	1.2	1.5	1.1	1.4	14.7	16.3	1.1	1.0
BB-b-7-D11	0.8	0.9	0.8	1.0	1.0	1.0	0.9	0.9	0.9	1.2	14.6	12.4	0.8	0.9
BB-i-12-B8	0.8	1.5	3.6	2.6	2.3	1.8	2.0	2.0	2.4	2.5	3.3	2.2	3.4	1.3
BB-i-12-E3	1.1	2.2	3.8	3.3	2.0	2.6	2.5	3.4	2.2	3.2	3.7	3.0	4.9	1.2
BB-i-12-F6	1.1	2.3	4.1	3.2	2.2	2.4	3.1	2.5	2.9	3.4	4.6	3.5	0.9	0.9
BB-i-12-G2	0.9	1.1	1.8	1.6	1.2	1.3	1.4	1.6	1.7	1.7	2.2	2.0	1.5	0.8
BB-i-12-G7	0.8	2.2	2.9	3.7	2.7	3.3	3.7	3.1	3.8	4.5	4.7	4.0	2.2	0.8
BB-i-12-H1	0.9	4.4	8.6	4.8	4.5	4.0	4.9	4.6	4.9	6.0	7.8	4.8	4.6	1.7
BB-k-12-A12	1.2	7.3	9.3	8.2	7.5	7.1	8.3	7.4	7.9	10.0	10.9	9.3	3.4	1.1
BB-k-12-B10	0.9	1.1	1.0	1.1	1.5	1.1	6.8	5.3	2.7	2.2	2.6	2.5	0.8	1.0
BB-k-12-B3	0.8	0.9	0.9	0.9	3.5	1.7	7.1	5.3	2.4	2.2	2.0	1.6	0.7	0.8
BB-k-12-C12	0.9	1.3	1.1	0.9	2.3	1.3	7.5	6.2	3.0	2.5	2.3	2.1	0.9	1.0
BB-k-12-C6	1.2	1.1	1.2	1.2	5.3	3.4	12.5	9.8	7.1	6.4	4.8	4.7	1.0	1.2
BB-k-12-C8	1.2	1.3	1.2	2.2	2.7	2.1	11.0	6.1	3.2	3.1	2.0	2.3	1.2	1.1
BB-k-12-D11	1.0	1.3	1.4	1.1	3.4	2.3	8.7	6.8	3.7	3.0	3.0	1.8	1.0	1.1
BB-k-12-D5	1.1	1.2	1.1	0.8	3.1	1.9	7.6	5.3	2.6	3.0	2.2	1.9	0.8	1.0
BB-k-12-D6	1.1	1.2	1.1	1.3	1.9	1.6	5.5	3.7	2.0	2.1	1.6	1.5	0.9	0.9
BB-k-12-D8	1.0	1.2	1.2	1.2	2.8	1.7	5.3	5.0	2.8	2.4	2.3	1.7	0.8	1.1
BB-k-12-G2	1.0	0.9	1.6	1.5	6.3	5.4	9.7	8.8	6.5	5.7	5.1	4.5	0.9	1.0
BB-k-12-H9	1.0	2.2	2.6	1.8	3.2	2.0	7.1	5.2	4.6	5.3	5.0	3.8	0.8	1.1
BB-k-7-A11	0.9	0.8	1.0	1.0	1.7	1.9	9.1	5.6	1.5	1.6	2.3	1.5	1.0	1.0
BB-k-7-B12	1.0	1.2	1.1	1.0	1.3	1.0	6.1	5.1	2.1	1.8	1.8	1.8	0.9	1.0
BB-k-7-E5	1.0	0.9	1.0	0.9	3.3	1.6	10.0	6.4	4.0	3.7	3.6	2.0	0.8	0.8
BB-k-7-F11	1.0	1.1	0.9	1.0	2.5	1.7	4.7	5.1	1.9	1.6	1.9	1.3	0.8	1.1

***Figure 36**: **Cross ELISA results**.*
Different time-points of animal K03135 were tested (week 0 (pre-bleed), week 23, week 44, week 52, week 60, week 64, week 68, week 72, week 76, week 80, week 83 and week 83 necropsy sample) as well as animal J02185 and animal L03165). All results are represented as ratio to a naïve pig-tailed macaque serum sample (M05118) and highlighted according to the following heat map (clones have been considered as truly positive when they showed a three times higher binding activity to the test sample compared to the naïve animal (orange colour in the heat map)).

Heat map for cross ELISA	< 1.5	1.5-2.0	2.1-3.0	3.1-5.0	5.1-7.0	7.1-10.0	> 10

As expected, none of the isolated mimotopes showed any binding signal when incubated with the pre-bleed sample of K03135. Mimotopes isolated with the first strategy (BB-a and BB-b, high neutralizing vs. naïve) did not show cross reactivity with earlier time-points or other SHIV-1157ipd3N4-infected pig-tailed macaques (only one clone BB-b-12-A11 reacted with serum sample of K03135 week 80). However, as seen before (phage ELISA), those mimotopes show a very strong reactivity with antibodies from the polyclonal sera used as positive selector (week 83 necropsy sample). In comparison, mimotopes isolated using the sequential antigen panning strategy (BB-i) showed a broad cross reactivity, once already starting at week 28 but the binding signal itself is much lower, compared to BB-a or BB-b mimotopes. Some clones, isolated in the third biopanning (BB-k, high neutralizing vs. low neutralizing), also showed a strong cross recognition, with the highest signal again for their positive selector (K03135 week 68). Only 6 out of 34 tested mimotopes reacted with a second SHIV-1157ipd3N4-infected pig-tailed macaque (L03165) and only one showed cross reactivity with all three tested pig-tailed macaques. All promising mimotopes and their cross reactivity are summarized in figure 39.

3.4.4. Conformationally Dependent Mimotopes – Conformational ELISA

In figure 37, one example of the performed conformational ELISAs is shown. All potential mimotopes (Top 35) have been tested with regard to their conformational dependence. To compare results of all tested clones, the ratio between binding activities of native and reduced phages was calculated and evaluated

according to a heat map (see figure 39). As a negative control the wild type phage M13KE was used. The ratio between native and reduced for the control phage was in average 2.0. Thus, only phages with a ratio higher than that can be considered as conformationally dependent. The anti-pIII antibody control confirmed the equal binding of native and reduced phages in all performed ELISAs.

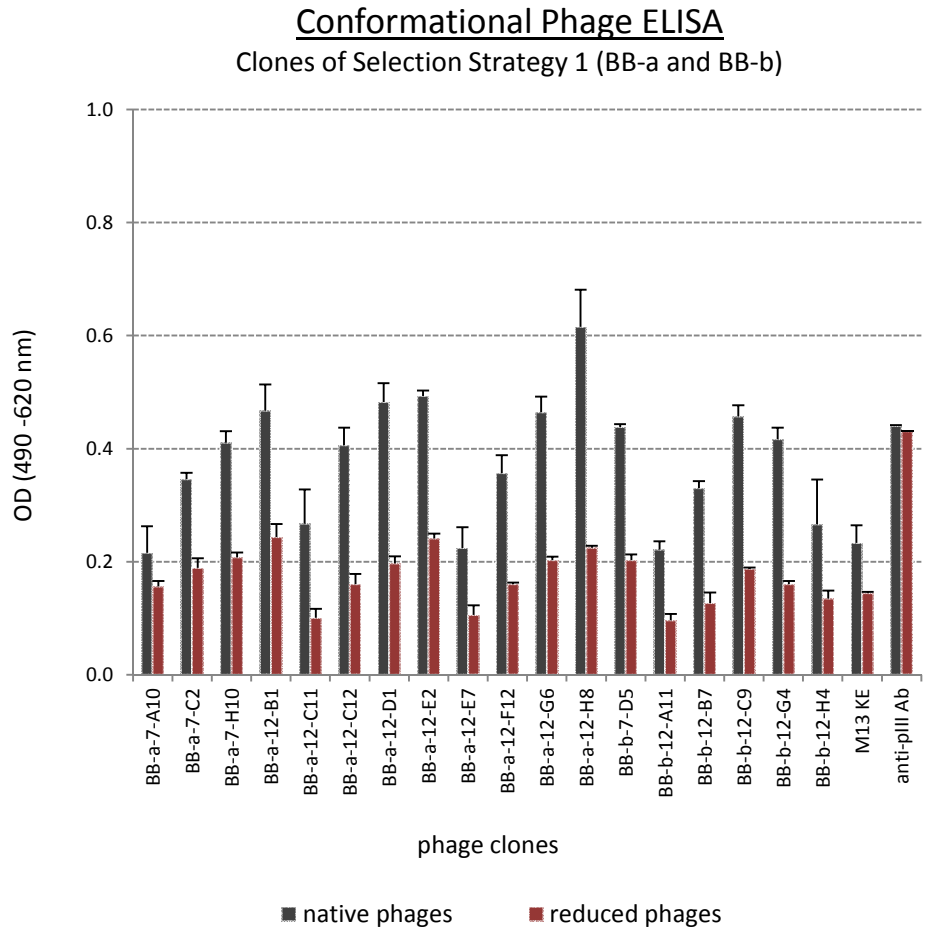

Figure 37: Typical conformational ELISA (BB-a and BB-b).
One example for the performed conformational ELISAs is shown. The native phages (resuspended in coating buffer) are illustrated in grey, the reduced phages (resuspended in reducing buffer) in red. To compare results of all tested clones, the ratio between native and reduced was calculated. Wild type phage M13KE showed an average ratio (of all performed assays) of 2.0. As a binding control (confirming the equal binding of native and reduced phages to the microtiter plate), one well with an anti-pIII antibody was included.

Looking at the resulting heat-map (in figure 39), 17 out of 35 clones showed a higher binding signal when immobilized in their native form compared to their reduced conformation (ratio of at least 2.5 (highlighted in orange)). Most of them had been isolated with the third selection strategy ("high neutralizing vs. low neutralizing", BB-k).

One of the 'KLIC' mimotopes, isolated with the sequential biopanning (BB-i) was included in the assay as well (BB-i-12-E3). The linear ^{589}KLIC^{592} motif is part of the immunodominant region (IDR) on gp41, a disulfide-bridged hydrophilic loop (connecting the two heptad-repeats on the ectodomain, see 1.3.2). Therefore, the 'KLIC' mimotopes was used as a positive control for the conformational phage ELISA and

included in all performed assays. As expected, the “KLIC” mimotope, BB-i-12-E3 showed the highest difference between binding activity of serum antibodies to immobilized native phages compared to reduced ones. According to the heat map, only three other clones (BB-i-12-F6, BB-k-12-G2 and BB-k-12-A12) seem to be as conformationally dependent as BB-i-12-E3.

Since none of the mimotopes isolated with the first selection strategy (BB-a and BB-b) showed a linear homology with SHIV-1157ipd3N4 gp160, we analyzed them with 3DEX by using the SHIV-1157idp3N4 gp120 model. The computational approach revealed some interesting motifs (overlapping with the CCR5 binding and the CD4 binding site, respectively). Unexpectedly, only 3 out of 13 tested clones from selection strategy 1 showed an at least 2.5 times higher binding signal when kept in their native conformation (BB-a-12-H8, BB-a-12-C12, BB-a-12-E7). For the third biopanning – selecting for nAb mimotopes - 10 out of 16 tested mimotopes showed a conformational dependence with a binding signal ratio of at least 2.5 (2 of them (BB-k-12-G2 and BB-k-12-A12) even more than 3.4 (see figure 39, according to color code highlighted in dark red)).

3.4.5. The Most Promising Mimotope – BB-k-12-A12

In figure 39, all Top 35 mimotopes are summarized with regard to their linear homologies with SHIV-1157ipd3N4gp160, their conformational homologies with the SHIV-1157ipd3N4 gp120 model, their cross-reactivity and their dependence on a maintained conformation. Isolated peptides are grouped according their selection strategy and their particular motifs are color coded (CCR5 binding site in blue, CD4 binding site and Phe43 cavity in red, on the surface of any of the five variable loops in green and the KLIC motif in grey.

After all performed tests (computational and experimental based), one clone BB-k-12-A12, showed the most promising results. It showed a specific binding activity for the target sample (at least three times higher binding signal to sample K03135 week 68 compared to J02185 week 68), broad cross recognition of all tested samples (but pre-bleed, naïve sample and negative selector) and a conformational dependence in the same range as the included “positive control” (immunodominant loop region “KLIC”). When first checked for linear homologies with the SHIV-1157ipd3N4 gp160 sequence, we thought to see again a KLIC mimicking peptide sequence. However, according to the 3DEX results, its peptide sequence seems to overlap with the Phe43 cavity, known to be essential for a first interaction of gp120 and the target cell receptor CD4.

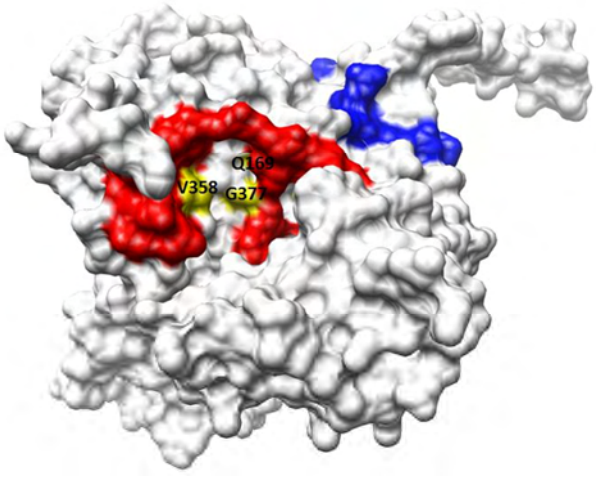

Visualized using CHIMERA software. Residues involved in the interaction with CD4 receptor highlighted in red, with chemokine receptor CCR5 in blue. Mimotope sequence ($S^{167}G^{377}Q^{169}L^{357}V^{358}$) in yellow.

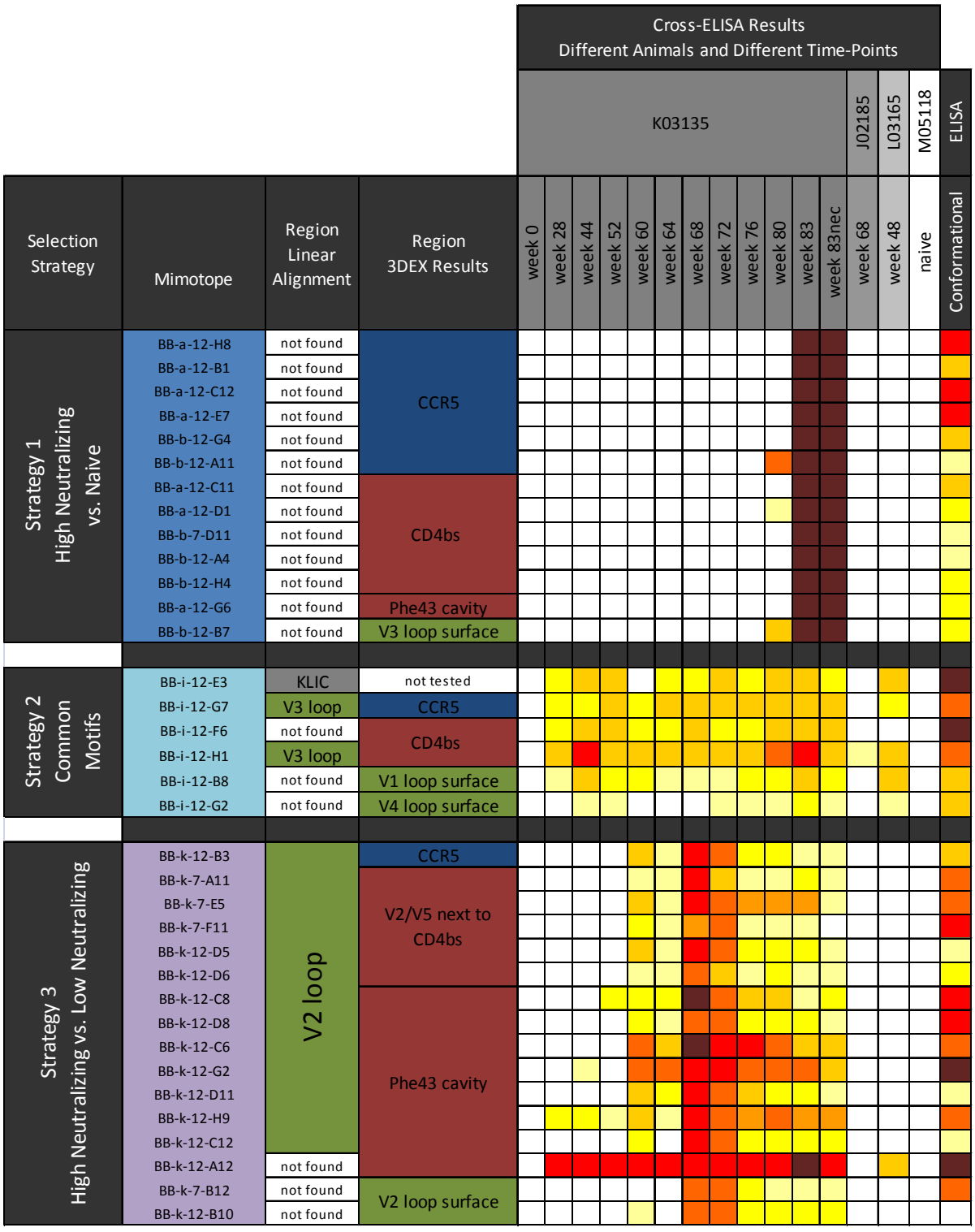

Figure 39: Top 35 - Summary of all promising mimotopes out of three different biopannings.

All promising clones are grouped according their selection strategy. Found motifs are highlighted in particular colours (overlapping with CCR5 binding site in blue, overlapping or close to CD4 binding site or Phe43 cavity in red, and on the surface of a variable loop in green. The immunodominant KLIC motif is illustrated in grey). Results of the cross and conformational ELISA were evaluated according to following heat maps (value is referring to binding signal ratio as described in text).

Heat map for cross ELISA	< 1.5	1.5-2.0	2.1-3.0	3.1-5.0	5.1-7.0	7.1-10.0	> 10
Heat map for conformational ELISA	< 1.1	1.1 -1.5	1.6 -1.9	2.0 - 2.4	2.5 - 2.9	3.0 - 3.4	> 3.4

4 DISCUSSION and FUTURE PERSPECTIVES

The overall goal of this study was the isolation of HIV-1 gp160 mimotopes by screening random peptide phage display libraries with polyclonal serum from three SHIV-C-infected pig-tailed. Three different selection strategies have been performed and resulting phagotopes have been analyzed for linear and conformational homologies to the homologous envelope protein. To identify conformational mimotopes, a monomeric gp120 core protein of SHIV-1157ipd3N4 was modelled and used for computational analysis with the 3D-Epitope Explorer software. Potentially conformational mimotopes have been visualized and evaluated with respect to their position on the gp120 surface. Cross-recognition patterns and conformational characteristics of promising clones have been analyzed experimentally.

In the first part of the discussion, the importance of epitope mapping approaches for vaccine development and our strategy to identify novel HIV specific epitopes will be outlined. Afterwards, the particular results of each performed selection strategy and further implications are discussed.

4.1. HIV Vaccine Approaches and Neutralizing Antibodies

More than 25 years ago HIV, the causative agent of the AIDS epidemic was described for the first time and since then, HIV research focused on understanding the pathogen's life cycle and finding potential drug and vaccine targets, respectively. Antiretroviral therapies have been developed, resulting in a remarkable decrease in morbidity and mortality associated with AIDS, mostly in industrialized countries. However, the HIV epidemic is still spreading, especially in emerging countries, where these therapies are not widely available. Moreover, countries with access to antiretroviral agents have to deal with low therapy tolerability and drug-resistant viral strains. Thus, a classic vaccine preventing HIV infection remains the ultimate goal. Ideally, an HIV vaccine will induce adaptive immune responses capable of clearing the virus completely and producing sterilizing immunity. Despite many vaccine approaches in more than two decades of HIV research have been designed, progress towards an effective immunization against the lentiviral infection is only modest. Reasons for the slow progress can be explained by some unique virus characteristics (e.g. creation of latent reservoirs), and its ability to escape from host immune responses (JOHNSTON et al., 2007; SPEARMAN, 2006; VIRGIN et al., 2010). Indeed, we still have to learn more about the quality and quantity of immune responses that should be induced (figure 40, "correlates of immunity") and how to overcome the enormous virus sequence variability due to the error-prone reverse transcriptase ("antigens to be targeted") (VIRGIN et al., 2010 and figure 40).

Early immunization approaches focused on developing recombinant forms of the viral envelope protein, which is believed to be the main target of neutralizing antibodies. Today, after many failed phase 1 and two phase 3 clinical trials, it became clear that eliciting broadly neutralizing antibodies against the envelope is not as simple as thought in the beginning. First of all, the spike molecules on the viral surface are not present as monomers but as trimeric proteins. Thus, conserved regions of the monomer are often

occluded in the native trimer and cannot be targeted by neutralizing antibodies. Second, a glycan shield hiding the virus from the immune system covers the native envelope protein. Third, until binding of gp120 to CD4 followed by extensive conformational changes, vulnerable co-receptor binding sites are protected. Fourth, the host's capacity to generate effective neutralizing antibodies will always lag behind the ability of the virus to generate neutralization escape variants due to sequence variations in the exposed variable loops. Last but not least, to prevent infection high titers of neutralizing antibodies are required. Despite all these challenging tasks, weak signals of protective immunity from vaccine studies in humans (a recent phase III trial in Thailand showed a 30% decrease in HIV acquisition after immunization; RERKS-NGARM et al., 2009) and more promising ones in animal models (BABA et al., 2000; FERRANTELLI et al., 2004; FERRANTELLI et al., 2007; MC CANN et al., 2005; PARREN et al., 2001; RUPRECHT et al., 2003) have been observed.

Besides trying to elicit high titers of neutralizing antibodies, most of the current vaccine approaches are focusing on inducing HIV specific T-cell immunity. $CD8^+$ cytotoxic T lymphocytes (CTL) are believed to help controlling early HIV infections by limiting viral replication to levels that can prevent or at least delay disease progression. Some of the designed $CD8^+$ T cell vaccines were already described in 1.4. Although protection was achieved in rhesus macaques by applying a vaccine vector for generating a SIV-specific effector memory T-cell response (HANSEN et al., 2009), a cell-based vaccine approach in humans (recombinant adenovirus encoding several HIV-1 proteins) failed to reduce viral replication in vaccinated people. (BUCHBINDER et al., 2008).

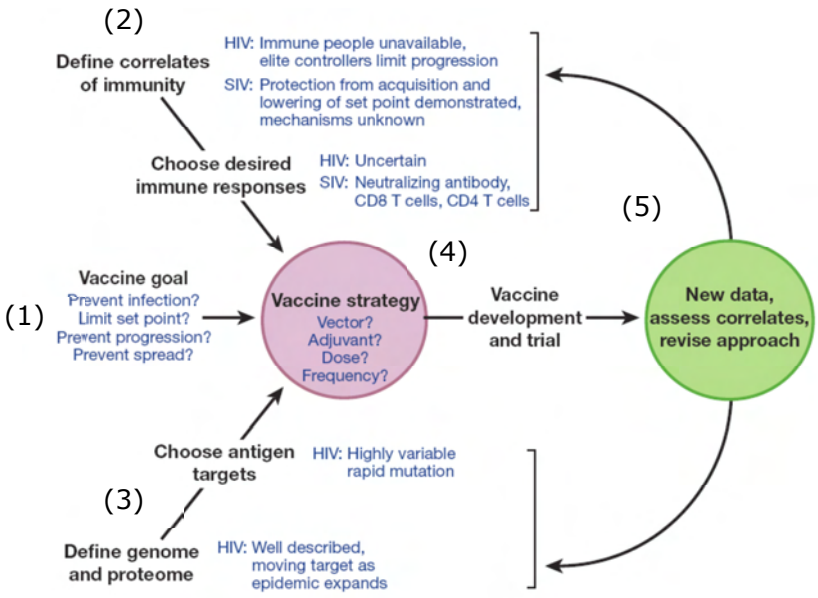

Figure 40: Vaccine approaches and remaining questions to be answered. Key steps in the development of a vaccine strategy (black) and still remaining questions are illustrated (blue). Three major questions (1-3) should be answered before starting with the vaccine development and clinical trials. (1) The vaccine goal has to be defined (e.g. prevent infection itself or prevent disease progression). (2) Possible and desired immune responses developed against HIV (correlates of immunity) should be described. Characterizing elite controllers (LTNPs, see 1.2.2) or protected monkeys might provide insight into the mechanism for protection. (3) By knowing the genome and proteome characteristics of HIV, possible antigen targets can be identified (e.g. conserved vs. variable regions). Based on the answers to these questions the vaccine strategy and factors of influence (such as dose or used adjuvants) can be defined (4). Vaccine trials will be helpful to assess correlates or, in the case of failure, revise performed approaches (5). Adapted from VIRGIN et al., 2010

For both vaccine approaches, certain limitations are well described. First of all, T-cell based vaccines are not able to clear HIV reservoirs completely or to provide sterilizing immunity. Further, escape mutants can develop quickly due to the ability of the virus to develop escape mutants by accumulating mutations in T-cell epitopes. Antibodies, on the other hand are indeed crucial for preventing infections by neutralizing or

eliminating virions during the phase of acute infection (see also 1.4). Not surprisingly, almost all current vaccines protecting against viral pathogens are based on the generation of neutralizing antibodies in serum or on mucosa (PLOTKIN, 2008). Nevertheless, numerous attempts to develop antibody-based vaccines against HIV showed only limited success. Detailed information on important epitopes of gp120 and gp41, known to be targeted by neutralizing antibodies and the implications for further antibody-based vaccine designs are summarized in HOXIE, 2009, PANTOPHLET et al., 2006 and ZOLLA-PAZNER, 2004.

To overcome the limitations of each arm of the adaptive immune response, it is believed that a successful vaccine should elicit responses provided by antibodies as well as T cells. To achieve protection, the humoral and the cellular arm of the immune system should be capable of recognizing diverse strains of HIV and should reach the sites of infection before the infection is established irreversibly. A summary of so far performed vaccine approaches and their limitations can be found in FAUCI et al., 2008; JOHNSTON et al., 2007; MCMICHAEL, 2006; MCMICHAEL et al., 2003; SPEARMAN, 2006; VIRGIN et al., 2010.

Taking the results from recent vaccine trials together, it is believed that one major part in vaccine development should focus on the identification and characterization of novel Env immunogens, targeted by broadly neutralizing antibodies. Screening polyclonal serum of HIV-infected patients or SHIV-infected monkeys with high nAb titers could help to isolate epitopes on gp120 and gp41 involved in the protection against virus strains from different subtypes (HOXIE, 2009). Keeping these goals in mind, we performed an epitope mapping methodology to analyze polyclonal serum samples of clade C SHIV-infected pig-tailed macaques, which showed nAb titers not only against the homologous virus (SHIV-1157ipd3N4) but also against heterologous clade B viruses (HO et al., 2009).

4.2. Three SHIV-1157ipd3N4-Infected Pig-Tailed Macaques

As explained in 1.5, non-human primates have played an important role in HIV and AIDS research. A detailed understanding of the biology and pathogenesis of SIV infections in natural hosts might be the key step to understand infection mechanisms of the closely related virus in humans just as well as the pathogenesis of the caused disease. Chimeric constructs of simian and human immunodeficiency viruses have been used to study immune responses developed against HIV Env. Most of the so far developed SHIV strains combined a SIVmac239 backbone with *env* derived from HIV-1 clade B-strains. Following UNAIDS, the global distribution of HIV-1 subtypes is dominated by subtype C (50% of all infections worldwide), followed by subtype A (12%), B (10%), D (3%) and G (6%) (HEMELAAR et al., 2006). To mimic human HIV-1 transmission as closely as possible, co-receptor tropism and the used transmission route should also be considered when designing vaccine studies using SHIV strains. Thus, a highly replication-competent clade C SHIV fulfilling biological relevant criteria was recently constructed and termed SHIV-1157ipd3N4 (SONG et al., 2006). SHIV-1157ipd3N4 contains an envelope gene from a HIV-

C isolate, uses R5 as a co-receptor, is mucosally transmissible and is susceptible to antibody-mediated neutralization.

Macaca mulatta have been frequently used as animal models in challenge studies and developed HIV gp160-specific antibody responses have been evaluated by analyzing polyclonal serum samples of SHIV-C-infected rhesus macaques (HUMBERT et al., 2008a). However, not much is known about the outcome of primate lentiviral infections in other macaque subspecies, such as *Macaca nemestrina.* Recently, the pathogenesis induced by SHIV-1157ipd3N4 in pig-tailed macaques was shown to be very similar to the pathogenesis observed in R5 SIV/SHIV-infected rhesus macaques (HO et al., 2009). In this follow-up study, we aimed to dissect the humoral immune response in these SHIV-C-infected pig-tailed macaques.

4.2.1. Evaluating Antibody Responses of SHIV-1157ipd3N4-Infected Pig-Tailed Macaques

For this study, three pig-tailed macaques infected with SHIV-1157ipd3N4 (from HO et al., 2009) were screened for specific antibody responses. To confirm that the selected animals developed an antibody binding titer against the HIV envelope protein, we performed two independent assays. A Western Blot showing the reactivity of antibodies with individual HIV viral antigens and an indirect ELISA detecting gp120 specific antibodies only. As explained in 1.5.2, SHIV-1157ipd3N4 was engineered by combining a SIVmac239 backbone with the envelope of HIV-1157i. Hence, the antibody response against the envelope is expected to be HIV-specific. Since SIV and HIV are closely related, antibody responses against other viral proteins are expected to cross-react and therefore it is not surprising that p31, p24 and p17 were detected (in all of the tested samples, but not in the negative controls) in the performed HIV-specific Western Blot (see 3.1.2 and figure 20). We were able to confirm previous results from Ho and co-workers in both assays (HO et al., 2009). All infected animals developed HIV-specific antibodies, with animal J02185 showing the lowest titer. However, it is known that for HIV, the antibody binding titer does not always correlate with the cross-clade neutralization capacity.

As described in the original publication, nAb activities were measured using a pseudotyped virus assay. Animal L03165 and animal K03135 showed the highest titers of neutralizing antibodies (see figure 46), not only against the homologous SHIV strain but also against subtype B, such as $HIV_{SF162LS}$ and $SHIV_{SF162P4}$. The neutralization assay was performed using TZM-bl cells (see 2.2.3). To measure neutralization activity of SHIV-1157ipd3N4-infected pig-tailed macaques 293T cell-grown pseudoviruses have been used. Although the TZM-bl assay is convenient as a high-throughput assay, some key points have to be considered. First of all, the HeLa cells are an immortal cell line derived from cervical cancer cells. Thus, they cannot be considered as natural HIV target cells. TZM-bl is a CXCR4 positive HeLa clone, which has been engineered to express CD4 and CCR5 in higher amounts than found on lymphocytes. Another approach to determine the neutralization activity is using the conventional PBMC (Peripheral Blood Mononuclear Cell)-based assay, where neutralization is measured as reduction in viral p24 (for HIV) or p27 (for SHIV). Compared to the TZM-bl assay, the primary cell based assay is more time-consuming but involves multiple rounds of virus replication and involves the most physiological target

cells (POLONIS et al., 2008). Keeping those facts in mind, it would be important to also evaluate the nAb activity of SHIV-1157ipd3N4-infected pig-tailed macaques with the biological more relevant PBMC assay.

Based on the original publication (HO et al., 2009) and nAb titer results shown in figure 46, we designed three different selection strategies. With the first biopanning we aimed to select mimotopes representing motifs of SHIV-1157ipd3N4 gp160. It is believed that broad specific neutralizing antibody responses are generated later in HIV infections (MCMICHAEL et al., 2010; STAMATATOS et al., 2009; ZOLLA-PAZNER et al., 2010) due to antibody maturation mechanisms (e.g. somatic hypermutation). Thus, we decided to use the latest available time point of animal K03135 - showing a high cross-clade nAb titer - as a positive selector. To deplete phagotopes mimicking non-HIV-specific epitopes we used a naïve animal as negative selector. The second goal of this study was to select for common mimotopes shared by three SHIV-1157ipd3N4-infected pig-tailed macaques (based on the “sequential antigen panning” strategy described in ZHANG et al., 2004). Non-HIV-specific mimotopes have been depleted by using the same naïve animal as in the first biopanning in the negative selection rounds. With the last biopanning we wanted to drive the selection towards neutralizing antibodies. Therefore, we improved our first selection strategy and used a SHIV-1157ipd3N4-infected pig-tailed monkey with a very low nAb activity as a negative selector. We hypothesized that by depleting binding-only antibodies we could enrich for phages representing neutralizing antibody epitopes. Unfortunately, the only monkey with low nAb titers (J02185) showed a much lower binding titer as well (see figure 20 and figure 21). To enrich for nAb epitopes it would be ideal to use serum samples showing a low nAb activity but the same amount of binding titers as the positive selector.

4.3. Epitope Mapping by Peptide Phage Display

Although the phage display technology is a very powerful tool for epitope mapping and identification of novel immunogens (examples discussed in the introducing chapters, 1.6.2 and 1.6.3), there are also some limitations to consider when working with phage-displayed random peptides libraries (PDPLs). As reviewed in MENENDEZ et al., 2005, every PDPL contains “target-specific binders” as well as a phage population displaying “target-unrelated peptides”. Those peptides are known to react with components of the screening system, such as constant regions of antibodies or the solid phase used for immobilization (in our case paramagnetic beads). The comprehensive review paper, lists common motifs of unspecific binders to system components, which were selected in various screenings throughout the years. This negative list should be considered when analyzing the results of screenings using random peptide libraries. It is important to mention that the problem of selecting unrelated sequences in such a phage display screening can be reduced by simply restricting potential phage peptide targets in the system to the minimum right from the beginning. Thus, all our protocols are set up in such a way that eventual selection of unrelated peptides would be eliminated in the included negative selections. Of note, none of our isolated mimotopes showed obvious similarities with any of the known target-unrelated motifs.

4.3.1. Using Polyclonal Serum to Isolate HIV gp160 Specific Mimotopes

To dissect the humoral immune response of three SHIV-1157ipd3N4-infected pig-tailed macaques we used polyclonal serum samples to screen for gp160 mimotopes. A previous study of the Ruprecht laboratory described the successful isolation of novel mimotope immunogens from polyclonal rhesus macaque samples, capable of inducing broadly reactive neutralizing antibodies in mice (HUMBERT et al., 2008a). As described elsewhere (LU, 2000), the percentage of total serum IgG in an HIV-infected individual directed against gp160 is only approximately 2.6%. By performing several rounds of positive and negative selection, we were able to enrich for gp160 mimotopes although polyclonal serum was used instead of purified, HIV-1-specific antibodies.

4.3.2. Computational Analysis of Isolated Mimotopes

Since many of the selected positive clones did not show any obvious linear homology to the primary SHIV-1157ipd3N4 gp160 sequence we used a SHIV-1157ipd3N4 gp120 model and 3DEX to identify discontinuous mimotopes on the three-dimensional structure. 3DEX was used in various publications to identify and describe potentially conformational mimotopes selected from phage display screenings (HUMBERT et al., 2007; HUMBERT et al., 2008a; SCHREIBER et al., 2005). The usefulness of applying computational analysis to identify conformational epitopes is also shown by the development of other software packages similar to 3DEX (HUANG et al., 2006; MOREAU et al., 2006; MUMEY et al., 2003; NEGI et al., 2009; PIZZI et al., 1995).

After the phage ELISA and sequencing of positive clones, approximately 100 peptide sequences have been checked for conformational homologies to the gp120 monomer. Due to probability most of them showed positive hits when analyzed with 3DEX, and thus we decided to include only sequences with homologies of at least five amino acid residues for 12mer mimotopes and at least four amino acid residues for 7mer mimotopes for further experiments. As calculated in 3.3.2 (equation 2), the probability to isolate a 4mer motif of the gp120 protein due to chance is lower than 0.5% and for a 5mer motif even lower than 0.02%. More than 50% of all, with 3DEX analyzed, mimotopes showed homologies with at least 4 amino acid residues. Some of the positive clones showed similarities of 7 out of 7 (BB-k-7-A11, BB-k-7-E5, BB-k-7-F11 and BB-k-7-B12) and one 9 out of 12 (BB-k-12-D6) amino acid residues.

To select promising peptide sequences, we used the gp120 model and checked predicted discontinuous mimotopes with regard to their location on the protein surface and if they are overlapping with epitopes known to be important either for neutralization or for virus entry (receptor and co-receptor binding sites). Before discussing the results in detail, some key points should be considered. First, as described in the original publication (SCHREIBER et al., 2005) the 3DEX-based analysis is not as detailed as other programmes, which consider more different parameters and include mathematical calculations as well as energy minimizations. However, just because 3DEX is very simple with regard to the adjustable parameters, it is – in contrary to other software packages – suitable for high-throughput analysis and thus helped us to select interesting mimotopes from a vast of sequences isolated in our biopannings. Second,

the SHIV-1157ipd3N4 model was based on a published X-ray structure of the HIV-1 subtype B strain JR-FL and shows only the monomeric form of gp120. Therefore, exposed epitopes on the monomer could be hidden in the trimeric form and hits found by 3DEX might have no biological relevance. Also, we would not be able to identify mimotopes which play an important role as mimicking epitopes for so called quaternary-specific antibodies (KWONG et al., 2009; PANCERA et al., 2010; ROBINSON et al., 2010; ZOLLA-PAZNER et al., 2010). Third, we have to keep in mind that the analysis was performed on a computer-based model and not on the actual structure. Variable loops 1, 2 and 4 have been modelled into the structure since they are not present in the original crystal structure. Also, the published structure is the conformation of the gp120 core after attachment to the CD4 receptor and in addition, the protein is co-crystallized with an antibody fragment. This means that the structure is not the native form present on the free virions and thus not ideal for the analysis of neutralizing antibody epitopes exposed prior CD4 binding. Of note, with some of the CCR5 mimotopes we performed an additional analysis using the original JR-FL structure and observed similar results as seen with the SHIV-1157ipd3N4 model (data not shown). Interestingly, most of the identified motifs seem to overlap with epitopes of the core structure (mainly amino acid residues of the conserved receptor and co-receptor binding sites) and only a very few ones map to the variable loops. It is known that broadly neutralizing antibodies target conserved regions on gp160 to evade the problem of virus diversity. If our selection strategy was successful and we were able to enrich for peptide sequences mimicking neutralizing antibody epitopes it is not surprising that most of them overlap with conserved regions. On the other hand, one could argue that the variable loops of our model have been calculated computationally and might not represent biological relevant structures. This question can only be answered with immunization studies in animal models to confirm that those mimotopes are able to induce neutralizing antibodies in vivo.

As a side note, an HIV subtype C structure was published this year (DISKIN et al., 2010) and since our model was based on a subtype B structure (HUANG et al., 2005) it might be interesting to analyze our mimotopes with a model based on a maybe more relevant structure.

Due to technical hurdles, no crystallized structure of the transmembrane part of Env (gp41) including all three major domains (summarized in 1.3.2) has been published so far. Three laboratories crystallized a proteolytically stable core of the extraviral domain of gp41 not including the N-terminal hydrophobic fusion peptide, the disulfide-loop region linking the N-HR and C-HR regions, and the membrane-proximal region (reviewed in ZWICK et al., 2004). Thus, the isolated mimotopes were not analyzed for conformational homologies to gp41. However, we have designed an approach to show gp41-specific mimotopes experimentally (see 4.5.1).

4.4. Isolated Mimotopes of 3 Different Selection Strategies

With the combination of peptide phage display and computational analysis we were able to identify potential mimotopes of gp160. Depending on the performed selection strategy, different kinds of mimotopes have been selected. For us, the most promising candidates for the intended pilot immunization study were those overlapping with - for virus entry important - residues of gp120 (sites involved in the

receptor or co-receptor binding). For this reason, mainly those mimotopes are discussed in the following parts.

4.4.1. Mimotopes of the Receptor and the Co-Receptor Binding Site

By using a late-time point serum sample of a SHIV-1157ipd3N4-infected pig-tailed macaque with a high neutralizing antibody titer (K03135 week 83) as a positive selector and a naïve pig-tailed macaque as a negative selector, we postulated, that we could deplete all non-HIV specific antibodies and select for gp160-specific mimotopes. For this biopanning we titered the eluted phages after three rounds of selection as well as the phages from the second positive eluate. The isolated phagotopes showed very similar motifs. The only difference, after three rounds of selection we saw approximately 25% more positive clones in the performed phage ELISA. However, all selected clones showed a highly specific binding activity to the positive serum.

Interestingly, 86% of the isolated motifs showed a common motif (PIxDxT), but none of them shared linear homologies with the envelope protein sequence or any other SHIV protein. Since neutralizing antibodies often target conformational epitopes, we analyzed them for structural homologies using the 3DEX software. With this approach, we could identify discontinuous gp120 mimotopes overlapping with the CCR5 binding site. To evaluate their potential for cross-reactivity, we tested them in a phage ELISA using twelve different time points of animal K03135 (the monkey which had been used as positive selector) as well as one serum sample each of SHIV-1157ipd3N4-infected animals J02185 and L03165 and of the naïve animal M05118. All clones showed a specific binding signal to animal serum K03135 of week 83, the used positive selector, but no cross-reactivity with any of the other tested sera. The identification of positive mimotopes confirms that the performed affinity selection has worked. However, it is possible that some clones might actually still mimic unrelated epitopes. Monkey K03135 developed heart problems between week 77 and week 80 post infection and had to be euthanized at week 83 (personal communication with Dr. Shiu-Lok Hu). Cardiac abnormalities have already been described in HIV-infected individuals (especially in infants and children, KEESLER et al., 2001; SANI et al., 2005; SUDANO et al., 2006) and SIV-infected rhesus macaques (YEARLEY et al., 2006; YEARLEY et al., 2007). Since all isolated mimotopes showed only significant binding for the polyclonal serum of week 83 and we isolated only one discontinuous, immunodominant mimotope (BB-b-12-B7, GPG motif on V3, see 3.3.3 and 4.4.2), it is possible that most of them mimic antibodies developed in response to opportunistic manifestations (such as the cardiac abnormalities). Thus, it will be important to confirm that these non-cross reactive mimotopes are indeed gp120-specific (see 4.5.1).

In 2000, Rizzuto and Sodroski described five highly conserved amino acid residues on gp120 (^{420}IKQ^{422}, P^{438} and G^{441}, numbers according to original publication, see figure 41A and table 8), important for the interaction with the co-receptor CCR5 on the target cell. (RIZZUTO et al., 2000). Of particular interest, one promising mimotope (BB-a-12-H8), shares homologies with three of those residues (K^{324}P^{341}G^{344}, see figure 41B, numbers according to SHIV-1157ipd3N4 gp120 model).

In 2003, Xiang and co-workers showed that two of these five important residues, K^{421} and Q^{422} are recognized by a so-called CD4-induced (CD4i) monoclonal antibody, E51 (XIANG et al., 2003). In general, the neutralizing activity of antibodies against the CCR5 binding site was described as weak or modest. However, they are known to react better with gp120 after attachment of gp120 to soluble CD4 (sCD4) (ZOLLA-PAZNER, 2004). Factors such as the conformational flexibility, variable loop masking of gp120 and steric hindrance of antibody binding are described to be crucial for the efficacy of such CD4i antibodies. CD4 binding and triggered conformational changes in gp120 expose the CD4i epitope. Several human monoclonal antibodies have been identified, although most of them did not show a broadly neutralizing activity. Furthermore, CD4i antibodies (such as 17b, X5, m9) are not able to neutralize most of the primary isolates in their complete IgG form. The antigen-binding fragment (Fab) and single-chain fragments on the other hand showed a broadly neutralizing activity (ZHANG et al., 2010). These observations can be explained by steric constraints, given that the distance between the CD4i epitope on gp120 and the target cell seems to be too small to accommodate an entire IgG molecule (LABRIJN et al., 2003). One of the best described CD4i antibodies is 17b (X-ray crystal structures complexed with gp120 core and CD4 are available; KWONG et al., 1998; KWONG et al., 2000). Three amino acid residues on gp120 have been described to be important for the interaction of 17b and the CCR5 binding site (I^{420}, Q^{422} and I^{423}). Two isolated mimotopes of this study (BB-a-12-E7 and BB-a-12-C12) showed conformational homologies with two of the three important residues (I^{323} and Q^{325}, on the SHIV-1157ipd3N4 gp120 model). Besides evaluating their ability to induce nAb activity, it would be interesting to see if the mimotopes can inhibit the binding of 17b to a gp120-sCD4 complex (see 4.5.3).

Besides the identification of CCR5 binding site mimotopes, 3DEX also found potential mimotopes overlapping with the CD4 binding site (mostly amino acid residue D^{277} of the PIxDxT motif). We included the mimotopes in our mouse vaccination study as well (see 4.5.4).

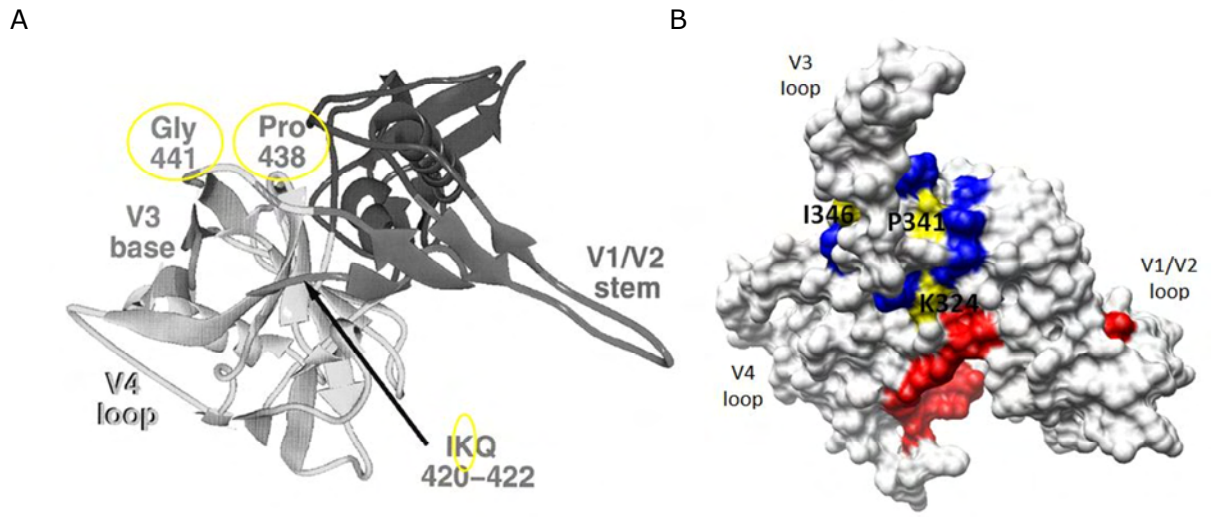

Figure 41: Illustration of conserved residues on gp120, important for interaction with CCR5 receptor.
(A) Ribbon drawing of the CD4-bound gp120 core, amino acid residues important for CCR5 binding are illustrated (^{420}IKQ^{422}, G^{441} and P^{438}). From RIZZUTO et al., 2000. (**B)** Corresponding gp120 model of SHIV-1157ipd3N4 is shown (visualized using CHIMERA). Amino acid residues important for CD4 binding are highlighted in red, those important for CCR5 binding in blue. Mimotope BB-a-12-H8 ($K^{324}P^{341}G^{344}P^{210}I^{346}$) is illustrated in yellow. This clone showed homologies with three of the five predicted amino acid residues (G^{344} can be found on the backside of the shown molecule, hidden by the V3 loop). For a better orientation V1-V4 are indicated.

4.4.2. Mimotopes of Immunodominant Epitopes

The third strategy was based on the "sequential antigen panning" approach (ZHANG et al., 2004). By changing the positive selector with each round of selection, we sought to select common and maybe conserved epitopes shared by all three SHIV-1157ipd3N4-infected pig-tailed macaques.

Not surprisingly, 70% of the isolated mimotopes showed similarities to the immunodominant ^{589}KLIC^{592} motif (see figure 42, amino acid numbering according to SHIV-1157ipd3N4 gp160), one clone (BB-i-12-H3) even sharing 7 identical amino acid residues (^{586}CSGKLIC^{592}). All of the selected KLIC motifs showed the two flanking cysteine residues (see figure 28), responsible for the loop formation (see figure 42) in that gp41 region. Moreover, two of the selected mimotopes overlapped with another immunodominant motif, which is found in the V3 loop (^{221}GPG^{223}; GORNY et al., 2004). Similar immunodominant mimotopes selected from HIV-1-infected individuals or SHIV-C-infected monkeys have already been described in the literature (CHEN, X. et al., 2001; HUMBERT et al., 2007; HUMBERT et al., 2008a; SCALA, G. et al., 1999) and can be considered as a "*proof of principle*" for a successful affinity selection procedure to isolate gp160 mimotopes using polyclonal serum samples.

Overall, the percentage of positive phages isolated was not as high as seen with biopannings using only one positive selector in all three biopanning rounds. In total, only 16 common clones were isolated (6%) and most of them showed a weak binding signal in the second phage ELISA. However, six clones have been included in further analysis and all of them showed a broad cross-reactivity for at least 2 out of 3 animals (although with an overall lower binding signal for each sample) confirming that our sequential biopanning approach was partly successful. It is not surprising that most of the clones showed higher binding for animal K03135 and animal L03165 since these two animals showed also the highest binding titers against gp160 in the Western Blot and against gp120 in the indirect ELISA (see

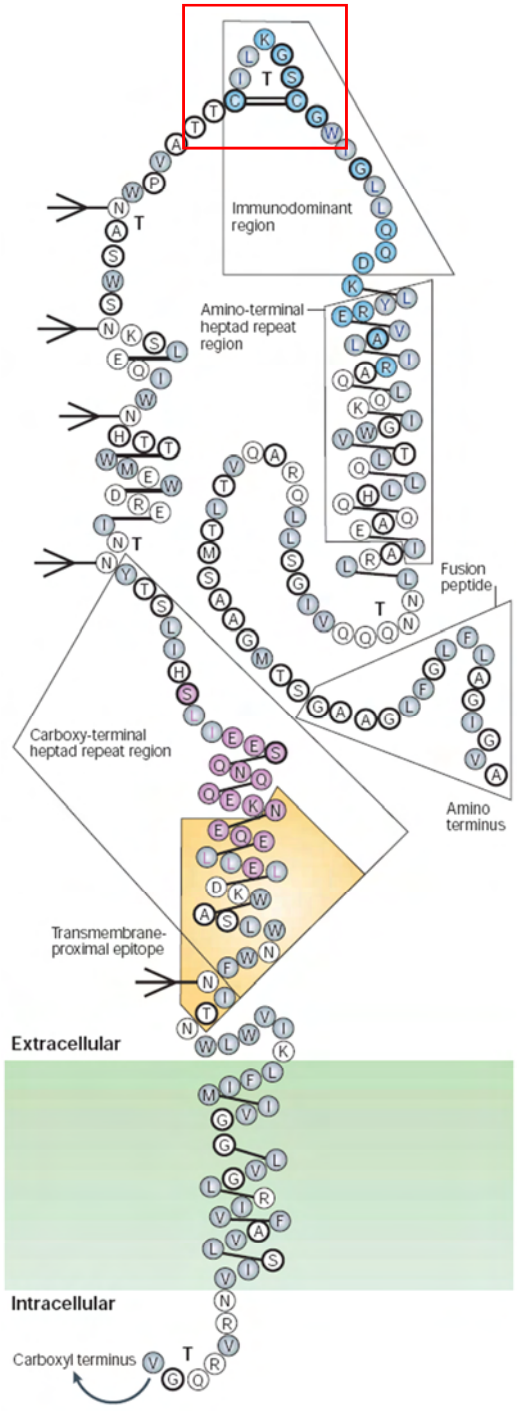

Figure 42: Schematic illustration of the gp41 structure.
Intracellular, transmembrane and extracellular parts are shown. The "KLIC" motif of the immunodominant region is boxed in red. Strong turns (T) and potential glycosylation sites (branched-stick figures) are indicated. From ZOLLA-PAZNER, 2004.

4.2.1). We included mimotope BB-i-12-H3 (see above) as a positive control in the conformational ELISAs. Giving the fact that the KLIC motif forms a small loop due to the flanking cysteine residues (see figure 42) we hypothesized a decreased binding activity after reducing the peptide conformation. Thus, mimotopes that showed similar results as the KLIC mimotope in our reduced ELISA have been considered as conformationally dependent (BB-i-12-F6, BB-k-12-G2 and BB-k-12-A12). Taken those observations together, the sequential biopanning did not lead us to novel immunogens, but was helpful as a proof of concept strategy.

4.4.3. Conformationally Dependent Mimotopes of the Phe43 cavity

With the third performed biopanning we aimed to drive the selection pressure towards neutralizing antibody epitopes. We designed an affinity selection strategy, using a serum sample with high neutralizing antibody titer as a positive selector (K03135) and a sample with a very low neutralizing antibody titer (J02185) as a negative selector (both from the same time point post infection (week 68), neutralization data see figure 46). The main goal of this selection strategy was to deplete mimotopes specific for binding-only antibodies and to enrich for mimotopes representing epitopes of antibodies with neutralizing activity. As already mentioned in 4.2.1, the negative selector also showed the lowest binding titer.

One linear motif was represented in approximately 80% of all analyzed peptide sequences. By comparing the motif with the SHIV-1157ipd3N4 gp160 sequence, we found linear homologies to the amino-terminal end of the V2 loop (^{73}TTEIR^{77}) (see figure 43). Two residues in the middle of this motif (^{74}TE^{75}) were highly conserved in all isolated mimotopes showing this peptide sequence.

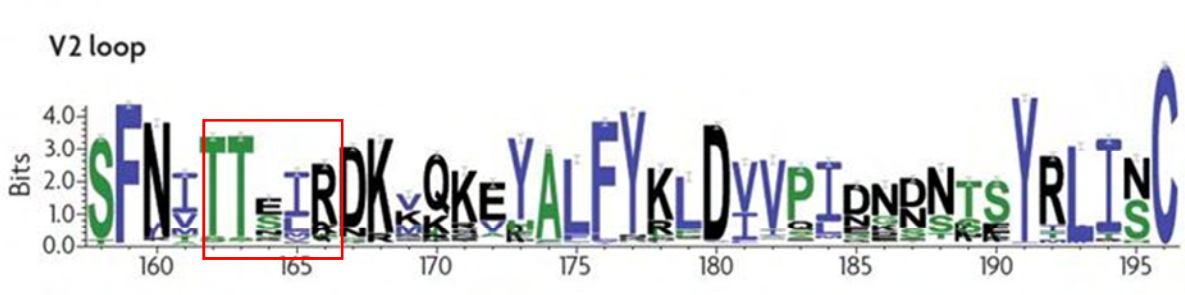

Figure 43: Conserved and variable residues in the V2 loop.
Degrees of amino acid conservations are shown. Discussed motif (^{73}TTEIR^{77}) is boxed in red (numbering different since we used our SHIV-1157ipd3N4 gp120 model). From ZOLLA-PAZNER et al., 2010

In general, the V2 loop mediates gp41-independent interaction with gp120 and shields certain regions responsible for the interaction with chemokine receptors. Thus far, a few V2 loop-specific antibodies with broad neutralizing activity have been described (ZOLLA-PAZNER et al., 2010). More recent studies showed that antibodies against complex epitopes, formed by both, V2 and V3 in the trimeric envelope protein (so called quaternary epitopes) have an extremely potent neutralization activity (KWONG et al., 2009; PANCERA et al., 2010; ROBINSON et al., 2010; ZOLLA-PAZNER et al., 2010). With our computational approach we are not able to identify quaternary mimotopes (see also 4.3.2). Nevertheless,

we analyzed all mimotopes with respect to conformational homologies to SHIV-1157ipd3N4 gp120. And we were able to detect that some of the ^{73}TTEIR^{77} mimotopes combine linear with structural homology (BB-k-7-A11, BB-k-7-E5, BB-k-12-D5, BB-k-12-D6, BB-k-7-F11, see figure 32), assigned either to the V2 or V5 loop. When analyzing the 3DEX hits with CHIMERA, we discovered that these mimotopes are in close proximity to the CD4 binding site (figures see 8.4).

In 1998, Kwong and co-workers published the structure of HIV gp120 in complex with the CD4 receptor. They described two residues of the CD4 receptor (Phe^{43} and Arg^{59}) that are important for the interaction with gp120. They showed that Phe^{43} is protruding a gp120 cavity (also referred as Phe43 cavity), which is surrounded by highly conserved amino acid residues (all listed, with corresponding numbers of SHIV-1157ipd3N4 gp120 model in table 8) (KWONG et al., 1998). Interestingly, nine mimotopes isolated from polyclonal serum of animal K03135 (one with the first biopanning (week 83) and eight with the last biopanning (week 68)) shared conformational homologies with amino acid residues of the Phe^{43} cavity. In figure 44, clone BB-k-12-C8 is illustrated (B) and compared to the schematic representation of the CD4-gp120 interface (A).

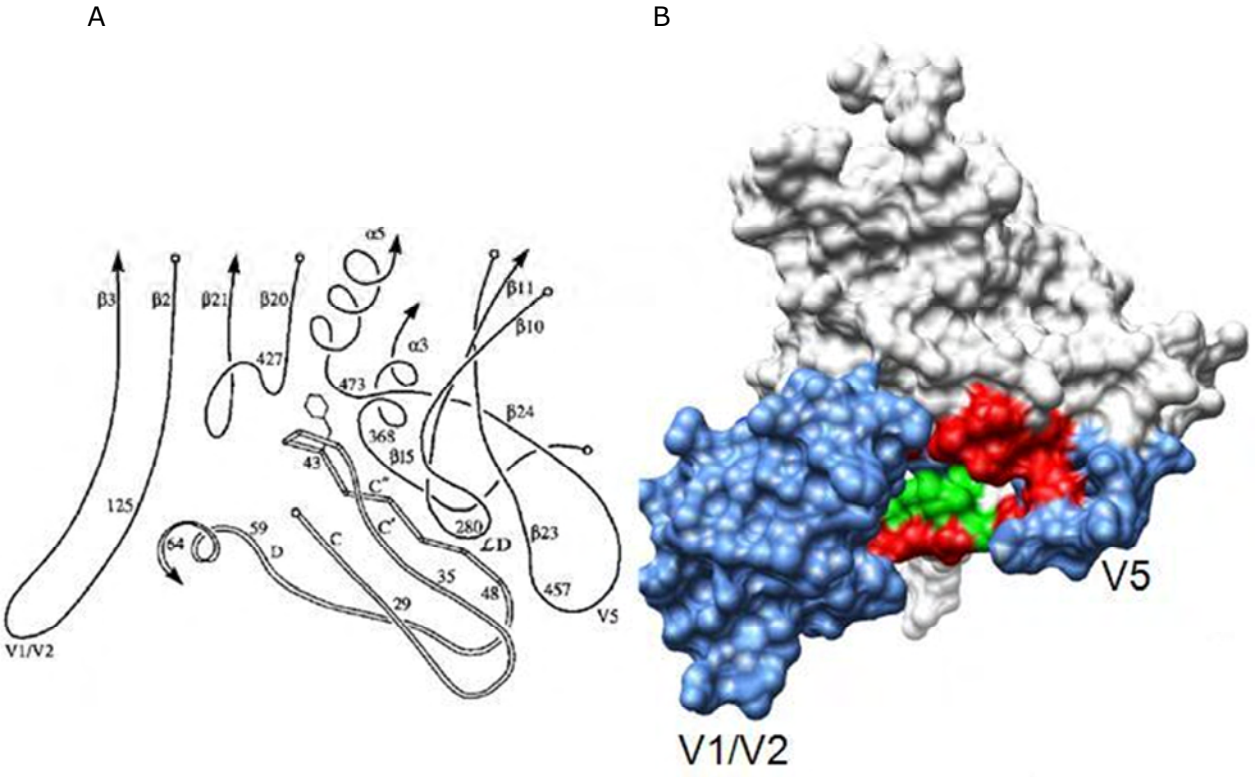

Figure 44: The CD4-gp120 interface.
(A) Schematic representation of six segments of gp120 (solid black lines) interacting with CD4 (double lines). The side chain of Phe^{43} is shown as well. V1/V2 and V5 loops are indicated. From KWONG et al., 1998. **(B)** The gp120 model of SHIV-1157ipd3N4 is shown in the same orientation as in A. V1/V2 and V5 loop are highlighted in blue for better orientation. The CD4 binding site is illustrated in red and the peptide sequence of BB-k-12-C8 in green.

As shown in figure 44, the mimotope sequence is overlapping with the CD4 interface and since amino acid residues of this domain are highly conserved, one could hypothesize that an antibody against this site has a broadly neutralizing activity. Thus, phages displaying Phe43 cavity peptide sequences have

been included in our pilot mouse immunization study as well. As described in 3.4.5, one promising clone, overlapping with the Phe43 cavity (BB-k-12-A12) showed also linear homologies with the KLIC epitope on gp41. Moreover, the cross-reactivity and conformational characteristics have been very similar to those observed with this immunodominant region. In this case it would be also important to check the gp120 or gp41 specificity of that particular clone (see 4.5.1).

Interestingly, most of the mimotopes from the third selection strategy showed a broad cross-reactivity starting with week 60 and one even at week 28 (BB-k-12-A12). Additionally, five clones displayed a conformational dependence with an - at least three times - higher binding activity when kept in their native conformation.

4.4.4. Concluding Remarks

Remarkably, 85% of the isolated mimotopes showed conformational homologies to highly conserved amino acid residues, either important for the interaction with the co-receptor CCR5 or with the receptor CD4 (see figure 45).

This could reflect the success of our selection strategies based on late time points (68 or 83 weeks after infection) and display the antibody repertoire developed in response to virus escape mutants. However, the used computational analysis can only give a hint for potential epitopes but is not a final proof (see 4.3.2). The biological relevance of the selected peptide sequences and potential location of epitopes needs to be confirmed in further studies. Nevertheless, the used approach helped us to select 34 promising phage clones, which can now be analyzed in functional assays (in-vitro and in-vivo) for gp160 specificity and their ability to induce neutralizing antibodies.

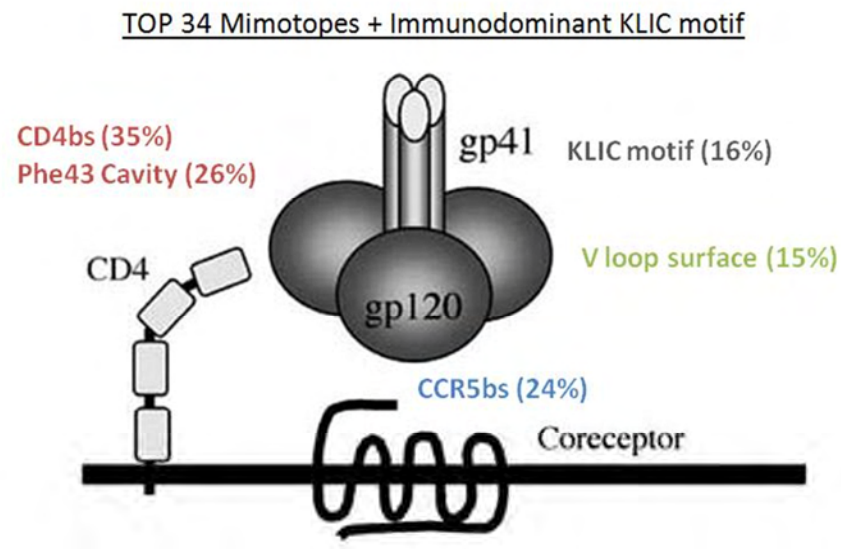

Figure 45: Top 34- and KLIC mimotopes and their location on gp160.
The distribution of Top 34 isolated mimotopes on gp120 (conformational homologies) and the KLIC mimotope on gp41 (linear homology) are illustrated. More than eighty percent of 3DEX results showed conformational homologies with highly conserved amino acid residues, important for the interaction with either CCR5 (24%) or CD4 (61%). Figure was adapted to SPEARMAN, 2006).

4.5. FUTURE PERSPECTIVES

The identification of possible antibody epitopes of gp160 with a computational approach needs to be confirmed for biological relevance (e.g. induction of nAbs). The next step of this study will be the design of in-vitro as well as in-vivo experiments to (1) confirm that the isolated mimotopes are representing gp160 epitopes and (2) to link selected clones to neutralization. In the following part, the hypotheses and planned assays are discussed.

4.5.1. HIV-1 gp160 Specific Mimotopes

Isolated mimotopes can be used to purify the corresponding antibodies out of the polyclonal serum samples. If the mimotopes are gp160-specific, the purified antibodies should recognize the protein. For this assay, selected recombinant phages are immobilized on ELISA plates and incubated with the polyclonal serum sample that was used as positive selector in the affinity selection procedure. After washing off unbound antibodies, bound ones can be eluted using a pH shift. Phage-affinity-purified antibodies can be evaluated for their specific binding to gp120 or gp160. With this approach, we would be able to confirm mimotope motifs overlapping with the known immunodominant regions on gp41 ("KLIC motif") by purifying antibodies which bind to gp160 but not gp120. This would be especially important for clone BB-k-12-A12 (see 3.4.5 and 4.4.3).

4.5.2. Discontinuous Mimotopes Identified by 3DEX

This antibody purification approach is also useful to answer the question of conformational characteristics. In an earlier study, Humbert and co-workers could show that a with 3DEX-predicted discontinuous mimotope was indeed conformational. Antibodies purified with this mimotope had a clear dependence on the native structure of gp160 for antibody binding (HUMBERT et al., 2008a). As discussed earlier, the conformational ELISA performed in this study showed some limitations with regard to the wild-type phage control. By reducing the target protein (gp160) instead of the phage conformation, we might get more significant results.

4.5.3. Mimotopes Overlapping with the CCR5 Binding Site Recognize the CCR5 Surface Receptor on Target Cells

According to the computer-based results, we hypothesize that mimotopes overlapping with the CCR5 binding site on gp120 are able to recognize the CCR5 surface receptors on the target cells. To confirm that idea, we have designed several experiments.

First, we want to perform a cell-based ELISA, immobilizing adherent cell lines expressing CCR5 in high amounts (such as GHOST (3) Hi-5 and/or U87.CD4.CCR5) on a microtiter plate and incubating with recombinant phages mimicking the CCR5 binding site on gp120. Additionally, natural CCR5 ligands, such as RANTES, MIP-1α and MIP-1β could be used as competitors in the same assay.

Using mimotope/GFP fusion proteins, we would be able to confirm the specific interaction of CCR5-binding site mimotopes and the CCR5 surface receptor by measuring green fluorescence signals exhibited by GFP (using fluorescence microscope and/or FACS).

A third approach to confirm that those mimotopes are overlapping with the CCR5 binding could be done by performing a inhibition ELISA, using either CCR5 peptides or monoclonal antibodies known to recognize the CCR5 binding site on gp120 (so called CD4-induced antibodies, such as 17b, X5 or m9, see 4.4.1; similar approach shown in ZHANG et al., 2010).

4.5.4. Mouse Immunization Study and Neutralization Assay

To evaluate the immunogenic characteristics of certain mimotopes we started a pilot vaccine study in mice. The most promising recombinant phages were grouped and combined according their peptide motifs and predicted localization on the envelope protein. In 2008, the Ruprecht Laboratory published a novel DNA prime/phage boost immunization strategy and we are going to use the same approach for mimotopes, isolated in this study (HUMBERT et al., 2008a). The mouse immune system has already been primed with the entire HIV-1 Env by one DNA inoculation (intramuscularly). In the next step, all mice will receive five phage boosts (subcutaneously) every 4-5 weeks, to focus the antibody response to a certain area of gp160 (10^{12} phage particles per boost). Binding and neutralizing antibody titers in mouse immune sera of three different groups (mimotopes overlapping with CCR5 binding site, Phe43 cavity or CD4 binding site) will be compared to titers of a control group that have received an empty DNA vector and have been boosted with wild-type phages.

4.5.5. Novel Selection Strategies

Since we isolated so many mimotopes overlapping with conserved sites on gp120, it would be interesting to perform a biopanning using earlier time points of animal K03135 to see if there is a shift towards epitopes of more variable regions.

Overall, the third selection strategy was successful in terms of depleting mimotopes representing immunodominant regions (such as the “KLIC motif”). Nevertheless, we might be able to increase the selection pressure towards neutralizing antibody mimotopes by using a serum sample with the same amount of binding titers as a negative selector (see 4.2.1 and 4.4.3).

5 ZUSAMMENFASSUNG

Auch nach 25 Jahren intensiver Forschung konnte noch kein Impstoff gegen das humane Immunodefizienz Virus (HIV) entwickelt werden. Um eine effektiven Schutz zu erreichen, müsste eine Vakkzine hohe Titer an breit neutralisierenden Antikörpern induzieren. Die Isolierung und Charakterisierung von neuen Immunogenen und korrespondierenden Antikörperepitopen stellt einen wichtigen Schritt in der Impfstoffentwicklung dar.

Im Juli 2009 haben Ho und Mitarber eine Studie veröffentlicht, in der Makaken der Spezies *Macaca nemestrina* mit einem R5-spezifischen Simianen-Humanen Immunodefizienz Virus (SHIV) vom Subtyp C infiziert wurden. Die mit dem als SHIV-1157ipd3N4 bezeichneten Virus infizierten Affen entwickelten AIDS und zeigten eine ähnliche Immunpathogenese wie auch schon in Rhesus Affen beobachtet werden konnte. Zwei der infizierten Affen zeigten eine neutralisierende Antikörperaktivität nicht nur gegen den homologen Virus, sondern auch gegen heterologe Viren vom Subtyp B ($HIV_{SF162.LS}$ und $SHIV_{SF162P4}$).

In der vorliegenden Arbeit wurden die polyklonalen Seren dieser SHIV-1157ipd3N4 infizierten Makaken verwendet, um Mimotope, die eventuell neutralisierende Antikörperepitope des HIV-1 Hüllproteins wiederspiegeln, zu isolieren. Dafür wurde die *Peptide Phage Display* Methodik unter der Verwendung einer kommerziell erhältlichen *Phage Display Library* angewendet. Nach einer Affinitätsselektion bestehend aus mehreren Runden positiver und negativer Selektionen, wurden isolierte Phagotope hinsichtlich ihrer spezifischen Bindung an die Zielstruktur im Phagen ELISA geteste und positive Klone auf ihre lineare Homologie mit der SHIV-1157ip3N4 gp160 Sequenz verglichen. Um auch eventuelle konformelle Homologien zu entdecken, wurde ein computergestütztes Model des monomeren Proteins von SHIV-1157ipd3N4 gp120 berechnet und die rekombinante Peptid Phagen Sequenz mittels einer speziellen Software (3DEX) potentiellen Regionen auf diesem Model zugeordnet. Vielversprechende Mimotope wurden auf ihre Kreuzreaktivität und hinsichtlich konformeller Eigenschaften in modifizierten Phagen ELISAs untersucht.

Unter Verwendung drei verschiedener Selektionsstrategien konnten wir unterschiedliche Mimotope des viralen Hüllproteins identifizieren. Mit dem ersten Ansatz wurden, für die Zielprobe spezifische, diskontinuierliche Mimotope der Rezeptor- und Korezeptorbindungsstellen isoliert. Im Gegensatz dazu, konnten wir mit einem sequentiellen Ansatz - unter der hintereinander geschaltetetn Verwendung von drei verschiedenen infizierten Affen - kreuzreagierende Mimotope identifizieren, die Ähnlichkeiten mit bekannten immunodominanten Antikörperepitopen aufweisen. Die meisten Peptidsequenzen, isoliert mit der dritten Selektionstrategie zeigen eine lineare Homologie mit einem V2 Loop Epitop und eine konformelle Ähnlichkeit mit einem stark konservierten Epitop der CD4 Bindungsstelle. Zusätzlich zeigten diese Klone eine breite Kreuzreaktivität und eine konformelle Abhängigkeit in den anschließenden in-vitro Experimenten. Die vielversprechendsten Mimotope sollen in einer Mausimmunisierungstudie auf ihr Potential breit neutralisierende Antikörperantworten zu induzieren getestet werden. Die Identifizierung von solchen neutralisierenden Antikörpermimotopen könnte eine wichtige Rolle in der Antikörper-basierten Impfstoffherstellung spielen.

Stichwörter: HIV-1, neutralisierende Antikörper, Peptide-Phage Display, 3DEX

6 SUMMARY

More than 25 years ago HIV, the causative agent of the AIDS epidemic was described. Since then, HIV research has intensely been focusing on understanding the virus life cycle and on finding potential drug or vaccine targets. Thus far, classical immunization approaches have not been able to prevent an HIV infection. To achieve sterilizing protection, a vaccine would have to elicit high titers of neutralizing antibodies capable of protecting against diverse HIV strains. The isolation and characterization of novel immunogens and antibody epitopes is an important step in antiviral vaccine development.

In July 2009, the consequences of intrarectal inoculation of pig-tailed macaques (*Macaca nemestrina*) with a R5-tropic clade C simian-human immunodeficiency virus (SHIV), termed SHIV-1157ipd3N4 was reported. SHIV-1157ipd3N4 caused AIDS and the virus-induced pathogenesis in pig-tailed macaques was very similar to that seen in R5-tropic SIV or SHIV-infected rhesus macaques. Some of the infected animals showed neutralizing antibody responses not only against the homologous virus but also against heterologous clade B viruses, such as $HIV_{SF162.LS}$ and $SHIV_{SF162P4.}$

In this follow-up study, polyclonal serum of the SHIV-1157ipd3N4-infected pig-tailed macaques was used to isolate phagotopes mimicking epitopes (mimotopes) of broadly neutralizing antibodies against the HIV-1 envelope protein. Mimotope isolation was performed by various selection strategies using commercially available random peptide phage libraries. After three rounds of affinity selection positive clones were identified via phage ELISA. Three different strategies have been performed to identify either (1) highly specific gp160 mimotopes, (2) common gp160 mimotopes shared by three different SHIV-1157ipd3N4-infected pig-tailed macaques or (3) phagotopes mimicking neutralizing antibody epitopes. The resulting motifs were analyzed for linear homologies to SHIV-1157ipd3N4 gp160. Potential conformational homologies were identified using a model of the SHIV-1157ipd3N4 gp120 monomer and 3DEX. Promising mimotopes were tested for cross-reactivity and binding characteristics in conformational phage ELISAs.

Using the first strategy, we were able to select conformational mimotopes representing gp120 epitopes, known to be important for virus entry (receptor and co-receptor binding site) and highly specific only for the used target sample. When all three infected animals were used in a sequential biopanning, common motifs with a cross-reactivity profile were isolated. Interestingly, approximately 70% of those mimotopes represented immunodominant regions on gp41. Isolated peptide sequences from the third selection strategy showed linear homologies to the V2 loop, and conformational similarities to highly conserved regions in the CD4 binding site. In-vitro experiments confirmed broad cross-reactivity as well as conformational dependence.

To evaluate the potential of inducing broadly neutralizing antibodies, the most promising mimotopes were included in a pilot mouse immunization study. Finding mimotopes which represent conserved, immunogenic regions of the HIV-1 Env and which have the potential to induce neutralizing antibody responses could be very useful for developing an antibody-based vaccine against HIV-1 in the future.

Keywords: HIV-1, neutralizing antibodies, peptide-phage display, 3DEX

7 REFERENCES

1 **AGRAWAL, L., LU, X., QINGWEN, J., VANHORN-ALI, Z., NICOLESCU, I. V., MCDERMOTT, D. H., MURPHY, P. M., ALKHATIB, G.** (2004). "Role for Ccr5delta32 Protein in Resistance to R5, R5x4, and X4 Human Immunodeficiency Virus Type 1 in Primary Cd4+ Cells." J Virol **78**(5): 2277-87.

2 **AGY, M. B., FRUMKIN, L. R., COREY, L., COOMBS, R. W., WOLINSKY, S. M., KOEHLER, J., MORTON, W. R., KATZE, M. G.** (1992). "Infection of Macaca Nemestrina by Human Immunodeficiency Virus Type-1." Science **257**(5066): 103-6.

3 **AMARA, R. R., VILLINGER, F., ALTMAN, J. D., LYDY, S. L., O'NEIL, S. P., STAPRANS, S. I., MONTEFIORI, D. C., XU, Y., HERNDON, J. G., WYATT, L. S., CANDIDO, M. A., KOZYR, N. L., EARL, P. L., SMITH, J. M., MA, H. L., GRIMM, B. D., HULSEY, M. L., MILLER, J., MCCLURE, H. M., MCNICHOLL, J. M., MOSS, B., ROBINSON, H. L.** (2001). "Control of a Mucosal Challenge and Prevention of AIDS by a Multiprotein DNA/Mva Vaccine." Science **292**(5514): 69-74.

4 **BABA, T. W., LISKA, V., HOFMANN-LEHMANN, R., VLASAK, J., XU, W., AYEHUNIE, S., CAVACINI, L. A., POSNER, M. R., KATINGER, H., STIEGLER, G., BERNACKY, B. J., RIZVI, T. A., SCHMIDT, R., HILL, L. R., KEELING, M. E., LU, Y., WRIGHT, J. E., CHOU, T. C., RUPRECHT, R. M.** (2000). "Human Neutralizing Monoclonal Antibodies of the IgG1 Subtype Protect against Mucosal Simian-Human Immunodeficiency Virus Infection." Nat Med **6**(2): 200-6.

5 **BARBAS, C. F., 3RD, BJORLING, E., CHIODI, F., DUNLOP, N., CABABA, D., JONES, T. M., ZEBEDEE, S. L., PERSSON, M. A., NARA, P. L., NORRBY, E., ET AL.** (1992). "Recombinant Human Fab Fragments Neutralize Human Type 1 Immunodeficiency Virus in Vitro." Proc Natl Acad Sci U S A **89**(19): 9339-43.

6 **BARBAS, C. F., 3RD;, BURTON, D. R.;, SCOTT, J. K.;, G.J.;, SILVERMAN** (2001) "Phage Display: A Laboratory Manual "; General Phage Methods 15.7; Protocol 15.6 Spectophotometric Quantitation of Phage; New York, Cold Spring Harbor Laboratory Press

7 **BARRE-SINOUSSI, F., CHERMANN, J. C., REY, F., NUGEYRE, M. T., CHAMARET, S., GRUEST, J., DAUGUET, C., AXLER-BLIN, C., VEZINET-BRUN, F., ROUZIOUX, C., ROZENBAUM, W., MONTAGNIER, L.** (1983). "Isolation of a T-Lymphotropic Retrovirus from a Patient at Risk for Acquired Immune Deficiency Syndrome (AIDS)." Science **220**(4599): 868-71.

8 **BERGER, E. A., DOMS, R. W., FENYO, E. M., KORBER, B. T., LITTMAN, D. R., MOORE, J. P., SATTENTAU, Q. J., SCHUITEMAKER, H., SODROSKI, J., WEISS, R. A.** (1998). "A New Classification for HIV-1." Nature **391**(6664): 240.

9 **BOTTGER, V., BOTTGER, A.** (2009). "Epitope Mapping Using Phage Display Peptide Libraries." Methods Mol Biol **524**: 181-201.

10 **BRATKOVIC, T.** (2010). "Progress in Phage Display: Evolution of the Technique and Its Application." Cell Mol Life Sci **67**(5): 749-67.

11 **BUCHBINDER, S. P., MEHROTRA, D. V., DUERR, A., FITZGERALD, D. W., MOGG, R., LI, D., GILBERT, P. B., LAMA, J. R., MARMOR, M., DEL RIO, C., MCELRATH, M. J., CASIMIRO, D. R., GOTTESDIENER, K. M., CHODAKEWITZ, J. A., COREY, L., ROBERTSON, M. N.** (2008). "Efficacy Assessment of a Cell-Mediated Immunity HIV-1 Vaccine (the Step Study): A Double-Blind, Randomised, Placebo-Controlled, Test-of-Concept Trial." Lancet **372**(9653): 1881-93.

12 **BURTON, D. R., DESROSIERS, R. C., DOMS, R. W., KOFF, W. C., KWONG, P. D., MOORE, J. P., NABEL, G. J., SODROSKI, J., WILSON, I. A., WYATT, R. T.** (2004). "HIV Vaccine Design and the Neutralizing Antibody Problem." Nat Immunol **5**(3): 233-6.

13 **BURTON, D. R., PYATI, J., KODURI, R., SHARP, S. J., THORNTON, G. B., PARREN, P. W., SAWYER, L. S., HENDRY, R. M., DUNLOP, N., NARA, P. L., ET AL.** (1994). "Efficient Neutralization of Primary Isolates of HIV-1 by a Recombinant Human Monoclonal Antibody." Science **266**(5187): 1024-7.

14 **CHEN, X., SCALA, G., QUINTO, I., LIU, W., CHUN, T. W., JUSTEMENT, J. S., COHEN, O. J., VANCOTT, T. C., IWANICKI, M., LEWIS, M. G., GREENHOUSE, J., BARRY, T., VENZON, D., FAUCI, A. S.** (2001). "Protection of Rhesus Macaques against Disease Progression from Pathogenic SHIV-89.6pd by Vaccination with Phage-Displayed HIV-1 Epitopes." Nat Med **7**(11): 1225-31.

15 **CLAVEL, F., GUETARD, D., BRUN-VEZINET, F., CHAMARET, S., REY, M. A., SANTOS-FERREIRA, M. O., LAURENT, A. G., DAUGUET, C., KATLAMA, C., ROUZIOUX, C., ET AL.** (1986). "Isolation of a New Human Retrovirus from West African Patients with AIDS." Science **233**(4761): 343-6.

16 **COFFIN, J., HAASE, A., LEVY, J. A., MONTAGNIER, L., OROSZLAN, S., TEICH, N., TEMIN, H., TOYOSHIMA, K., VARMUS, H., VOGT, P., ET AL.** (1986a). "What to Call the AIDS Virus?"; Nature **321**(6065): 10.

17 **COFFIN, J., HAASE, A., LEVY, J. A., MONTAGNIER, L., OROSZLAN, S., TEICH, N., TEMIN, H., TOYOSHIMA, K., VARMUS, H., VOGT, P., ET AL.** (1986b). "Human Immunodeficiency Viruses." Science **232**(4751): 697.

18 **DAS, A. T., BERKHOUT, B.** (1995). "Efficient Extension of a Misaligned Trna-Primer During Replication of the HIV-1 Retrovirus." Nucleic Acids Res **23**(8): 1319-26.

19 **DI MARZO VERONESE, F., WILLIS, A. E., BOYER-THOMPSON, C., APPELLA, E., PERHAM, R. N.** (1994). "Structural Mimicry and Enhanced Immunogenicity of Peptide Epitopes Displayed on Filamentous Bacteriophage. The V3 Loop of HIV-1 gp120." J Mol Biol **243**(2): 167-72.

20 **DISKIN, R., MARCOVECCHIO, P. M., BJORKMAN, P. J.** (2010). "Structure of a Clade C HIV-1 gp120 Bound to Cd4 and Cd4-Induced Antibody Reveals Anti-Cd4 Polyreactivity." Nat Struct Mol Biol **17**(5): 608-13.

21 **ENSHELL-SEIJFFERS, D., DENISOV, D., GROISMAN, B., SMELYANSKI, L., MEYUHAS, R., GROSS, G., DENISOVA, G., GERSHONI, J. M.** (2003). "The Mapping and Reconstitution of a Conformational Discontinuous B-Cell Epitope of HIV-1." J Mol Biol **334**(1): 87-101.

22 **FAUCI, A. S., JOHNSTON, M. I., DIEFFENBACH, C. W., BURTON, D. R., HAMMER, S. M., HOXIE, J. A., MARTIN, M., OVERBAUGH, J., WATKINS, D. I., MAHMOUD, A., GREENE, W. C.** (2008). "HIV Vaccine Research: The Way Forward." Science **321**(5888): 530-2.

23 **FERRANTELLI, F., BUCKLEY, K. A., RASMUSSEN, R. A., CHALMERS, A., WANG, T., LI, P. L., WILLIAMS, A. L., HOFMANN-LEHMANN, R., MONTEFIORI, D. C., CAVACINI, L. A., KATINGER, H., STIEGLER, G., ANDERSON, D. C., MCCLURE, H. M., RUPRECHT, R. M.** (2007). "Time Dependence of Protective Post-Exposure Prophylaxis with Human Monoclonal Antibodies against Pathogenic SHIV Challenge in Newborn Macaques." Virology **358**(1): 69-78.

24 **FERRANTELLI, F., RASMUSSEN, R. A., BUCKLEY, K. A., LI, P. L., WANG, T., MONTEFIORI, D. C., KATINGER, H., STIEGLER, G., ANDERSON, D. C., MCCLURE, H. M., RUPRECHT, R. M.** (2004). "Complete Protection of Neonatal Rhesus Macaques against Oral Exposure to Pathogenic Simian-Human Immunodeficiency Virus by Human Anti-HIV Monoclonal Antibodies." J Infect Dis **189**(12): 2167-73.

25 **GALLO, R. C., SALAHUDDIN, S. Z., POPOVIC, M., SHEARER, G. M., KAPLAN, M., HAYNES, B. F., PALKER, T. J., REDFIELD, R., OLESKE, J., SAFAI, B., ET AL.** (1984). "Frequent Detection and Isolation of Cytopathic Retroviruses (Htlv-Iii) from Patients with AIDS and at Risk for AIDS." Science **224**(4648): 500-3.

26 **GELDERBLOM, H. R.** (1997). "Fine Structure of HIV and SIV "; In: Los Alamos National Laboratory (Ed) HIV Sequence Compendium, 31-44

27 **GERSHONI, J. M., ROITBURD-BERMAN, A., SIMAN-TOV, D. D., TARNOVITSKI FREUND, N., WEISS, Y.** (2007). "Epitope Mapping: The First Step in Developing Epitope-Based Vaccines." BioDrugs **21**(3): 145-56.

28 **GEYSEN, H. M., RODDA, S. J., MASON, T. J.** (1986). "A Priori Delineation of a Peptide Which Mimics a Discontinuous Antigenic Determinant." Mol Immunol **23**(7): 709-15.

29 **GORNY, M. K., REVESZ, K., WILLIAMS, C., VOLSKY, B., LOUDER, M. K., ANYANGWE, C. A., KRACHMAROV, C., KAYMAN, S. C., PINTER, A., NADAS, A., NYAMBI, P. N., MASCOLA, J. R., ZOLLA-PAZNER, S.** (2004). "The V3 Loop Is Accessible on the Surface of Most Human Immunodeficiency Virus Type 1 Primary Isolates and Serves as a Neutralization Epitope." J Virol **78**(5): 2394-404.

30 **HALL, T.A.** (1999). "Bioedit: A User-Friendly Biological Sequence Alignment Editor and Analysis Program for Windows 95/98/Nt." Nucl. Acids. Symp. Ser. **45**: 95-98.

31 **HANSEN, S. G., VIEVILLE, C., WHIZIN, N., COYNE-JOHNSON, L., SIESS, D. C., DRUMMOND, D. D., LEGASSE, A. W., AXTHELM, M. K., OSWALD, K., TRUBEY, C. M., PIATAK, M., JR., LIFSON, J. D., NELSON, J. A., JARVIS, M. A., PICKER, L. J.** (2009). "Effector Memory T Cell Responses Are Associated with Protection of Rhesus Monkeys from Mucosal Simian Immunodeficiency Virus Challenge." Nat Med **15**(3): 293-9.

32 **HAYNES, B. F., FLEMING, J., ST CLAIR, E. W., KATINGER, H., STIEGLER, G., KUNERT, R., ROBINSON, J., SCEARCE, R. M., PLONK, K., STAATS, H. F., ORTEL, T. L., LIAO, H. X., ALAM, S. M.** (2005). "Cardiolipin Polyspecific Autoreactivity in Two Broadly Neutralizing HIV-1 Antibodies." Science **308**(5730): 1906-8.

33 **HEMELAAR, J., GOUWS, E., GHYS, P. D., OSMANOV, S.** (2006). "Global and Regional Distribution of HIV-1 Genetic Subtypes and Recombinants in 2004." AIDS **20**(16): W13-23.

34 **HEWER, R., MEYER, D.** (2003). "Peptide Immunogens Based on the Envelope Region of HIV-1 Are Recognized by HIV/AIDS Patient Polyclonal Antibodies and Induce Strong Humoral Immune Responses in Mice and Rabbits." Mol Immunol **40**(6): 327-35.

35 **HIRSCH, V. M., OLMSTED, R. A., MURPHEY-CORB, M., PURCELL, R. H., JOHNSON, P. R.** (1989). "An African Primate Lentivirus (Sivsm) Closely Related to HIV-2." Nature **339**(6223): 389-92.

36 **HO, O., LARSEN, K., POLACINO, P., LI, Y., ANDERSON, D., SONG, R., RUPRECHT, R. M., HU, S. L.** (2009). "Pathogenic Infection of Macaca Nemestrina with a Ccr5-Tropic Subtype-C Simian-Human Immunodeficiency Virus." Retrovirology **6**: 65.

37 **HOFMANN-LEHMANN, R., VLASAK, J., CHENINE, A. L., LI, P. L., BABA, T. W., MONTEFIORI, D. C., MCCLURE, H. M., ANDERSON, D. C., RUPRECHT, R. M.** (2002). "Molecular Evolution of Human Immunodeficiency Virus Env in Humans and Monkeys: Similar Patterns Occur During Natural Disease Progression or Rapid Virus Passage." J Virol **76**(10): 5278-84.

38 **HOLMES, E. C.** (2001). "On the Origin and Evolution of the Human Immunodeficiency Virus (HIV)." Biol Rev Camb Philos Soc **76**(2): 239-54.

39 **HOXIE, J. A.** (2009). "Toward an Antibody-Based HIV-1 Vaccine." Annu Rev Med **61**: 135-52.

40 **HU, S. L.** (2005). "Non-Human Primate Models for AIDS Vaccine Research." Curr Drug Targets Infect Disord **5**(2): 193-201.

41 **HUANG, C. C., TANG, M., ZHANG, M. Y., MAJEED, S., MONTABANA, E., STANFIELD, R. L., DIMITROV, D. S., KORBER, B., SODROSKI, J., WILSON, I. A., WYATT, R., KWONG, P. D.** (2005). "Structure of a V3-Containing HIV-1 gp120 Core." Science **310**(5750): 1025-8.

42 **HUANG, J., GUTTERIDGE, A., HONDA, W., KANEHISA, M.** (2006). "Mimox: A Web Tool for Phage Display Based Epitope Mapping." BMC Bioinformatics **7**: 451.

43 **HUET, T., CHEYNIER, R., MEYERHANS, A., ROELANTS, G., WAIN-HOBSON, S.** (1990). "Genetic Organization of a Chimpanzee Lentivirus Related to HIV-1." Nature **345**(6273): 356-9.

44 **HUMBERT, M., ANTONI, S., BRILL, B., LANDERSZ, M., RODES, B., SORIANO, V., WINTERGERST, U., KNECHTEN, H., STASZEWSKI, S., VON LAER, D., DITTMAR, M. T., DIETRICH, U.** (2007). "Mimotopes Selected with Antibodies from HIV-1-Neutralizing Long-Term Non-Progressor Plasma." Eur J Immunol **37**(2): 501-15.

45 **HUMBERT, M., DIETRICH, U.** (2006). "The Role of Neutralizing Antibodies in HIV Infection." AIDS Rev **8**(2): 51-9.

46 **HUMBERT, M., RASMUSSEN, R. A., ONG, H., KAISER, F. M., HU, S. L., RUPRECHT, R. M.** (2008a). "Inducing Cross-Clade Neutralizing Antibodies against HIV-1 by Immunofocusing." PLoS One **3**(12): e3937.

47 **HUMBERT, M., RASMUSSEN, R. A., SONG, R., ONG, H., SHARMA, P., CHENINE, A. L., KRAMER, V. G., SIDDAPPA, N. B., XU, W., ELSE, J. G., NOVEMBRE, F. J., STROBERT, E., O'NEIL, S. P., RUPRECHT, R. M.** (2008b). "SHIV-1157i and Passaged Progeny Viruses Encoding R5 HIV-1 Clade C Env Cause AIDS in Rhesus Monkeys." Retrovirology **5**: 94.

48 **IRVING, M. B., PAN, O., SCOTT, J. K.** (2001). "Random-Peptide Libraries and Antigen-Fragment Libraries for Epitope Mapping and the Development of Vaccines and Diagnostics." Curr Opin Chem Biol **5**(3): 314-24.

49 **JANEWAY, C.A, JR.** (2001) "Immunobiology"; The Immune System in Health and Disease; Acqiured immune deficiency syndrom; Online version, (http://www.ncbi.nlm.nih.gov/bookshelf/br.fcgi?book=imm); 5th edition New York, Garland Science

50 **JOHNSTON, M. I., FAUCI, A. S.** (2007). "An HIV Vaccine--Evolving Concepts." N Engl J Med **356**(20): 2073-81.

51 **JULG, B., GOEBEL, F. D.** (2005). "HIV Genetic Diversity: Any Implications for Drug Resistance?"; Infection **33**(4): 299-301.

52 **KARLSSON HEDESTAM, G. B., FOUCHIER, R. A., PHOGAT, S., BURTON, D. R., SODROSKI, J., WYATT, R. T.** (2008). "The Challenges of Eliciting Neutralizing Antibodies to HIV-1 and to Influenza Virus." Nat Rev Microbiol **6**(2): 143-55.

53 **KASLOW, R. A., CARRINGTON, M., APPLE, R., PARK, L., MUNOZ, A., SAAH, A. J., GOEDERT, J. J., WINKLER, C., O'BRIEN, S. J., RINALDO, C., DETELS, R., BLATTNER, W., PHAIR, J., ERLICH, H., MANN, D. L.** (1996). "Influence of Combinations of Human Major Histocompatibility Complex Genes on the Course of HIV-1 Infection." Nat Med **2**(4): 405-11.

54 **KEESLER, M. J., FISHER, S. D., LIPSHULTZ, S. E.** (2001). "Cardiac Manifestations of HIV Infection in Infants and Children." Ann N Y Acad Sci **946**: 169-78.

55 **KEHOE, J. W., KAY, B. K.** (2005). "Filamentous Phage Display in the New Millennium." Chem Rev **105**(11): 4056-72.

56 **KOEFOED, K., FARNAES, L., WANG, M., SVEJGAARD, A., BURTON, D. R., DITZEL, H. J.** (2005). "Molecular Characterization of the Circulating Anti-HIV-1 gp120-Specific B Cell Repertoire Using Antibody Phage Display Libraries Generated from Pre-Selected HIV-1 gp120 Binding Pbls." J Immunol Methods **297**(1-2): 187-201.

57 **KONTHUR, Z., WALTER, G.** (2002). "Automation of Phage Display for High-Throughput Antibody Development." Targets **1**(1): 30-36.

58 **KRAMER, V. G., SIDDAPPA, N. B., RUPRECHT, R. M.** (2007). "Passive Immunization as Tool to Identify Protective HIV-1 Env Epitopes." Curr HIV Res **5**(6): 642-55.

59 **KRUMPE, L. R., MORI, T.** (2007). "Potential of Phage-Displayed Peptide Library Technology to Identify Functional Targeting Peptides." Expert Opin Drug Discov **2**(4): 525.

60 **KWONG, P. D., WILSON, I. A.** (2009). "HIV-1 and Influenza Antibodies: Seeing Antigens in New Ways." Nat Immunol **10**(6): 573-8.

61 **KWONG, P. D., WYATT, R., MAJEED, S., ROBINSON, J., SWEET, R. W., SODROSKI, J., HENDRICKSON, W. A.** (2000). "Structures of HIV-1 gp120 Envelope Glycoproteins from Laboratory-Adapted and Primary Isolates." Structure **8**(12): 1329-39.

62 **KWONG, P. D., WYATT, R., ROBINSON, J., SWEET, R. W., SODROSKI, J., HENDRICKSON, W. A.** (1998). "Structure of an HIV gp120 Envelope Glycoprotein in Complex with the Cd4 Receptor and a Neutralizing Human Antibody." Nature **393**(6686): 648-59.

63 **LABRIJN, A. F., POIGNARD, P., RAJA, A., ZWICK, M. B., DELGADO, K., FRANTI, M., BINLEY, J., VIVONA, V., GRUNDNER, C., HUANG, C. C., VENTURI, M., PETROPOULOS, C. J., WRIN, T., DIMITROV, D. S., ROBINSON, J., KWONG, P. D., WYATT, R. T., SODROSKI, J., BURTON, D. R.** (2003). "Access of Antibody Molecules to the Conserved Coreceptor Binding Site on Glycoprotein gp120 Is Sterically Restricted on Primary Human Immunodeficiency Virus Type 1." J Virol **77**(19): 10557-65.

64 **LACKNER, A. A., VEAZEY, R. S.** (2007). "Current Concepts in AIDS Pathogenesis: Insights from the SIV/Macaque Model." Annu Rev Med **58**: 461-76.

65 **LEVY, J. A.** (2009). "HIV Pathogenesis: 25 Years of Progress and Persistent Challenges." AIDS **23**(2): 147-60.

66 **LEVY, J. A., HOFFMAN, A. D., KRAMER, S. M., LANDIS, J. A., SHIMABUKURO, J. M., OSHIRO, L. S.** (1984). "Isolation of Lymphocytopathic Retroviruses from San Francisco Patients with AIDS." Science **225**(4664): 840-2.

67 **LU, F. X.** (2000). "New Method for Quantifying Anti-Hiv1-Gp160 Antibodies in Saliva, Cervicovaginal Secretions, and Serum of Infected Women." J Clin Lab Anal **14**(4): 188-92.

68 **MARKOVIC, I., CLOUSE, K. A.** (2004). "Recent Advances in Understanding the Molecular Mechanisms of HIV-1 Entry and Fusion: Revisiting Current Targets and Considering New Options for Therapeutic Intervention." Curr HIV Res **2**(3): 223-34.

69 **MASCOLA, J. R., MONTEFIORI, D. C.** (2009). "The Role of Antibodies in HIV Vaccines." Annu Rev Immunol **28**: 413-44.

70 **MC CANN, C. M., SONG, R. J., RUPRECHT, R. M.** (2005). "Antibodies: Can They Protect against HIV Infection?"; Curr Drug Targets Infect Disord **5**(2): 95-111.

71 **MCGAUGHEY, G. B., CITRON, M., DANZEISEN, R. C., FREIDINGER, R. M., GARSKY, V. M., HURNI, W. M., JOYCE, J. G., LIANG, X., MILLER, M., SHIVER, J., BOGUSKY, M. J.** (2003). "HIV-1 Vaccine Development: Constrained Peptide Immunogens Show Improved Binding to the Anti-HIV-1 gp41 Mab." Biochemistry **42**(11): 3214-23.

72 **MCMICHAEL, A. J.** (2006). "HIV Vaccines." Annu Rev Immunol **24**: 227-55.

73 **MCMICHAEL, A. J., BORROW, P., TOMARAS, G. D., GOONETILLEKE, N., HAYNES, B. F.** (2010). "The Immune Response During Acute HIV-1 Infection: Clues for Vaccine Development." Nat Rev Immunol **10**(1): 11-23.

74 **MCMICHAEL, A. J., HANKE, T.** (2003). "HIV Vaccines 1983-2003." Nat Med **9**(7): 874-80.

75 **MENENDEZ, A., SCOTT, J. K.** (2005). "The Nature of Target-Unrelated Peptides Recovered in the Screening of Phage-Displayed Random Peptide Libraries with Antibodies." Anal Biochem **336**(2): 145-57.

76 **MIKHAIL, M., WANG, B., SAKSENA, N. K.** (2003). "Mechanisms Involved in Non-Progressive HIV Disease." AIDS Rev **5**(4): 230-44.

77 **MONTERO, M., VAN HOUTEN, N. E., WANG, X., SCOTT, J. K.** (2008). "The Membrane-Proximal External Region of the Human Immunodeficiency Virus Type 1 Envelope: Dominant Site of Antibody Neutralization and Target for Vaccine Design." Microbiol Mol Biol Rev **72**(1): 54-84, table of contents.

78 **MOREAU, V., GRANIER, C., VILLARD, S., LAUNE, D., MOLINA, F.** (2006). "Discontinuous Epitope Prediction Based on Mimotope Analysis." Bioinformatics **22**(9): 1088-95.

79 **MOULARD, M., PHOGAT, S. K., SHU, Y., LABRIJN, A. F., XIAO, X., BINLEY, J. M., ZHANG, M. Y., SIDOROV, I. A., BRODER, C. C., ROBINSON, J., PARREN, P. W., BURTON, D. R., DIMITROV, D. S.** (2002). "Broadly Cross-Reactive HIV-1-Neutralizing Human Monoclonal Fab Selected for Binding to gp120-Cd4-Ccr5 Complexes." Proc Natl Acad Sci U S A **99**(10): 6913-8.

80 **MUMEY, B. M., BAILEY, B. W., KIRKPATRICK, B., JESAITIS, A. J., ANGEL, T., DRATZ, E. A.** (2003). "A New Method for Mapping Discontinuous Antibody Epitopes to Reveal Structural Features of Proteins." J Comput Biol **10**(3-4): 555-67.

81 **NEGI, S. S., BRAUN, W.** (2009). "Automated Detection of Conformational Epitopes Using Phage Display Peptide Sequences." Bioinform Biol Insights **3**: 71-81.

82 **PANCERA, M., MCLELLAN, J. S., WU, X., ZHU, J., CHANGELA, A., SCHMIDT, S. D., YANG, Y., ZHOU, T., PHOGAT, S., MASCOLA, J. R., KWONG, P. D.** (2010). "Crystal Structure of Pg16 and Chimeric Dissection with Somatically Related Pg9: Structure-Function Analysis of Two Quaternary-Specific Antibodies That Effectively Neutralize HIV-1." J Virol.

83 **PANTALEO, G., MENZO, S., VACCAREZZA, M., GRAZIOSI, C., COHEN, O. J., DEMAREST, J. F., MONTEFIORI, D., ORENSTEIN, J. M., FOX, C., SCHRAGER, L. K., ET AL.** (1995). "Studies in Subjects with Long-Term Nonprogressive Human Immunodeficiency Virus Infection." N Engl J Med **332**(4): 209-16.

84 **PANTOPHLET, R., BURTON, D. R.** (2006). "Gp120: Target for Neutralizing HIV-1 Antibodies." Annu Rev Immunol **24**: 739-69.

85 **PARKER, C. E., DETERDING, L. J., HAGER-BRAUN, C., BINLEY, J. M., SCHULKE, N., KATINGER, H., MOORE, J. P., TOMER, K. B.** (2001). "Fine Definition of the Epitope on the gp41 Glycoprotein of Human Immunodeficiency Virus Type 1 for the Neutralizing Monoclonal Antibody 2F5." J Virol **75**(22): 10906-11.

86 **PARREN, P. W., MARX, P. A., HESSELL, A. J., LUCKAY, A., HAROUSE, J., CHENG-MAYER, C., MOORE, J. P., BURTON, D. R.** (2001). "Antibody Protects Macaques against Vaginal Challenge with a Pathogenic R5 Simian/Human Immunodeficiency Virus at Serum Levels Giving Complete Neutralization in Vitro." J Virol **75**(17): 8340-7.

87 **PERRIN, L., KAISER, L., YERLY, S.** (2003). "Travel and the Spread of HIV-1 Genetic Variants." Lancet Infect Dis **3**(1): 22-7.

88 **PETERLIN, B. M., TRONO, D.** (2003). "Hide, Shield and Strike Back: How HIV-Infected Cells Avoid Immune Eradication." Nat Rev Immunol **3**(2): 97-107.

89 **PETTERSEN E.F., GODDARD T.D., HUANG C.C., COUCH G.S., GREENBLATT D.M., MENG, E.C., FERRIN T.E.** (2004). "Uscf Chimera - a Visualization System for Exploratory Research and Analysis." J Comput Chem **25**(13): 1605-12.

90 **PIZZI, E., CORTESE, R., TRAMONTANO, A.** (1995). "Mapping Epitopes on Protein Surfaces." Biopolymers **36**(5): 675-80.

91 **PLANTIER, J. C., LEOZ, M., DICKERSON, J. E., DE OLIVEIRA, F., CORDONNIER, F., LEMEE, V., DAMOND, F., ROBERTSON, D. L., SIMON, F.** (2009). "A New Human Immunodeficiency Virus Derived from Gorillas." Nat Med **15**(8): 871-2.

92 **PLOTKIN, S. A.** (2008). "Vaccines: Correlates of Vaccine-Induced Immunity." Clin Infect Dis **47**(3): 401-9.

93 **POLONIS, V. R., BROWN, B. K., ROSA BORGES, A., ZOLLA-PAZNER, S., DIMITROV, D. S., ZHANG, M. Y., BARNETT, S. W., RUPRECHT, R. M., SCARLATTI, G., FENYO, E. M., MONTEFIORI, D. C., MCCUTCHAN, F. E., MICHAEL, N. L.** (2008). "Recent Advances in the Characterization of HIV-1 Neutralization Assays for Standardized Evaluation of the Antibody Response to Infection and Vaccination." Virology **375**(2): 315-20.

94 **RERKS-NGARM, S., PITISUTTITHUM, P., NITAYAPHAN, S., KAEWKUNGWAL, J., CHIU, J., PARIS, R., PREMSRI, N., NAMWAT, C., DE SOUZA, M., ADAMS, E., BENENSON, M., GURUNATHAN, S., TARTAGLIA, J., MCNEIL, J. G., FRANCIS, D. P., STABLEIN, D., BIRX, D. L., CHUNSUTTIWAT, S., KHAMBOONRUANG, C., THONGCHAROEN, P., ROBB, M. L., MICHAEL, N. L., KUNASOL, P., KIM, J. H.** (2009). "Vaccination with Alvac and Aidsvax to Prevent HIV-1 Infection in Thailand." N Engl J Med **361**(23): 2209-20.

95 **RIZZUTO, C., SODROSKI, J.** (2000). "Fine Definition of a Conserved Ccr5-Binding Region on the Human Immunodeficiency Virus Type 1 Glycoprotein 120." AIDS Res Hum Retroviruses **16**(8): 741-9.

96 **ROBINSON, J. E., FRANCO, K., ELLIOTT, D. H., MAHER, M. J., REYNA, A., MONTEFIORI, D. C., ZOLLA-PAZNER, S., GORNY, M. K., KRAFT, Z., STAMATATOS, L.** (2010). "Quaternary Epitope Specificities of Anti-HIV-1 Neutralizing Antibodies Generated in Rhesus Macaques Infected by the Simian/Human Immunodeficiency Virus Shivsf162p4." J Virol **84**(7): 3443-53.

97 **ROSE, N. F., MARX, P. A., LUCKAY, A., NIXON, D. F., MORETTO, W. J., DONAHOE, S. M., MONTEFIORI, D., ROBERTS, A., BUONOCORE, L., ROSE, J. K.** (2001). "An Effective AIDS Vaccine Based on Live Attenuated Vesicular Stomatitis Virus Recombinants." Cell **106**(5): 539-49.

98 **ROUX, K. H., TAYLOR, K. A.** (2007). "AIDS Virus Envelope Spike Structure." Curr Opin Struct Biol **17**(2): 244-52.

99 **RUPRECHT, R. M., FERRANTELLI, F., KITABWALLA, M., XU, W., MCCLURE, H. M.** (2003). "Antibody Protection: Passive Immunization of Neonates against Oral AIDS Virus Challenge." Vaccine **21**(24): 3370-3.

100 **SANI, M. U., OKEAHIALAM, B. N., ALIYU, S. H., ENOCH, D. A.** (2005). "Human Immunodeficiency Virus (HIV) Related Heart Disease: A Review." Wien Klin Wochenschr **117**(3): 73-81.

101 **SCANLAN, C. N., PANTOPHLET, R., WORMALD, M. R., OLLMANN SAPHIRE, E., STANFIELD, R., WILSON, I. A., KATINGER, H., DWEK, R. A., RUDD, P. M., BURTON, D. R.** (2002). "The Broadly Neutralizing Anti-Human Immunodeficiency Virus Type 1 Antibody 2G12 Recognizes a Cluster of Alpha1-->2 Mannose Residues on the Outer Face of gp120." J Virol **76**(14): 7306-21.

102 **SCHREIBER, A., HUMBERT, M., BENZ, A., DIETRICH, U.** (2005). "3D-Epitope-Explorer (3DEX): Localization of Conformational Epitopes within Three-Dimensional Structures of Proteins." J Comput Chem **26**(9): 879-87.

103 **SHIVER, J. W., FU, T. M., CHEN, L., CASIMIRO, D. R., DAVIES, M. E., EVANS, R. K., ZHANG, Z. Q., SIMON, A. J., TRIGONA, W. L., DUBEY, S. A., HUANG, L., HARRIS, V. A., LONG, R. S., LIANG, X., HANDT, L., SCHLEIF, W. A., ZHU, L., FREED, D. C., PERSAUD, N. V., GUAN, L., PUNT, K. S., TANG, A., CHEN, M., WILSON, K. A., COLLINS, K. B., HEIDECKER, G. J., FERNANDEZ, V. R., PERRY, H. C., JOYCE, J. G., GRIMM, K. M., COOK, J. C., KELLER, P. M., KRESOCK, D. S., MACH, H., TROUTMAN, R. D., ISOPI, L. A., WILLIAMS, D. M., XU, Z., BOHANNON, K. E., VOLKIN, D. B., MONTEFIORI, D. C., MIURA, A., KRIVULKA, G. R., LIFTON, M. A., KURODA, M. J., SCHMITZ, J. E., LETVIN, N. L., CAULFIELD, M. J., BETT, A. J., YOUIL, R., KASLOW, D. C., EMINI, E. A.** (2002). "Replication-Incompetent Adenoviral Vaccine Vector Elicits Effective Anti-Immunodeficiency-Virus Immunity." Nature **415**(6869): 331-5.

104 **SIDHU, S. S.** (2001). "Engineering M13 for Phage Display." Biomol Eng **18**(2): 57-63.

105 **SIMON, V., HO, D. D.** (2003). "HIV-1 Dynamics in Vivo: Implications for Therapy." Nat Rev Microbiol **1**(3): 181-90.

106 **SMITH, G. P.** (1985). "Filamentous Fusion Phage: Novel Expression Vectors That Display Cloned Antigens on the Virion Surface." Science **228**(4705): 1315-7.

107 **SONG, R. J., CHENINE, A. L., RASMUSSEN, R. A., RUPRECHT, C. R., MIRSHAHIDI, S., GRISSON, R. D., XU, W., WHITNEY, J. B., GOINS, L. M., ONG, H., LI, P. L., SHAI-KOBILER, E., WANG, T., MCCANN, C. M., ZHANG, H., WOOD, C., KANKASA, C., SECOR, W. E., MCCLURE, H. M., STROBERT, E., ELSE, J. G., RUPRECHT, R. M.** (2006). "Molecularly Cloned SHIV-1157ipd3n4: A Highly Replication- Competent, Mucosally Transmissible R5 Simian-Human Immunodeficiency Virus Encoding HIV Clade C Env." J Virol **80**(17): 8729-38.

108 **SPEARMAN, P.** (2006). "Current Progress in the Development of HIV Vaccines." Curr Pharm Des **12**(9): 1147-67.

109 **STAMATATOS, L., MORRIS, L., BURTON, D. R., MASCOLA, J. R.** (2009). "Neutralizing Antibodies Generated During Natural HIV-1 Infection: Good News for an HIV-1 Vaccine?"; Nat Med **15**(8): 866-70.

110 **STREMLAU, M., OWENS, C. M., PERRON, M. J., KIESSLING, M., AUTISSIER, P., SODROSKI, J.** (2004). "The Cytoplasmic Body Component Trim5alpha Restricts HIV-1 Infection in Old World Monkeys." Nature **427**(6977): 848-53.

111 **SUDANO, I., SPIEKER, L. E., NOLL, G., CORTI, R., WEBER, R., LUSCHER, T. F.** (2006). "Cardiovascular Disease in HIV Infection." Am Heart J **151**(6): 1147-55.

112 **SZARDENINGS, M.** (2003). "Phage Display of Random Peptide Libraries: Applications, Limits, and Potential." J Recept Signal Transduct Res **23**(4): 307-49.

113 **THOMSON, M. M., PEREZ-ALVAREZ, L., NAJERA, R.** (2002). "Molecular Epidemiology of HIV-1 Genetic Forms and Its Significance for Vaccine Development and Therapy." Lancet Infect Dis **2**(8): 461-71.

114 **TRKOLA, A., POMALES, A. B., YUAN, H., KORBER, B., MADDON, P. J., ALLAWAY, G. P., KATINGER, H., BARBAS, C. F., 3RD, BURTON, D. R., HO, D. D., ET AL.** (1995). "Cross-Clade Neutralization of Primary Isolates of Human Immunodeficiency Virus Type 1 by Human Monoclonal Antibodies and Tetrameric Cd4-IgG." J Virol **69**(11): 6609-17.

115 **TRKOLA, A., PURTSCHER, M., MUSTER, T., BALLAUN, C., BUCHACHER, A., SULLIVAN, N., SRINIVASAN, K., SODROSKI, J., MOORE, J. P., KATINGER, H.** (1996). "Human Monoclonal Antibody 2G12 Defines a Distinctive Neutralization Epitope on the gp120 Glycoprotein of Human Immunodeficiency Virus Type 1." J Virol **70**(2): 1100-8.

116 **UNAIDS** (2009). "AIDS Epidemic Update: November 2009." from www.unaids.org.

117 **VIRGIN, H. W., WALKER, B. D.** (2010). "Immunology and the Elusive AIDS Vaccine." Nature **464**(7286): 224-31.

118 **VLASAK, J., RUPRECHT, R. M.** (2006). "AIDS Vaccine Development and Challenge Viruses: Getting Real." AIDS **20**(17): 2135-40.

119 **WANG, L. F., YU, M.** (2004). "Epitope Identification and Discovery Using Phage Display Libraries: Applications in Vaccine Development and Diagnostics." Curr Drug Targets **5**(1): 1-15.

120 **WYATT, R., KWONG, P. D., DESJARDINS, E., SWEET, R. W., ROBINSON, J., HENDRICKSON, W. A., SODROSKI, J. G.** (1998). "The Antigenic Structure of the HIV gp120 Envelope Glycoprotein." Nature **393**(6686): 705-11.

121 **XIANG, S. H., WANG, L., ABREU, M., HUANG, C. C., KWONG, P. D., ROSENBERG, E., ROBINSON, J. E., SODROSKI, J.** (2003). "Epitope Mapping and Characterization of a Novel Cd4-Induced Human Monoclonal Antibody Capable of Neutralizing Primary HIV-1 Strains." Virology **315**(1): 124-34.

122 **YEARLEY, J. H., PEARSON, C., CARVILLE, A., SHANNON, R. P., MANSFIELD, K. G.** (2006). "SIV-Associated Myocarditis: Viral and Cellular Correlates of Inflammation Severity." AIDS Res Hum Retroviruses **22**(6): 529-40.

123 **YEARLEY, J. H., PEARSON, C., SHANNON, R. P., MANSFIELD, K. G.** (2007). "Phenotypic Variation in Myocardial Macrophage Populations Suggests a Role for Macrophage Activation in SIV-Associated Cardiac Disease." AIDS Res Hum Retroviruses **23**(4): 515-24.

124 **ZHANG, M. Y., BORGES, A. R., PTAK, R. G., WANG, Y., DIMITROV, A. S., ALAM, S. M., WIECZOREK, L., BOUMA, P., FOUTS, T., JIANG, S., POLONIS, V. R., HAYNES, B. F., QUINNAN, G. V., MONTEFIORI, D. C., DIMITROV, D. S.** (2010). "Potent and Broad Neutralizing Activity of a Single Chain Antibody Fragment against Cell-Free and Cell-Associated HIV-1." MAbs **2**(3).

125 **ZHANG, M. Y., SHU, Y., RUDOLPH, D., PRABAKARAN, P., LABRIJN, A. F., ZWICK, M. B., LAL, R. B., DIMITROV, D. S.** (2004). "Improved Breadth and Potency of an HIV-1-Neutralizing Human Single-Chain Antibody by Random Mutagenesis and Sequential Antigen Panning." J Mol Biol **335**(1): 209-19.

126 **ZOLLA-PAZNER, S.** (2004). "Identifying Epitopes of HIV-1 That Induce Protective Antibodies." Nat Rev Immunol **4**(3): 199-210.

127 **ZOLLA-PAZNER, S., CARDOZO, T.** (2010). "Structure-Function Relationships of HIV-1 Envelope Sequence-Variable Regions Refocus Vaccine Design." Nat Rev Immunol **10**(7): 527-35.

128 **ZWICK, M. B., LABRIJN, A. F., WANG, M., SPENLEHAUER, C., SAPHIRE, E. O., BINLEY, J. M., MOORE, J. P., STIEGLER, G., KATINGER, H., BURTON, D. R., PARREN, P. W.** (2001). "Broadly Neutralizing Antibodies Targeted to the Membrane-Proximal External Region of Human Immunodeficiency Virus Type 1 Glycoprotein gp41." J Virol **75**(22): 10892-905.

129 **ZWICK, M. B., SAPHIRE, E. O., BURTON, D. R.** (2004). "gp41: Hiv's Shy Protein." Nat Med **10**(2): 133-4.

8 APPENDIX

8.1. Neutralization Data – Dr. Shiu-Lok Hu

Study: SHIV-1157ipd3N4 titration (Dr. Shiu-Lok Hu)
Assays: Neutralization in TZM-bl cells
Virus stocks: All are 293T-grown pseudoviruses, stock ID# shown in table
Report Date: August 28, 2009

			ID50 in TZM-bl cells[1]										
			Clade B						Clade C				
Animal	Bleed date	Bleed Wk	SF162.LS ID#1720	SHIV-SF162P4 ID#726	6535.3 ID#1720	QH0692.42 ID#2190	PVO.4 ID#1503	RHPA4259.7 ID#839	SHIV-1157ipd3N4 ID#942	Du156.12 ID#2151	Du422.1 ID#582	ZM197M.PB7 ID#2538	CAP45.2.00.G3 ID#2365
J02185	11/19/07	-1	<20	21					<20	<20	<20	<20	<20
	08/04/08	36	82	85					45	<20	<20	<20	<20
	03/16/09	68	47	60	<20	<20	<20	<20	32	<20	<20	<20	<20
K03135	11/19/07	-1	<20	<20					<20	<20	<20	<20	<20
	08/04/08	36	6765	4156					53	<20	<20	<20	<20
	03/16/09	68	6952	2911	<20	<20	<20	<20	153	<20	<20	<20	<20
	04/13/09	72	4091	1656	<20	<20	<20	<20	443	<20	<20	<20	<20
	05/11/09	76	8451	3575	<20	<20	<20	<20	460	<20	<20	<20	<20
	06/08/09	80	15986	9192	21	29	<20	<20	424	<20	<20	<20	<20
	06/29/09	83	11604	7220	<20	37	<20	<20	415	<20	<20	<20	<20
M05118	06/29/09	--	<20	<20	<20	<20	<20	<20	<20	<20	<20	<20	<20
L03165	01/31/08	-1	<20	<20					<20	<20	<20	<20	<20
	10/16/08	36	9307	2202					34	<20	<20	<20	<20
Plasma B			755	331	<20	<20	<20	<20	<20	<20	<20	<20	<20
Plasma C			341	176	<20	<20	<20	<20	<20	45	<20	<20	<20

[1] *Values are the sample dilution at which relative luminescence units (RLUs) were reduced 50% compared to virus control wells (no test sample).*

Figure 46: Neutralization data of SHIV-1157ipd3N4 infected pig-tailed macaques (J02185, K03135, L03165) and one naïve pig-tailed macaque (M05118). Neutralization assay was performed in TZM-bl cells, different clade B and clade C HIV and SHIV isolates have been tested.

8.2. Important Residues on gp120 (Receptor and Co-Receptor Binding Sites)

Table 8: Overview of important residues on gp120, important for interaction with CD4 and CCR5

Conserved Residues of CCR5 binding site		Interacting Residues of Phe43 cavity		Residues that line the Phe43 cavity	
HIV2B4C gp120 (KWONG et al., 1998)	Corresponding residues SHIV-1157ipd3N4 gp120	HIV2B4C gp120 (KWONG et al., 1998)	Corresponding residues SHIV-1157ipd3N4 gp120	HIV2B4C gp120 (KWONG, P.D. et al., 1998)	Corresponding residues SHIV-1157ipd3N4 gp120
Ile 420	Ile 323	Asp 368	Asp 277	Trp 112	Trp 29
Lys 421	Lys 324	Glu 370	Glu 279	Val 255	Val 166
Gln 422	Gln 325	Ile 371	Ile 289	Thr 257	Thr 168
Ile 423	Ile 326	Asn 425	Asn 328	Glu 370	Glu 279
Pro 438	Pro 341	Met 426	Met 329	Phe 382	Phe 291
Gly 441	Gly 344	Trp 427	Trp 330	Tyr 384	Tyr 293
		Gly 473	Gly 378	Trp 427	Trp 330
				Met 475	Met 389

8.3. Phage ELISA Results

A

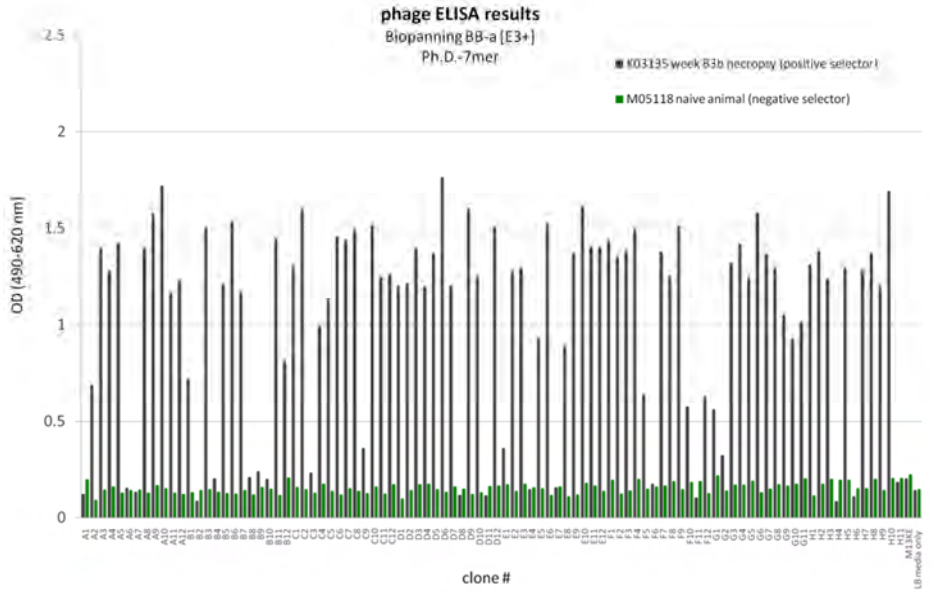

B

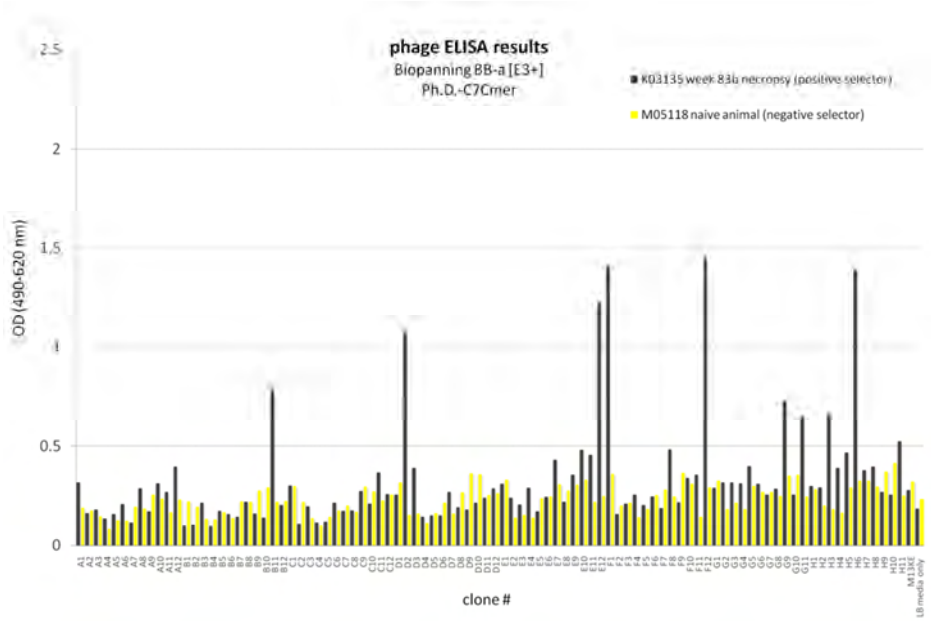

Figure 47: Phage ELISA results of BB-a; 3rd positive eluate [E3+].
(A) Ph.D-7mer library, **(B)** Ph.D-C7Cmer library

A

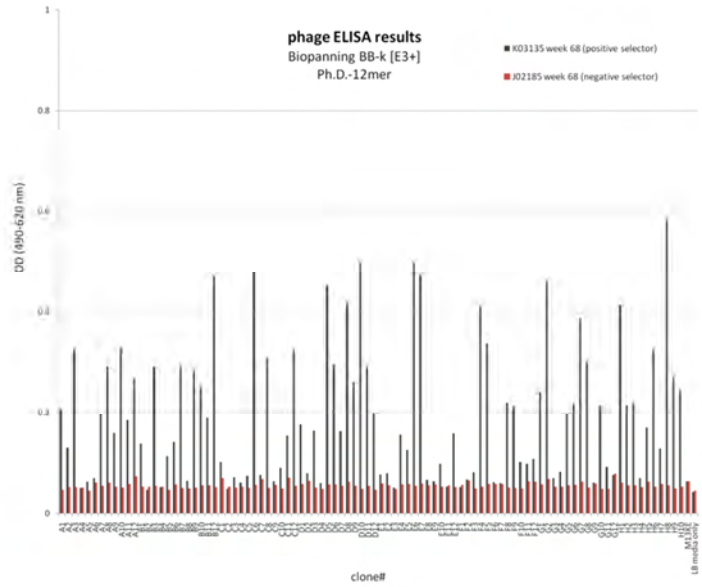

B

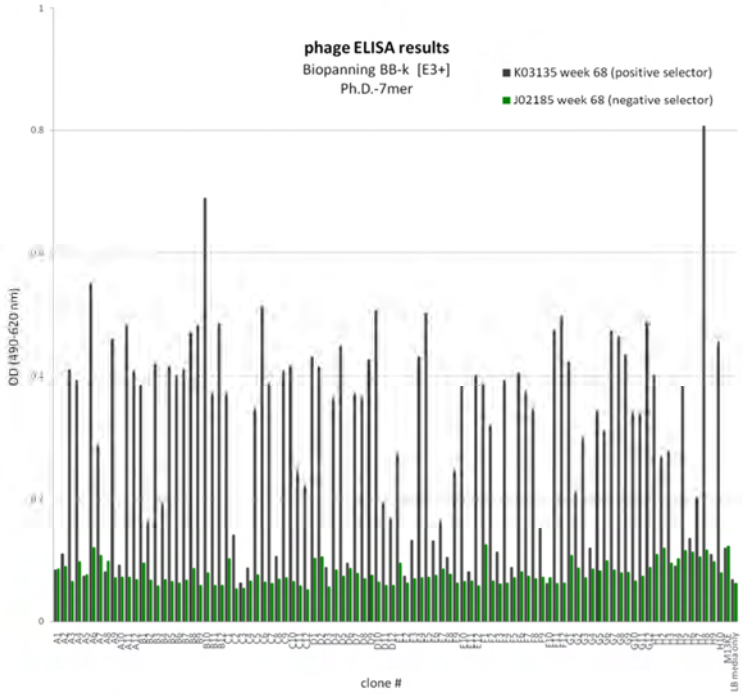

C

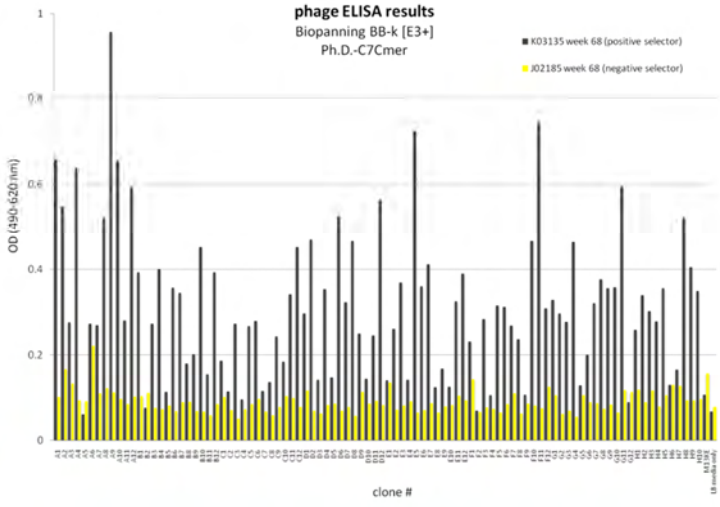

Figure 48: ***Phage ELISA results of BB-k; 3rd positive eluate [E3+.]***
(A) *Ph.D-12mer library,* ***(B)*** *Ph.D-7mer library.* ***(C)*** *Ph.D-C7Cmer library*

8.4. Promising Mimotopes from 3 Different Biopannings

The most promising 3DEX results are shown (clone number according to figure 32), visualized using the surface command of the CHIMERA software.

CCR5 Mimotopes

BB-a-12-B1

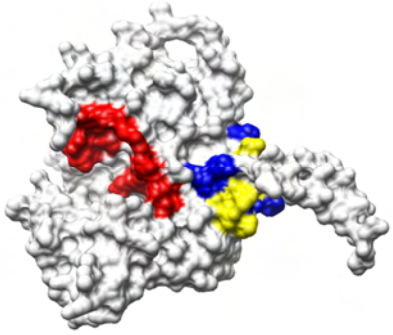

BB-a-12-H8_1

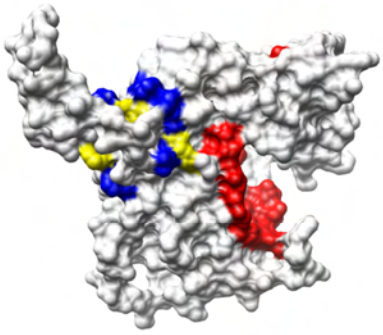

BB-a-12-C12_1

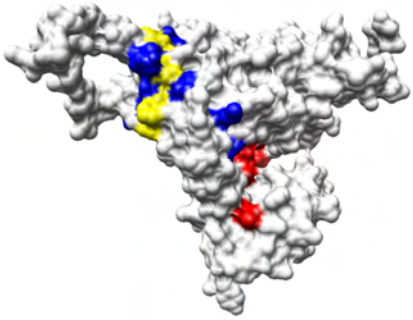

BB-b-12-A11

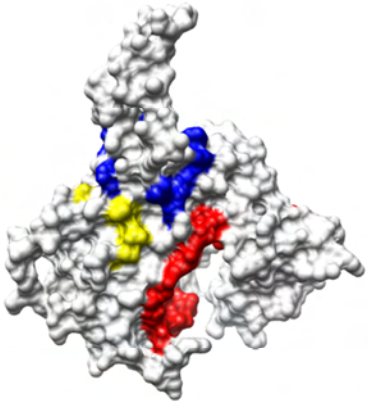

BB-a-12-E7_1

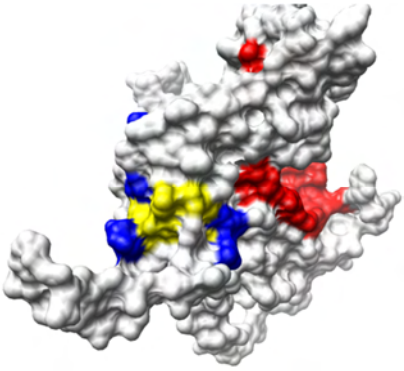

BB-b-12-G4

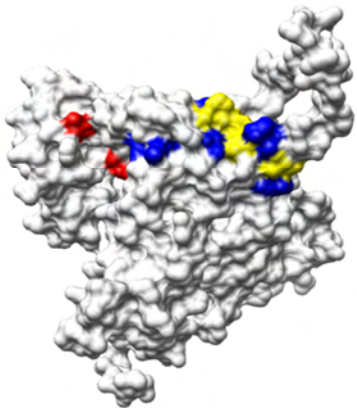

BB-a-12-E7_2

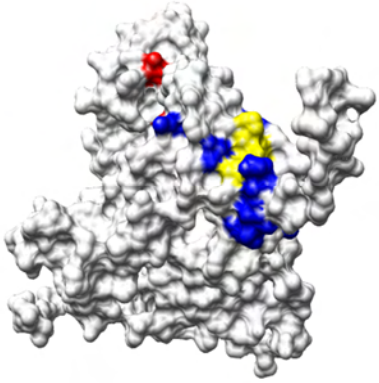

BB-i-12-G7

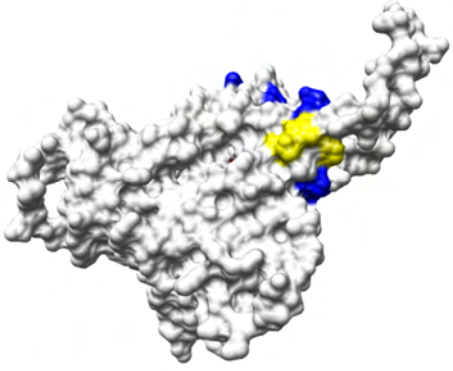

BB-k-12-B3

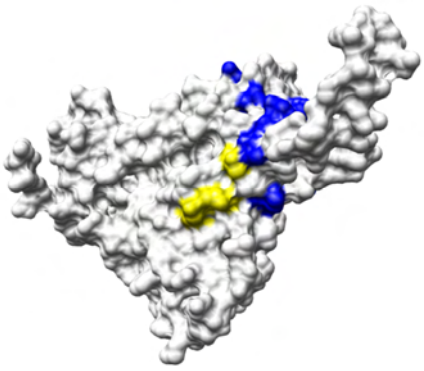

BB-k-12-D5_3

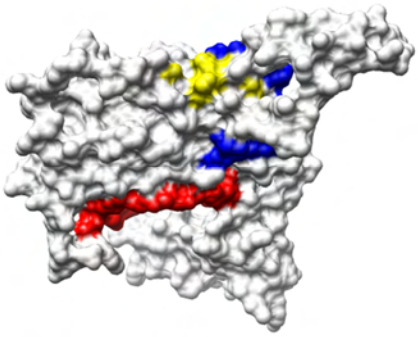

CD4 Mimotopes

BB-b-7-D11_1

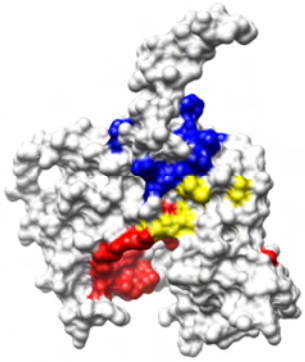

BB-a-12-D1

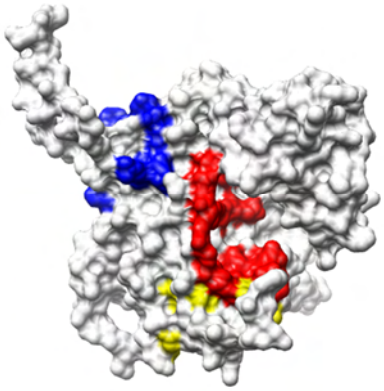

BB-a-12-C11

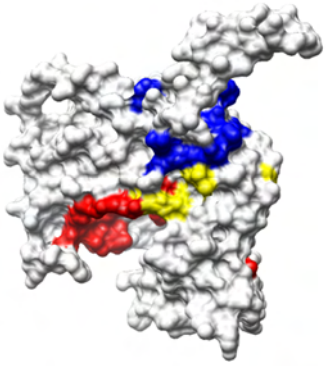

BB-a-12-E7_3

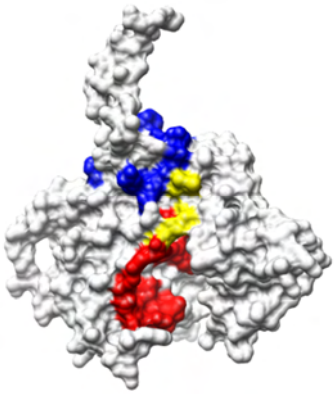

BB-a-12-C12_2

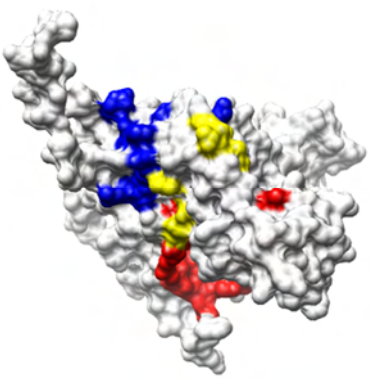

BB-a-12-H8_3

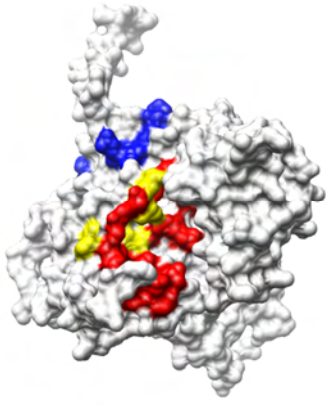

BB-b-12-A4

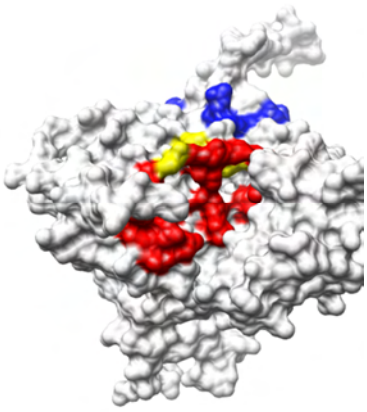

BB-i-12-F6

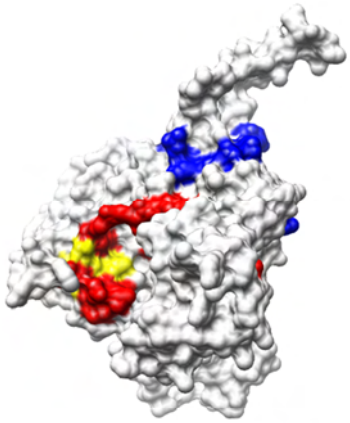

BB-b-12-H4

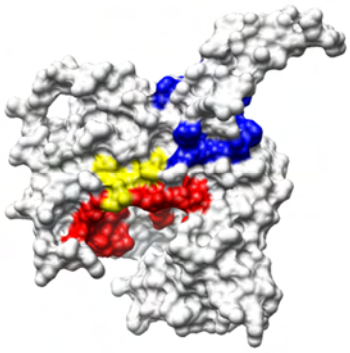

BB-k-12-D6_2

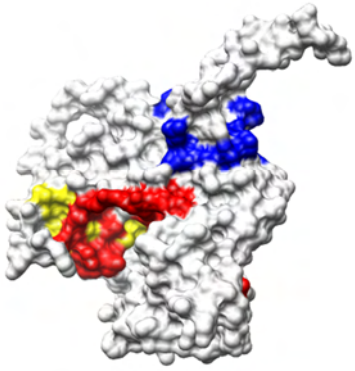

Phe43 Cavity Mimotopes

BB-a-12-H8_2

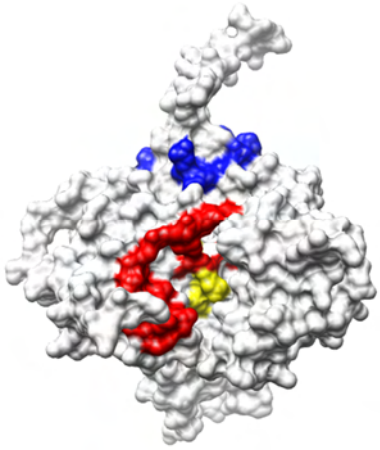

BB-i-12-H1

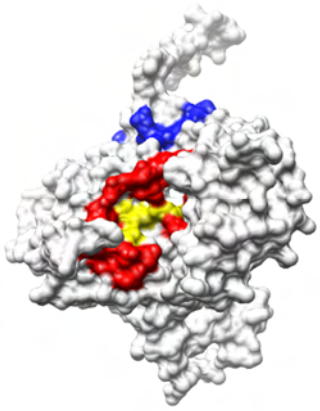

BB-a-12-G5

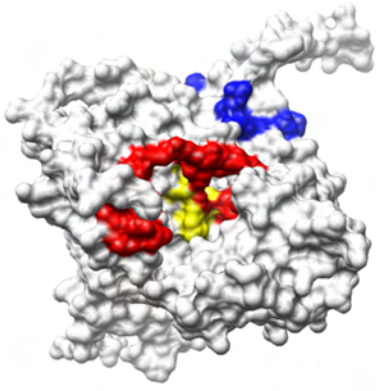

BB-k-12-C6

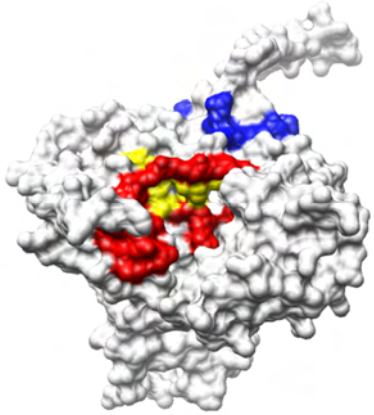

BB-k-12-C8

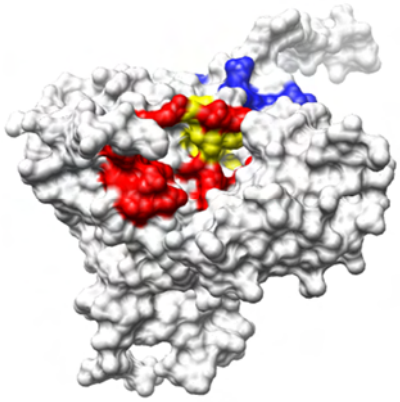

BB-k-12-G2

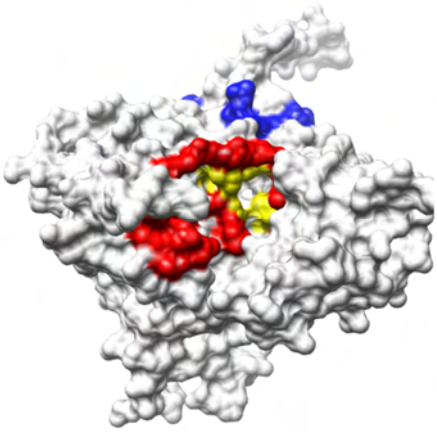

BB-k-12-C12

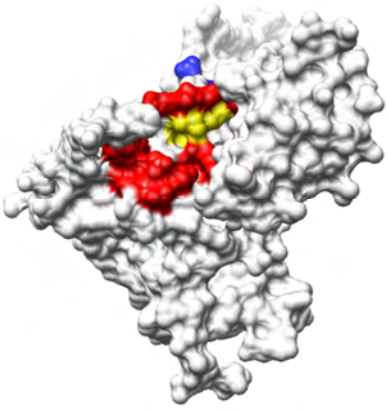

BB-k-12-H9_1

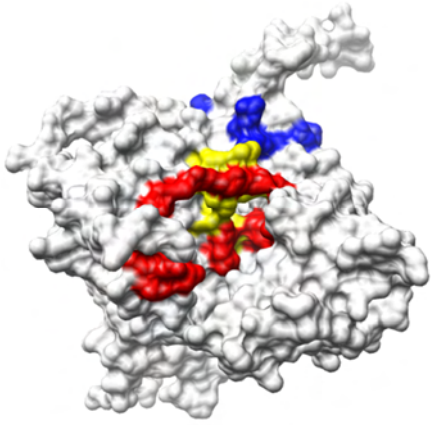

BB-k-12-D8

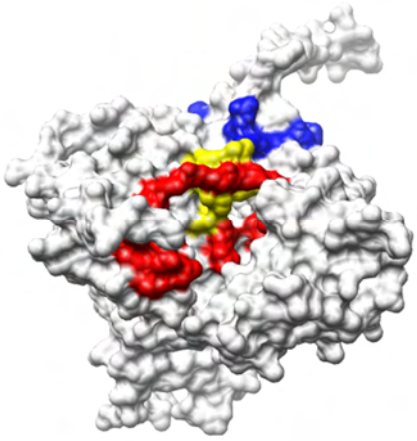

BB-k-12-H9_2

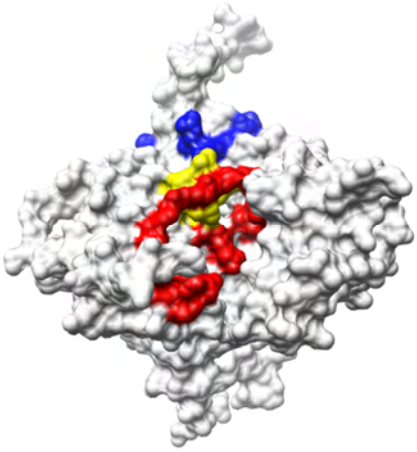

BB-k-12-D11

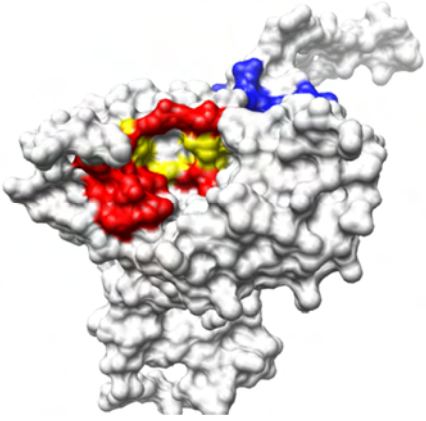

BB-k-12-A12

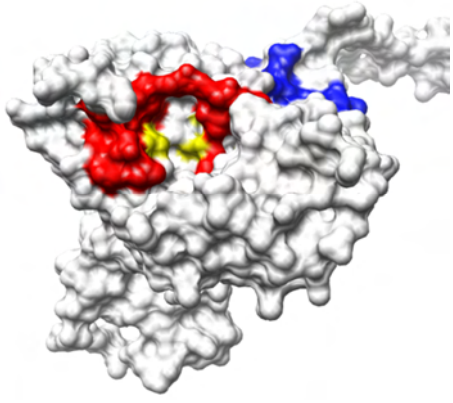

Variable Loop Mimotopes

BB-b-7-D11_2

V4 loop

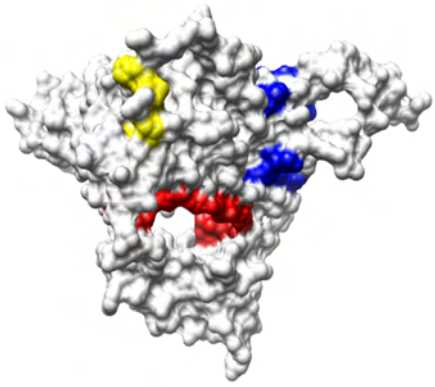

BB-k-7-A11_1

V2 loop
close to CD4bs

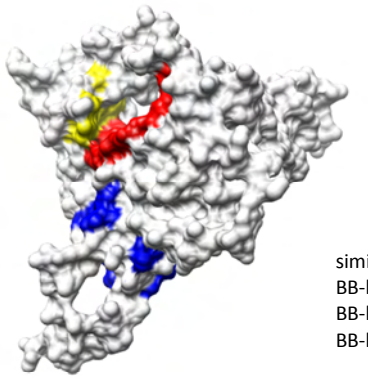

similar in:
BB-k-7-E5_1
BB-k-12-D5_1
BB-k-7-F11_1

BB-b-12-B7

V3 loop

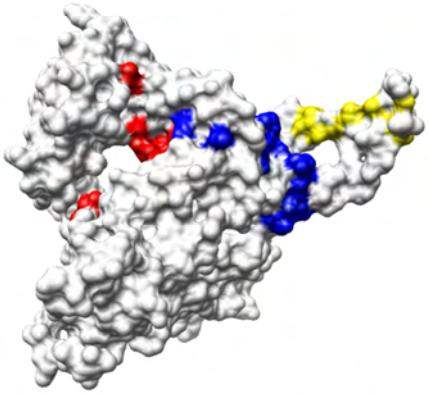

BB-k-7-A11_2

V5 loop
close to CD4bs

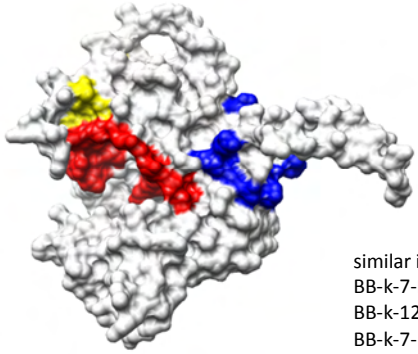

similar in:
BB-k-7-E5_2
BB-k-12-D5_2
BB-k-7-F11_2

BB-i-12-B8

V1 loop

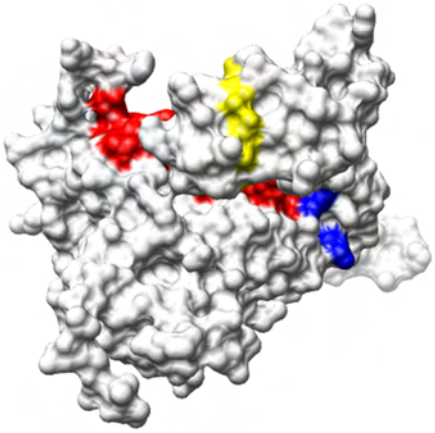

BB-k-12-D6_1

V2 loop
close to CD4bs

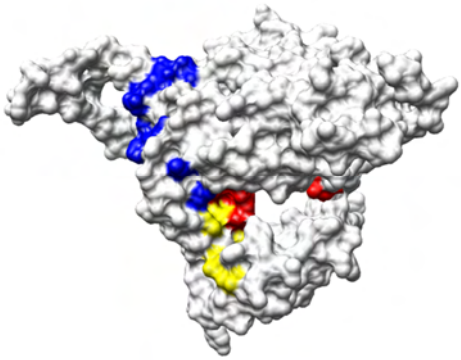

BB-i-12-G2

V4 loop

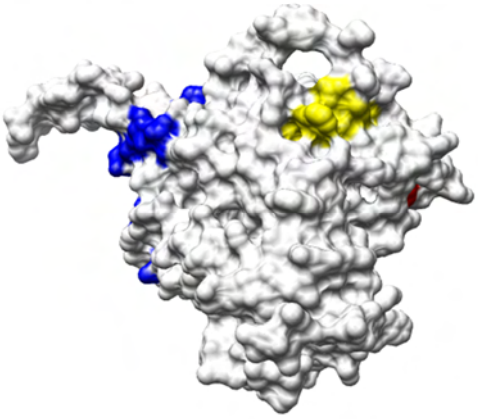

BB-k-7-B12

V2 loop

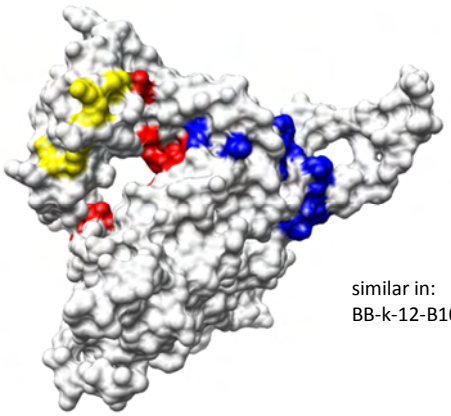

similar in:
BB-k-12-B10

8.5. Alignment of SHIV-1157ipd3N4 gp120 and HIV-1 JR-FL

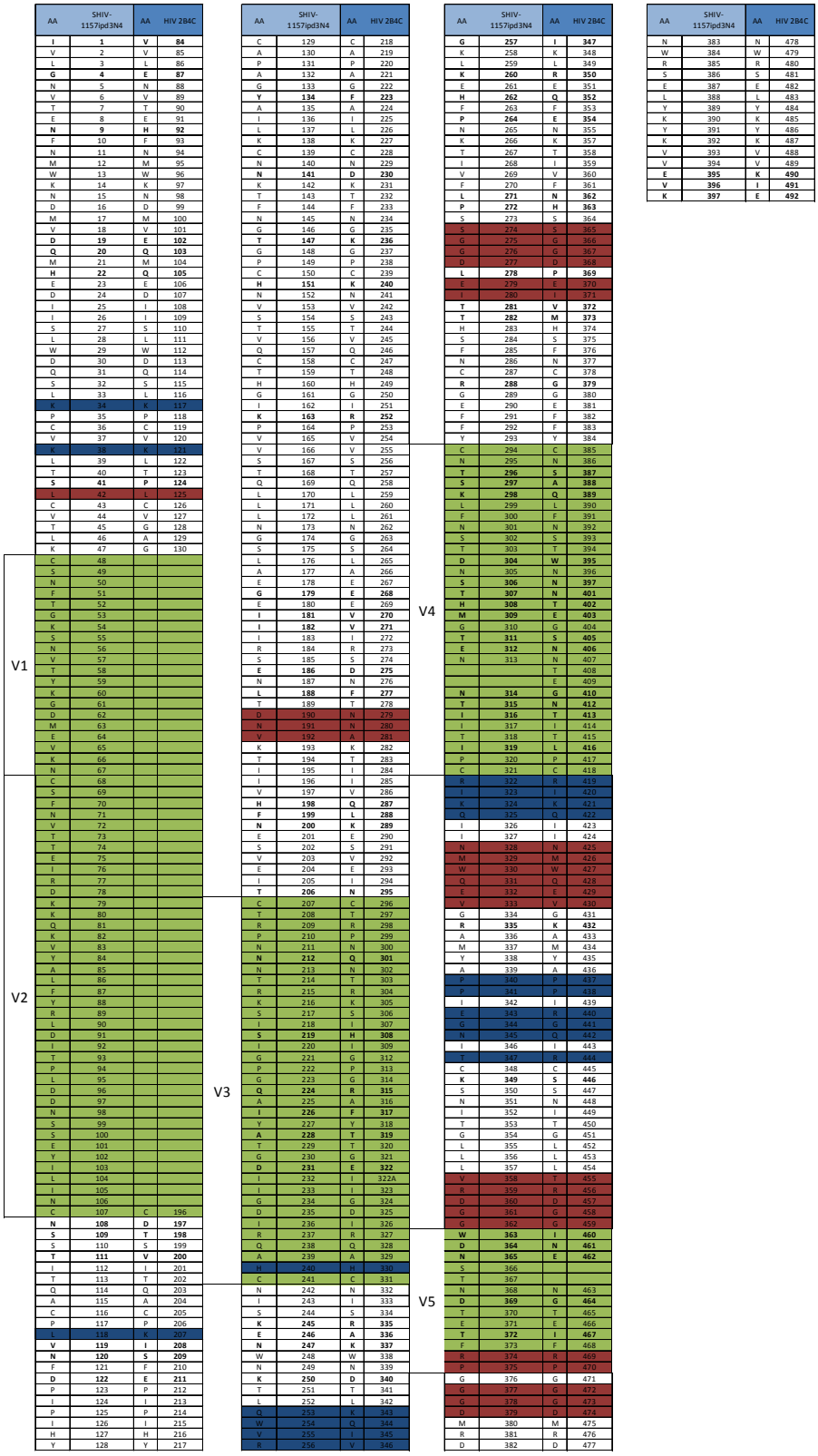

Figure 49: Alignment of HIV-1 JR-FL and SHIV-1157ipd3N4 gp120 sequence.
Loop regions are highlighted in green, amino acid residues important for CCR5 binding in blue and for CD4 binding in red.

9 ACKNOWLEDGEMENTS

First of all, I want to thank Ruth Ruprecht for giving me the opportunity to join her lab at the Dana-Farber Cancer Institute. It was a great experience and with her help I was able to improve my technical, social and language skills. She integrated me in her research group from the very first day and was very supportive with my future plans to make the Ph.D. in her lab as well. Additionally, without her agreement to fund the last five months I would have never been able to extend my stay in Boston. In this context, I also want to thank the Austrian Marshallplan Foundation for the financial support in the first seven months of my stay in the United States.

My special acknowledgement goes to Michael Humbert, who supervised me with a lot of patience throughout the whole year. He was not only a great mentor at work, but listened to my problems and doubts also outside of the lab. Moreover, he always made me feel a little bit like I am home. Danke dafür Michi!

In addition, I want to thank Dieter Klein and Regina Hofmann-Lehmann who always supported my ideas. Without them I would not have had the courage to apply at the Dana-Farber Cancer Institute for my Master Thesis or for my Ph.D.

I want to thank all members of the Ruprecht-Lab for their help in all kind of situations and special thanks to Jennifer Watkins, John Yoon, Brisa Palikuqi and Nadja Kopp who have always been great companions also outside the lab. For a great time outside of the lab, I also want to thank my roommates Micki and Alex, with whom I shared so many funny as well as difficult situations.

Last but not least, I want to thank my family and friends back in Austria for their help and advices during all my years of study and especially during the times abroad. They always believed in me and my plans, and offered me a great home when I decided to come back.